ENVIRONMENTAL AND BIOLOGICAL EFFECTS ON NUTRITIONAL MODE AND RESOURCE PARTITIONING IN SCLERACTINIAN CORALS

A DISSERTATION SUBMITTED TO THE GRADUATE DIVISION OF THE UNIVERSITY OF HAWAI‘I AT MĀNOA IN PARTIAL FULFILLMENT OF THE REQUIREMENTS FOR THE DEGREE OF

DOCTOR OF PHILOSOPHY

IN

MARINE BIOLOGY

May 2019

By

Christopher B. Wall

Dissertation Committee:
Megan Donahue, Chairperson
Anthony Amend
Amy Moran
Brian Popp
Christopher Sabine

Keywords: Corals, Isotopes, Symbiodiniaceae, Energetics, Nutrition, Climate Change

DEDICATION

For my family and our times together by the ocean that set me on this path

ACKNOWLEDGEMENTS

I am eternally thankful for my family and their investments in my life and career. To the Walls and Colemans and inlaws Wesleys and Holmes: I am fortunate to have you all in my life and in my heart. To my wife Megan: your support for me has been unyielding. It has survived long tours, longer field seasons, and our shared world travels. You inspire me; you make life beautiful. This accomplishment is ours, together. To my daughter Alana Jane: your love of the ocean rekindles my own fascination with nature. There is nothing in this world I enjoy more than being your father. To my mother Jane: I wish you could have seen the last twenty years come together. I know you were watching, holding your breath in anticipation. To my father James: your extraordinary journey through life has been a constant reminder that adversity and tribulations are speed bumps, not road blocks, and commitment and hard work pay off. Thank you for instilling in me the value of self-reliance, plus a bit of bullheadedness. To my grandmother Geneva: your love of nature made me a botanist prior to being a marine biologist. Thank you for teaching me to appreciate the serenity of a garden and the study of plants. To my brother Matthew and my sister-in-law Jennifer, I am exceptionally proud of you both and love your enduring curiosity and passion for learning. Matthew, thank you for being my confidant, sounding board, and best friend through smooth and rough seas; the quest lives on.

To my advisor, Dr. Ruth Gates: Ruth, I wish we could have crossed the finish line together. I am grateful for your optimism, your energy, and the opportunity to have worked with you and learned from you. I am grateful for my committee – Dr. Megan Donahue, Dr. Brian Popp, Dr. Amy Moran, Dr. Anthony Amend, Dr. Chris Sabine – for their contributions to my training and for the fruitful discussions and intellectual challenges provided along the way. I appreciate the

time you spent guiding and consulting me in my research over the past size years. In particular, Megan Donahue, thank you for taking me under your wing and keeping me on path during a hard time; and Brian Popp, thank you for sharing your expertise and insights on stable isotopes (and introducing me to the extended IsoCamp hui), and always having your door open to an isotope neophyte. Your mentorship has been invaluable.

To my mainland and island ohana, I am blessed beyond words to have you all in my life. The best memories of my Ph.D. are thost spent with you – sharing stories and laughs around a grill, by the water, or in the surf. To my extended scientific family – The Ruth Gates Coral Lab, The Megan Donahue Lab, and the Peter Edmunds Polyp Lab – thank you all for the training, experience, and friendships that carried me through this journey. In particular, thank you Peter Edmunds, Hollie Putnam, Ross Cunning, Raphael Ritson-Williams, Crawford Drury, John Burns, Maggie Sogin, Robert Mason, Beth Lenz, Shayle Matsuda, Ariana Huffmyer, Carlo Caruso, Mariana Rocha de Souza for the fruitful discussions, Jen Davidson, Kira Hughes, and invaluable assistance of undergraduate scholars (William Ellis, Mario Kaluhiokalani, Alexandra Wen, Kelly Wyrick, Pansa Cecchini) for logistical support in pursuit of my dissertation research.

ABSTRACT

Reef corals are threatened by climate change. Increasing atmospheric CO_2 has resulted in ocean acidification (OA) and ocean warming, which contribute to reductions in coral growth and to widespread coral bleaching events. The resilience of coral reef ecosystems to climate change fundamentally relies on the physiological resilience of reef corals to environmental change. Coral resilience may be supported by (i) biomass reserves, (ii) the capacity to switch feeding modes from autotrophy to heterotrophy, and (iii) the flexibility to associate with stress tolerant endosymbionts (Family: Symbiodiniaceae). To better understand the physiological response of corals to natural and human-induced environmental stress, I used a combination of laboratory and field studies to examine the tradeoffs in these three aspects of coral physiological resilience under ocean acidification stress, bleaching and post-bleaching recovery, and light limitation.

First, under ecologically relevant irradiances, the coral *Pocillopora acuta* does not exhibit OA-driven reductions in calcification as reported for other corals. Instead, reductions in biomass reserves suggest that OA induced an energetic deficit and contributed to the catabolism of tissue biomass. Second, coral bleaching had extensive effects on the biomass of *Montipora capitata* and *Porites compressa*, and isotope mass balance revealed that changes in coral $\delta^{13}C$ values were best explained by changes in tissues (proteins:lipids:carbohydrates) not a greater reliance on heterotrophy during bleaching or recovery. Finally, *M. capitata*-Symbiodiniaceae holobionts exhibited distinct traits and $\delta^{13}C$ isotope values that differed between seasons and were modulated by light-availability. $\delta^{13}C$ isotopic values did not reveal changes in nutritional modes, but instead suggest lower rates of carbon fixation/translocation by the symbiont *Durusdinium,* in agreement with laboratory studies identifying *Durusdinium* as an opportunist symbiont providing

less nutritional benefit to the host. Together, my research provides insights into the complex consequences of environmental change on reef-building corals. Moreover, physiological tradeoffs that underlie coral resilience may mask the full effects of climate stressors on coral reefs. My work highlights the need for future research to consider (i) energetic costs and growth tradeoffs, (ii) biomass compound-specific isotope values, (iii) and the role of seasonality and (iv) symbiont community effects.

TABLE OF CONTENTS

LIST OF TABLES

LIST OF FIGURES

CHAPTER 1
INTRODUCTION

Introduction

The coral-algal symbiosis and environmental stress

Coral reefs are among the most biologically diverse and productive ecosystems on Earth, providing habitat for a multitude of marine organisms including those of high commercial value and cultural significance, as well as threatened and endangered species (Wilkinson 2008). Reef corals (Order: Scleractinia) and their symbiont algae (formerly, *Symbiodinium* spp.) (Division: Dinophyceae, Family: Symbiodiniaceae) function as autogenic and allogenic ecosystem engineers (Jones et al. 1994) of coral reef ecosystems by modifying the chemistry of reef seawater, contributing to the architectural complexity of the benthos, transforming organic and inorganic nutrients through primary productivity and excretory processes (Wild et al. 2011). In the oligotrophic tropical and subtropical seas (30°N – 30°S latitude) (Sheppard et al. 2010), reef corals and Symbiodiniaceae have thrived as a result of nutrient recycling within the symbiotic partnership (Porter 1976), wherein photosynthetically fixed carbon and nitrogen compounds are translocated and conserved within the coral holobiont (i.e., animal + alga + assorted microbes) (Muscatine and Porter 1977; Rahav et al. 1989; Tanaka et al. 2006). However, resource assimilation and utilization, as well as the level of resource sharing among symbiotic partners, is shaped by environmental conditions (Tremblay et al. 2012b, 2013).

Coral reefs worldwide are in a state of decline due to direct human impacts (e.g., nutrient pollution) and global climate change (GCC). Reef corals are sensitive to changing environmental conditions, including elevated sea surface temperatures, terrigenous pollutants (e.g., dissolved nutrients, coastal runoff, sewage), and reduced ocean pH (Lesser et al. 1990; Glynn 1993; Hoegh-Gulberg 1999; Kleypas et al. 1999). Such abiotic stressors have the

potential to reduce the ecosystem function of reef corals, destabilize the coral-algal symbiosis, disrupt symbiont photosynthesis and the transfer of symbiont-derived metabolites to the coral host, and cause coral mortality (Lesser 1990; Hughes et al. 2010). At the local level point source nutrient pollution (e.g., sewage outfall) and land-based runoff (e.g., agriculture and urban runoff, sediment discharge) degrade the quality of reef habitat by increasing seawater turbidity and the concentration of dissolved nutrients and contributing to macroalgal proliferation (Fabricius 2005; Friedlander et al. 2005). At larger spatial scales GCC and the burning of fossil fuels are increasing sea surface temperatures (SST) and perturbing the chemical composition and pH of seawater, a process termed ocean acidification (OA).

Increased pCO_2 in the atmosphere and seawater is projected to increase from current pCO_2 (ca. 400 μatm; NOAA) to 490 μatm – 850 μatm pCO_2 (RCP 2.6 and 6.0, respectively) (Moss et al. 2010; van Vuuren et al. 2011) commiserate with a 0.1 – 0.3 unit decrease in ocean pH_T and a 1.8 – 4.0 °C increase in global temperatures (IPCC 2007). Corals live near their upper thermal limit during summer months (Coles 1976), and abrupt or prolonged exposure to elevated temperatures initiate a stress response that results in the quantitative reduction in symbiont cells within coral tissues (i.e., coral bleaching). Thermal bleaching can negatively affect numerous aspects of coral performance and cause reductions in coral tissue biomass, altered metabolic states and nutritional modes, attenuated reproductive investments (Porter et al. 1989; Szmant and Gassman 1990; Hughes et al. 2010), and cause widespread mortality (Glynn and D'Croz 1990; Loya et al. 2001). Additionally, OA reduces the rates of biomineralization in marine calcifiers and may exacerbate the effects of thermal stress on reef corals (Kleypas et al. 1999; Anthony et al. 2008). Together changes in the thermal content and carbonate chemistry of seawater will interact with direct

human impacts (e.g., nutrient enrichment) to have profound affects on the physiology of reef corals and will challenge the capacity for coral reefs to remain in coral-dominated states (Kleypas et al., 1999; Silverman et al. 2009).

Reef corals resilient to multiple (local and global) environmental stressors will dominate the reefs of the future. This acknowledgement has led to considerable research effort identify factors contributing to stress resilience in reef corals. Corals show considerable variation in their response to environmental stress as a result of a matrix of host and symbiont traits, as well as abiotic factors contributing to stress acclimatization and adaptation (i.e., thermal history, environmental variability). In particular, coral physiological resilience associates with the following factors: high energy reserves concentrations (i.e., lipids) (Rodrigues and Grottoli 2007; Anthony et al. 2009); the ability to opportunistically transition from autotrophy to heterotrophy (i.e., nutritional flexibility) (Grottoli et al. 2006); and the association with stress-tolerant Symbiodiniaceae genotypes (Rowan et al. 1997; Baker 2003). Increased lipid biomass and heterotrophic feeding have been hypothesized as pathways for the resilience (Hughes and Grottoli 2013) and attenuation (Edmunds 2011; Towle et al. 2015) of climate change stressors and coral mortality (Anthony et al. 2009), including ocean warming and acidification. The energy content of coral biomass (i.e., energetics) and lipid content has long been considered a proxy for coral fitness (Anthony 2006; Anthony et al. 2009) and can support physiological recovery from bleaching (Rodrigues and Grottoli 2007). Therefore, evaluating factors affecting the nutritional modes and energetics of corals has the potential to inform the physiological resilience of reef corals in an uncertain world shaped by climate change.

Nutritional modes: Autotrophic and heterotrophic nutrition

Corals are mixotrophic organisms that rely on symbiont-derived metabolites and exogenous materials to fuel growth and metabolism (Muscatine et al. 1981). While autotrophic nutrition is the *status quo* in reef coral metabolism, it is becoming clear that corals exist along a continuum of autotrophic and heterotrophic nutritional states. The degree to which corals exhibit either opportunistic or obligate nutritional flexibility is affected by a matrix of biological, environmental, and genetic effects only beginning to be understood. However, reef corals are generally thought to rely more heavily on heterotrophic nutrition in conditions where symbiont photosynthesis is reduced, such is the case with increasing depth or water turbidity (Muscatine et al. 1989; Palardy et al. 2005), in response to environmental disturbance (i.e., thermal stress and bleaching recovery) (Grottoli et al. 2006), and may be affected by the genetic diversity of a coral's Symbiodiniaceae community (Leal et al. 2015).

i. Autotrophic nutrition

Corals are reliant on their symbiont algae (Symbiodiniaceae) for autotrophic nutrition to support growth and metabolism. The fixation and release of photosynthates from symbiont to host is stimulated under light exposure (Muscatine and Cernichiari 1969; Trench 1971a; Muscatine et al. 1984) and by the presence of host tissues (Muscatine 1967; Trench 1971b, Trench 1971c) through the action of a low molecular weight compound(s) termed the "host factor" (Gates et al. 1995; Grant et al. 1998). Under conditions optimum for photosynthesis, > 90% of photosynthetically fixed carbon may be translocated to the coral host forms including simple, low molecular weight compounds (i.e., glycerol and glucose, amino acids, organic acids) and complex high molecular weight compounds (i.e., free fatty acids, lipids) (Muscatine and

Cernichiari 1969; Patton et al. 1977; Papina et al. 2003). Translocated products may meet the majority (~ 90 – 100%) of a coral's daily metabolic costs, and translocated metabolites may be used as respiratory substrate, become incorporated into tissue biomass, contribute to skeletal calcification and reproduction, or may be excreted from the association as mucus (Trench 1971a; Muscatine et al. 1984). The products of photosynthesis, however, are deficient in nitrogen, phosphorous and amino acids essential for the production of tissue biomass (Falkowski et al. 1984), requiring corals to obtain exogenous nutrients through heterotrophic feeding or the uptake of dissolved compounds in seawater.

Carbon translocated to the coral host may is ultimately affected by the photosynthetic capacity (net photosynthesis per unit area and per algal cell) and the photoacclimatory state of its symbiont community and the health of the holobiont (Anthony and Hoegh-Guldberg 2003; Tremblay et al. 2012b, 2014). High carbon translocation rates relate to nutrient limitations in the coral-*Symbiodiniaceae* association, where fixed carbon is released to the coral host and incorporated into algal biomass. However, changes in the availability of organic and inorganic nitrogen from heterotrophic feeding or exogenous seawater conditions can affect symbiont photosynthesis as well as the retention, translocation, and utilization of carbon in the symbiotic association (Davy and Cook 2001; Tanaka et al. 2007; Tremblay et al. 2012a, 2012b, 2014). Carbon translocation also differs among host species, Symbiodiniaceae genotypes, the interaction of environmental conditions altering symbiont productivity (i.e., temperature, irradiance), and the nutritional status of the coral holobiont (Falkowski et al. 1984; Davy and Cook 2001; Loram et al. 2007: Stat et al. 2008). For instance, temperature and photo-stress reduce autotrophic nutrition available and increase the loss of total organic carbon to the

environment (Tremblay et al. 2012). Similarly, shade-adapted corals receive less autotrophic carbon than sun-adapted corals, and require heterotrophic nutrition to cover energetic costs of growth and metabolism (Muscatine et al. 1984). However, light and temperature alone do not offer a complete explanation for coral bioenergetics. For instance, in the absence of heterotrophic feeding carbon translocated was not affected by irradiance (120 vs. 250 μmol photons m^{-2} s^{-1}), however heterotrophic feeding affected carbon translocation rates in a light dependent fashion, reducing translocation by ~ 20% at low irradiances relative to high irradiances (Tremblay et al. 2014). However, high rates of autotrophic nutrition do not necessarily equate to greater biomass or skeletal production, and surplus translocated carbon may be excreted. Therefore, heterotrophic nutrition appears to be an important input for the bioeconomy of corals even under conditions of replete autotrophic nutrition.

ii. Heterotrophic nutrition

Heterotrophic feeding represents an important nutritional constituent in the diet of reef coals. Corals are voracious predators capable of the capture of living organisms (e.g., microbes, plankters), filter feeding on detritus or suspended particulates, and utilizing dissolved organic/inorganic compounds from seawater (collectively, "heterotrophy") (Davies 1984; McCloskey and Muscatine 1984; Houlbrèque and Ferrier-Pagès 2009). Heterotrophy can supply 15 – 60% of a healthy coral's daily metabolic energy demand >100% of energy requirements in bleached corals (Muscatine et al. 1981; Grottoli et al., 2006; Palardy et al. 2008). In laboratory feeding experiments, heterotrophy stimulates coral calcification, tissue growth, symbiont and photopigment density, and symbiont photosynthesis (Ferrier-Pagès et al. 2003; Houlbreque et al. 2003; Tolosa et al. 2011).

Rates of heterotrophic feeding vary among coral taxa due to biological factors—such as feeding effort (Palardy et al. 2005; Ferrier-Pagès et al. 2010), zooplankton concentrations (Palardy et al. 2006), corallum morphology (Porter 1976; Palardy et al. 2005), polyp size (Porter 1976; Alamaru et al. 2009) and environmental conditions such as, water temperature (Palardy et al. 2005), flow (Sebens et al. 1998) light levels (Ferrier-Pagès et al. 1998) and depth (Palardy et al. 2005; Alamaru et al. 2009; Lesser et al., 2010). Further, heterotrophic feeding may be stimulated during periods of environmental stress where symbiont photosynthesis and autotrophic nutrition contributing to animal respiration is reduced (Grottoli et al. 2006; Ferrier-Pagès 2010). The degree of heterotrophic nutrition in corals may be dynamic and regulated by the coral animal's feeding effort and not by feeding capacity. However, the ability to opportunistically exploit heterotrophic feeding in response to environmental stress is largely species-specific. For instance, feeding rates increased in the corals *Turbinaria reinformis* and *Galaxea fasciularis* at 31 °C relative to 26 °C but heterotrophic feeding declined in thermally stressed *Stylophora pistillata* (Ferrier-Pagès 2010). Similarly, feeding rates increased in bleached *Montipora capitata* relative to non-bleached controls, but feeding was reduced in bleached *Porites compressa* and unchanged in bleached *Porites lobata* (Palardy et al. 2008). The disparity in feeding responses may reflect coral metabolic needs or demands and associated costs of prey capture and digestion and the relative disruption of carbon fixation and translocation in Symbiodiniaceae. Using the sea anemone, *Aiptasia pallida,* Leal and colleagues demonstrated the cnidarian's trophic plasticity was affected by its Symbiodiniaceae community, and the disruption of carbon fixation and translocation and reductions in symbiont density positively correlated with reduced prey capture and digestion (Leal et al. 2015).

iii. Functional and genetic diversity of Symbiodiniaceae

Reef corals associate with distinct genotypes of Symbiodiniaceae that differ in their evolutionary relatedness (hereafter, *clades*) (Baker 2003). Previously, clades – now genera (LaJeunesse et al. 2018) – identified as A – I were annotated by either small subunit (18S) or large subunit (5.8S, 28S) ribosomal nuclear DNA (rDNA), with further evolutionary distinctions at the species (previously, sub-clade) level using the internal transcribed spacer (ITS2) region of rDNA (Stat et al. 2006, 2009). Symbiodiniaceae genera and species show functional differences, both in their capacity to tolerate environmental stress (Rowan 1997; Jones et al. 2008) and to supply autotrophic nutrition (Stat et al. 2008; Leal et al. 2015). The quality and quantity of carbon translocated to coral is affected by symbiont genotype, the genetic composition of the symbiont community and may also be affected by host-symbiont combinations (Loram et al. 2007; Stat et al. 2008; Starzak et al. 2014; Leal et al. 2015). The ability for thermotolerant Symbiodiniaceae genotypes to confer tolerance to environmental stress has gained much attention (Rowan et al. 1997), however the nutritional and functional performance of Symbiodiniaceae at the genus and species (i.e., previously clade and subclade) level is not well understood (Starzak et al. 2014; Leal et al. 2015).

Environmental disturbances disrupt the exchange of nutrients in the coral-algal symbiosis and may drive shifts in a reef coral's symbiont community over time (Baker 2003). However, corals hosting stress sensitive clades and subclades may also suffer mortality and be progressively removed from the population gene pool (Sampayo et al. 2008). According to the adaptive bleaching hypothesis (Buddemeier and Fautin 1993), corals will bleach and expel temperature

sensitive symbionts and retain (or uptake) temperature labile genotypes thereby gaining temperature resilience. However, thermotolerant symbionts, such as those in clade D, appear less nutritionally beneficial to the growth and metabolism of their coral hosts (Cantin et al. 2009; Jones and Berkelmans 2010), potentially harming coral performance and acting as parasites under non-stressful conditions (Cunning et al. 2014, 2015; Lesser et al 2013). Considering the differences in the nutrient transfer and autotrophic capacity of Symbiodiniaceae genotypes (Leal et al. 2015), shifts in coral-algal associations may have unforeseen tradeoffs affecting ecological outcomes for reef corals under environmental stress and climate change.

Recent works have significantly contributed to the understanding of the functional diversity of Symbiodiniaceae as it pertains to the coral ecology, carbon and nitrogen assimilation and translocation from symbiont to host, and the nutritional (i.e., trophic) flexibility of reef corals. For instance, reef corals and sponges associating with *Cladocopium* spp. symbionts (e.g., ITS2 types C1, C3) poses higher rates of carbon fixation and translocation, ammonium and nitrate translocation, and stimulate the growth of their coral hosts to a greater degree than *Durusdinium* spp. symbionts (formerly clade D) (Baker et al., 2013; Pernice et al., 2014). Furthermore, *Cladocopium* spp. symbionts (e.g., ITS2 types C1 and C2) have greater photosynthetic performance and have been shown to contributed more to coral growth, energetics and egg production and than *Durusdinium* spp. symbionts (Cantin et al., 2009; Jones and Berkelmans 2010, 2011). Similarly, adult corals hosting *Durusdinium* spp. symbionts grew ~ 30% slower than *Cladocopium* sp. (ITS2 type C2) hosting conspecifics in laboratory and the field settings (Jones and Berkelmans 2010). In cultures, *Cladocopium* spp. symbionts in the presence of synthetic host factor showed carbon fixation and carbon release (a proxy for translocation)

relative to purportedly less mutualistic *Symbiodinium* spp. (formerly clade A) symbionts (Stat et al. 2008).

The autotrophic performance of a coral's symbionts also appears to be affected by the composition of the resident community (Loram et al. 2007), which may consist of several clades and subclades genotypes within a single colony. Using the giant sea anemone, Loram *et al*. (2007) found *Symbiodinium* sp. (clade A) and *Brevolium* sp. (formerly clade B) symbionts to translocate ~ 30 and 40% of fixed carbon to the animal, respectively, while mixed communities of (*Symbiodinium* sp. + *Brevolium* sp.) symbiont released intermediate percentages (~ 35% of fixed carbon) to the animal. Furthermore, a larger percentage of translocated carbon was stored in the lipid fraction of the host's biomass in anemones associating with *Symbiodinium* relative to *Brevolium* (Loram et al. 2007). The genetic identity of a coral's Symbiodiniaceae community may also influence the reliance of corals on different modes of nutrition (i.e., heterotrophy) and may provide an evolutionary context for the disparate nutritional strategies utilized among coral species in response to stress (Leal et al. 2015). A coral's symbiont community may affect the utilization and storage of materials relevant to the health and function of the coral animal and may also impact the degree to which corals are nutritionally flexible. Investigating the role of the functional diversity in Symbiodiniaceae may offer insight into the anabolism and catabolism of energy reserve and the requirement for select coral taxa to exhibit greater nutritional plasticity under normal and stressful conditions.

Conclusions

The maintenance of nutrient exchanges in reef corals is critical to the function of both symbiotic

partners and identifies nutritional interactions within the coral holobiont as a focal point to provide insight on the success and failures of this symbiotic system in response to environmental change. However, there is a need to better understand the role of abiotic and biotic factors affecting the partitioning of autotrophic and heterotrophic nutrients within the holobiont across symbiotic states and environmental conditions. Indeed, the need for such research is supported by new evidence of the functional diversity of Symbiodiniaceae in affecting both autotrophic and heterotrophic nutrition of reefs corals—a previously unknown property of reef coral performance—and in modulating coral's response to GCC.

This dissertation seeks to test for the effects of changing environmental conditions and host-symbiont combinations on the nutrition of corals. This will be accomplished by using a series of field collections and laboratory experimentation to evaluate autotrophic and heterotrophic nutrition, coral tissue energetics, and the functional diversity of Symbiodinium genera in Hawaiian corals (1) in response to changing light conditions and ocean acidification, (2) during and following a regional bleaching event, (3) and within and among reef habitats across a light-resource gradient in two seasons.

CHAPTER 2

ELEVATED pCO_2 AFFECTS TISSUE BIOMASS COMPOSITION, BUT NOT CALCIFICATION, IN A REEF CORAL UNDER TWO LIGHT REGIMES

Abstract

Ocean acidification (OA) is predicted to reduce reef coral calcification rates and threaten the long-term growth of coral reefs under climate change. Reduced coral growth at elevated pCO_2 may be buffered by sufficiently high irradiances, however, the interactive effects of OA and irradiance on other fundamental aspects of coral physiology, such as the composition and energetics of coral biomass, remain largely unexplored. This study tested the effects of two light treatments (7.5 *vs*. 15.7 mol photons m^{-2} d^{-1}) at ambient- or elevated-pCO_2 (435 *vs*. 957 µatm) on calcification, photopigment and symbiont densities, biomass reserves (lipids, carbohydrates, proteins), and biomass energy content (kJ) of the reef coral *Pocillopora acuta* from Kāne'ohe Bay, Hawai'i. While pCO_2 and light had no effect on either area- or biomass-normalized calcification, tissue lipids gdw^{-1} and kJ gdw^{-1} were reduced 15% and 14% at high pCO_2, and carbohydrate content increased 15% under high light. The combination of high light and high pCO_2 reduced protein biomass (per unit area) by ~ 20%. Thus, under ecologically relevant irradiances, *P. acuta* in Kāne'ohe Bay does not exhibit OA-driven reductions in calcification reported for other corals; however, reductions in tissue lipids, energy content, and protein biomass suggest OA induced an energetic deficit and compensatory catabolism of tissue biomass. The null effects of OA on calcification at two irradiances support a growing body of work concluding some reef corals may be able to employ compensatory physiological mechanisms that maintain present-day levels of calcification under OA. However, negative effects of OA on *P. acuta* biomass composition and energy content may impact the long-term performance and scope for growth of this species in a high pCO_2 world.

Introduction

Scleractinian corals are engineers of tropical coral reef ecosystems, directing the architecture and bioenergetics of these communities (Wild et al. 2011). These ecosystems are, however, threatened by rapid seawater warming and ocean acidification (OA) associated with increasing concentrations of carbon dioxide (pCO_2) in the atmosphere (Raven 2005), which is predicted to double by the end of the century (650 – 850 μatm pCO_2) (Moss et al. 2010). Dissolution of atmospheric CO_2 in the upper-ocean alters the carbonate chemistry of seawater and reduces seawater pH and the saturation state of aragonite (Ω_{arag}) (Gattuso et al. 1999). These changes in seawater chemistry negatively impact many marine organisms, for example, by reducing rates of biogenic calcification in ecologically and economically important marine calcifiers (Kroeker et al. 2010; Chan and Connolly 2013). The magnitude of OA effects on coral calcification, however, may be buffered by biological mechanisms (e.g., upregulation of internal pH) (McCulloch et al. 2012), environmental conditions (e.g., light, temperature, water motion) (Reynaud et al. 2003; Dufault et al. 2013; Comeau et al. 2014c; Bahr et al. 2016) and increasing energy available for metabolism (e.g., heterotrophy) (Edmunds 2011; Towle et al. 2015).

Light availability impacts reef corals by modulating Symbiodiniaceae photosynthesis, which influences both the formation of skeleton (Gattuso et al. 1999) and the generation of lipid biomass (Patton et al. 1977) from translocated photosynthates (Crossland et al. 1980; Stimson 1987). Despite the importance of light to coral biology, the role of light in modulating coral responses to elevated pCO_2 has only recently been considered (Dufault et al. 2013). Many OA experiments have been performed under low light levels (Table 2.1) that likely do not saturate photosynthesis and calcification rates, which may increase OA-sensitivity. Indeed, low light exacerbates the negative effects of high pCO_2 on the growth of at least some corals (Dufault et al.

2013; Vogel et al. 2015), whereas increased light availability can mitigate negative effects of OA on growth observed at lower irradiances (Suggett et al. 2013). The role of light in modulating OA effects on skeletal growth is gaining attention, however, few studies have addressed whether other equally important aspects of coral physiology—such as tissue biomass growth and composition, and the allocation of energy resources—are impacted by pCO_2 (Schoepf et al. 2013; Comeau et al. 2014a; Hoadley et al. 2015) and its interaction with light availability.

Understanding the interactive impacts of OA and light availability on coral tissue biomass is critically important, given that the quantity (Fitt et al. 2000) and biochemical composition (e.g., lipids, carbohydrates, proteins) of biomass has important ecological implications for corals, including their response to environmental stress. In particular, lipids, which comprise ~ 30 – 45% of dry biomass (Stimson 1987), are a critical energy source in the early life history of reef corals (Harii et al. 2010), for parental provisioning of brooded larvae (Ward 1995), and in adult corals recovering from bleaching (Grottoli et al. 2004). Indeed, corals with greater lipid content (Anthony et al. 2007) and/or tissue biomass (Thornhill et al. 2011) may avoid post-bleaching mortality.

The quantity and quality (e.g., lipid proportion or energy content) of tissue biomass may be impacted by OA as a response to altered metabolic demands or resource allocation. For instance, physiological stress from OA may increase the energetic costs of calcification and cellular homeostasis (e.g., ion transport, protein turnover) (Allemand et al. 2011; Pan et al. 2015), and in turn promoting the catabolism of lipid energy reserves to meet these demands (Vidal-Dupiol et al. 2013). Indeed, OA produces both positive and negative effects on coral biomass. Tissue

biomass (Comeau et al. 2013b, 2013c) (and lipid content [Schoepf et al. 2013]) can increase in some corals under elevated pCO_2, while in other corals, tissue carbohydrates, proteins, and lipids decline (Hoadley et al. 2015). Despite mixed pCO_2 effects (< 2,000 μatm) on coral respiration and photosynthesis (Kaniewska et al. 2012; Suggett et al. 2013; Wall et al. 2014; Comeau et al. 2017), multiple lines of evidence indicate high pCO_2 can affect resource allocation (Comeau et al. 2014a), anabolic and catabolic processes (Edmunds and Wall 2014), and gene expression in corals indicative of changing metabolic demands (Kaniewska et al. 2012; Vidal-Dupiol et al. 2013). For instance, elevated pCO_2 can increase photosynthetic and heterotrophic energy acquisition (Suggett et al. 2013; Tremblay et al. 2013; Towle et al. 2015), and may also alter the allocation of resources to growth (e.g., tissue and skeletal) or maintenance (Anthony et al. 2002; Pan et al. 2015). Such changes in resource acquisition or allocation may therefore influence biomass quantity (Comeau et al. 2013c) and composition (Schoepf et al. 2013; Hoadley et al. 2015) with concomitant consequences for coral physiology. However, OA effects on coral biomass observed to date appear complex and non-linear (Schoepf et al. 2013; Hoadley et al. 2015; Comeau et al. 2013c), and effects vary (i.e., positive, negative, or null effects) with light availability (Comeau et al. 2014a) and across species (Schoepf et al. 2013; Hoadley et al. 2015). Considering the importance of tissue biomass to coral performance, the uncertainty of OA effects on coral biomass represents a significant knowledge gap that we aim to address here.

We tested the effects of pCO_2 and light on the calcification, tissue biomass (total biomass, lipids, carbohydrates, proteins), energy equivalents (kiloJoule (kJ) or energy content), and densities of symbiont cells and concentrations of chlorophylls (*a* and c_2) in the coral *Pocillopora acuta* (Lamarck, 1816) (Schmidt-Roach et al. 2014). We address the following questions: (1) Does

elevated pCO_2 affect calcification, coral biomass and tissue energy content, symbiont cell density, and chlorophyll concentration? (2) Are the effects of pCO_2 on coral biomass and calcification modulated by light availability? We reasoned high pCO_2 effects on energy reserves and calcification would be attenuated by increased light availability (Suggett et al. 2013) due to stimulatory effects of light on coral tissue and skeletal growth (Chalker 1981; Stimson 1987; Gattuso et al. 1999). We also normalized energy reserves and calcification at two levels (Edmunds and Gates 2002)—the surface area of the skeleton and the quantity of tissue biomass—to evaluate the scale at which these responses were affected by pCO_2 and light.

Material and Methods

Taxonomic identification

Coral samples were identified as *Pocillopora acuta* rather than the morphologically similar *P. damicornis* (Schmidt-Roach et al. 2014). Our laboratory has performed molecular identifications of pocilloporid colonies at Moku o Loʻe Island (Hawaiʻi Institute of Marine Biology, HIMB) and within the larger Kāneʻohe Bay reef system that revealed that *P. acuta* is overwhelmingly the dominant coral of the two species at our sampling location. We also consulted several scientists at HIMB regarding species identifications at our collection site.

Experimental Design

Four experimental treatments of low and high light (LL and HL) fully crossed with ambient and high pCO_2 (ACO_2 and HCO_2) were produced in 24 flow-through aquaria (45 L; Aqualogic, Inc., USA) (n = 6 tanks treatment^{-1}) receiving sand-filtered natural seawater (ca. >100 μm) and maintained at seasonally ambient seawater temperatures (24.94°C ± 0.05) (mean ± SE, n = 680). pCO_2 treatments reflected ambient Kāneʻohe Bay seawater (ACO_2; ca. 440 μatm pCO_2), and

elevated levels (HCO_2; ca. 900 µatm pCO_2) projected for the end of the century (RCP 6.0) (Moss et al. 2010). Light treatments were created by suspending a 75 W light emitting diode module over each tank (AI Sol White, Blue, Royal Blue; Aqua Illuminations, USA), calibrated with a 4π quantum sensor (LI-193, Li-Cor, USA) connected to an LI-1400 light meter (Li-Cor). Lights were programmed to increase each day from 0500 – 1000 hrs, sustain maximum (400 or 800 µmol photons m^{-2} s^{-1}) for 2 h, and decrease to darkness by 1700 hrs, resulting in a 12h light : 12h dark diel cycle. Light treatments were programmed to a ramping 12 : 12 h light : dark diel cycle that contrasted high light (HL; 800 μmol photons m^{-2} s^{-1} daily maximum) and 50% light attenuation conditions (LL; 400 μmol photons m^{-2} s^{-1} daily maximum) equivalent to 15.7 and 7.5 mol photons m^{-2} d^{-1}. These light treatments are ecologically relevant to reef corals on Kāne‘ohe Bay patch reefs, where daily integrated light intensities at 1 m depth near our collection site range from 10 – 20 mol photons m^{-2} d^{-1} and ~ 300 – 1,100 µmol photons m^{-2} s^{-1} maximum daily irradiance for the period of November – January (Cunning et al. 2016).

pCO_2 treatments were maintained by bubbling either ambient air (i.e., ACO_2) or CO_2-enriched air (i.e., HCO_2) into four header tanks (n = 2 header tanks per pCO_2 treatment). pCO_2 in each header tank was controlled by a pH-stat system (Apex AquaController, Neptune Systems, USA) that dynamically regulated the flow of air or CO_2 gas through a solenoid based on a static set-point for each seawater treatment (ACO_2 or HCO_2). Seawater in each header tank was delivered to six flow-through treatment tanks at ca. 1.5 l min^{-1}. Seawater temperature, salinity, pH_T (pH on the total scale) and total alkalinity (A_T) were measured in all tanks every third day of the experiment. Seawater temperature (24.59˚C ± 0.06) (mean ± SE, n = 153) during the 32 d experimental period was independently maintained in each treatment tank using digital

temperature controllers (Model TR115DN; Aqualogic Inc., USA) and submersible heaters. Temperature in tanks was monitored using a certified digital thermometer (5-077-8, +/- 0.05°C, Control Company, USA), and the salinity of incoming seawater (ca. 34 salinity) was monitored using a conductivity meter (YSI 63, YSI Inc., USA); pH_T was measured using a benchtop pH meter (Orion 3-Star, Thermo Fisher Scientific, USA) and pH probe (DG115-SC, Mettler-Toledo, LLC, USA) calibrated against certified Tris standard at a range of temperatures (Dickson Lab, UCSD) (Dickson et al. 2007). Titrations were performed using an open-cell, potentiometric automatic titrator (T50, Metler-Toledo, USA) filled with certified acid titrant (Dickson Lab, UCSD). Titrations of certified reference materials of known A_T (Batch 137 and 140) provided by A.G. Dickson (UCSD) were titrated prior to and alongside treatment seawater titrations, with our analyses differing on average < 0.8% or 17 μmol kg^{-1} (n = 21) from certified values. Final values for seawater carbonate chemistry were calculated using the *seacarb* package (Gattuso et al. 2015) in *R* (R Core Team 2016).

Coral collection

Seven adult colonies of *Pocillopora acuta* were collected on 13 and 29 October 2014 at ~ 1 m from windward facing reefs of Moku o Loʻe (Coconut Island) in Kāneʻohe Bay on the island of Oʻahu, Hawaiʻi, USA (21°26'08.9"N, 157°47'12.0"W). Twenty-four ramets (≤ 4 cm height) from each coral colony were attached to PVC-bases with Z-spar (A-788) and hot-glue, and allowed to recover for 3 – 5 weeks in outdoor flow-through tanks (1,300 l) under attenuated natural sunlight (≤ 6 mol photons m^{-2} d^{-1}) receiving sand-filtered seawater and maintained at 26.05 °C ± 0.01 (mean ± SE, n = 4,869) using a chiller (Model MT3, Aqualogic, Inc.). Subsequently, one fragment from each of the seven colonies was assigned to each of the twenty-

four indoor treatment aquaria (n = 7 colony fragments tank^{-1}) and allowed to acclimate for 25 d to treatment irradiances (7.5 and 15.7 mol photons m^{-2} d^{-1}), acclimation-period temperatures 25.73 ± 0.03 °C (mean ± SE, n = 192), progressively increasing pCO_2 (for HCO_2 tanks), and flow. Supplemental heterotrophic feedings were not provided during acclimation or experimental periods, however, corals had access to heterotrophic food sources in the form of microbes, dissolved organic matter, and < 100 μm plankters. Corals were exposed to pCO_2 and light treatments for 32 d from 16 December 2014 – 16 January 2015 and frozen (-80 °C) until further processing.

Physiological parameters

All coral fragments (n = 7 tank^{-1}) were analyzed for net calcification, photopigment densities, carbohydrates, proteins, and total biomass. Quantification of symbiont cell densities, lipid biomass, and tissue energy content was performed on four fragments in each tank. Net calcification was determined by the change in buoyant weight (Davies 1989) (converted to dry weight using a density of aragonite of 2.93 g cm^{-3}) and standardized to both skeletal surface area determined by wax dipping (Stimson and Kinzie 1991) and coral biomass determined by ash-free dry weight (AFDW). To quantify tissue biomass characteristics, tissues were removed from the skeleton using an airbrush filled with filtered seawater (0.2 μm). The host and symbiont extract (hereafter, tissue slurry) was briefly homogenized, subsampled, and frozen at -20 °C. Symbiont cell densities were determined from replicate counts (n = 6 – 8) of tissue slurry on a haemocytometer and normalized to surface area. The concentration of chlorophyll a and c_2 was quantified following a modified protocol from (Fitt et al. 2000). An aliquot of homogenized tissue slurry (1 ml) was centrifuged (1,600 × g for 3 min), pelleting symbiont cells. The

supernatant was decanted and 1 ml of 100% acetone was added to the pellet and allowed to incubate in darkness at -20 °C for 36 h. Chlorophyll concentrations were calculated using trichromatic equations for dinoflagellates (Jeffrey and Humphrey 1975) and normalized to both surface area and symbiont cells.

Total biomass was measured from the difference in dried (60 °C) and burned (4 h at 450 °C) masses of an aliquot of tissue slurry, and the ash-free dry weight of biomass was expressed as mg biomass cm^{-2}. Total lipid biomass (hereafter, lipids) was measured by lyophilizing a subsample of the coral slurry (host + symbiont) for 12 h, and extracting lipids from the freeze-dried tissue in 2:1 chloroform:methanol, following (Schoepf et al. 2013). The lipid extract was filtered through a GF/F filter (0.7 μm), washed with 0.88% KCl, followed by 100% chloroform and 0.88% KCl washes, evaporated to dryness under nitrogen gas (5.0 purity grade), and quantified gravimetrically on a microbalance. Carbohydrates were determined spectrophotometrically using the phenol-sulfuric acid method with glucose as a standard (Dubois et al. 1956). Total soluble and insoluble protein (hereafter, proteins) was determined by adding 0.1 M NaOH to the tissue slurry, heating (90 °C for 1 h), and using the bicinchoninic acid method (Pierce BCA Protein Assay Kit, Thermo Fisher Scientific) with a bovine serum albumin standard. The equivalent energetic value of biomass (i.e., energetic content) was determined by summing the specific enthalpy of combustion (kJ g^{-1}) lipids (−39.5 kJ g^{-1}), proteins (−23.9 kJ g^{-1}), and carbohydrates (−17.5 kJ g^{-1}) biomass (Gnaiger and Bitterlich 1984). Biomass energy reserves (lipids, carbohydrates, proteins) and energy content were each normalized to skeletal surface area and tissue AFDW.

Statistical analyses

Studies of coral physiology commonly standardize response variables to either skeletal area or biomass units (e.g., dry weight, protein) (Edmunds and Gates 2002). In scleractinian corals, tissue biomass can vary across the surface of individual coral colonies (Oku et al. 2002) and among colonies differing in size (Anthony et al. 2002). In some cases, normalizing physiological metrics to a quantity reflecting the amount of live material (i.e., biomass) may be preferable (Edmunds and Gates 2002) in order to account for effects of colony size or if metrics are not rate-limited by metabolite flux across coral tissues (e.g., respiration, photosynthesis). However, the mass of tissue energy reserves has been normalized to skeletal surface area (Anthony et al. 2002), and sometimes to biomass (Grottoli et al. 2004), with one recent outcome being that the trends as a function of pCO_2 treatment conditions are inconsistent (Schoepf et al. 2013; Hoadley et al. 2015). In order to evaluate treatment effects on coral biomass and calcification, and address the potential role of normalization (i.e., surface area *vs.* grams of dry weight) in the interpretation of treatment effects, we took the following approach. First, we tested the broad hypothesis that corals responded to treatments by using a multivariate principal component (PC) analysis that included coral calcification and biomass metrics normalized to either surface area or biomass. This approach provided a test of the overall treatment effect without inflated Type I error rate. Second, to evaluate which variables were most influential in driving multivariate effects, we applied univariate hypothesis tests on individual metrics to determine where treatment effects existed.

A principal component analysis (PCA) using a scaled and centered correlation matrix was used to test the relationship among net calcification, total biomass, tissue reserves and energy content

among data normalization approach (area-normalized vs. biomass-normalized response variables) and experimental treatments. The PCA data matrix included those fragments where all tissue biomass metrics and calcification had been measured (n = 4 fragments tank^{-1}); total biomass from AFDW (mg cm^{-2}) was included in both data matrices. The multivariate relationship between the two principal components (PC) explaining the greatest variance (PC1 and PC2) was graphically examined for area- and biomass-normalized response variables. Correlations between PCs and response variables were tested using Pearson's correlation coefficient using cor.test in *R*. To interpret treatments effects on PCs, component loadings with eigenvalues > 1.0 were tested to meet assumptions of ANOVA and examined using linear mixed effect models.

Analyses of seawater carbonate chemistry among replicate treatment tanks were examined using separate one-way ANOVAs with tank as a predictor and pCO_2, pH_T and A_T as explanatory variables. pCO_2 and light effects on biological response variables and multivariate PCs were analyzed using a linear mixed-effect model in the *lme4* package in *R* (Bates et al. 2015). pCO_2 and light treatments were treated as fixed effects, colony as a random effect (1|Colony), and tank as a random effect nested within pCO_2 × light treatment (1|Treatment:Tank). The decision to retain or exclude random effects in models was determined by sequentially dropping random effects and performing likelihood ratio tests among models. Assumptions of normality and homoscedasticity of response variables and principal components were confirmed by graphical analysis of residuals; data transformations were applied when assumptions were violated. ANOVA tables were generated for fixed effects using Type II sum of squares with Satterthwaite degrees of freedom using *lmerTest* (Kuznetsova et al. 2016). Significant interactive effects (p <

0.05) were examined by least-square means with a Tukey adjustment in the *lsmeans* package (Lenth 2016). All analyses were performed using *R* version 3.2.1 (R Core Team 2016). Raw data and code to reproduce this work is archived at Dryad (doi.org/10.5061/dryad.5vg70) (Wall et al. 2017a).

Results

Treatment conditions

Experimental treatments were precisely regulated at target levels (Table 2.2). Mechanical issues in two replicate HL–HCO_2 tanks towards the end of the experiment led to the *a priori* removal of these tanks and constituent corals from further analyses. Therefore, final replication for HL–HCO_2 treatments was four tanks per treatment and for all other treatments, six. Corals were maintained under mean pCO_2 treatments of 435 ± 8 µatm pCO_2 (ACO_2) and 957 ± 30 µatm pCO_2 (HCO_2) equivalent to a pH_T of 8.00 ± 0.01 and 7.71 ± 0.01 (± SE, n = 84 and 69) (Table 2.2). Seawater treatments differed in pCO_2 ($p < 0.001$) and pH_T conditions ($p < 0.001$) and A_T was not affected by CO_2-treatment ($p = 0.110$). pCO_2 and pH_T did not differ among replicate CO_2-treatment tanks ($p \geq 0.060$).

Multivariate response analysis

Complete outputs from all statistical models can be found in Appendix Table 2.S1 – 2.S4; summarized model outputs are displayed in Table 2.3. Two principal components with eigenvalues > 1.0 explained 62% and 72% of observed variance for area- and biomass-normalized variables, respectively (Table 2.3; Appendix Table 2.S1). Graphical inspection of PC-biplots for area-normalized responses showed poor separation according to experimental

treatments (Figure 2.1*a*), and PC1 and PC2 were not affected by light or pCO_2 ($p \geq 0.114$) (Table 2.3; Appendix Table 2.S1). Area-normalized PC1 (41.0% variance explained) was positively correlated with all responses ($p < 0.001$), except calcification ($p = 0.105$). PC2 negatively correlated with lipids and energy content ($p \leq 0.008$) and positively correlated with all other metrics ($p \leq 0.019$). Conversely, PC-biplots for biomass-normalized responses showed the greatest degree of divergence between ambient and high pCO_2-treatments along PC2 (Figure 2.1*b*), and PC2 was affected by CO_2 treatment ($p = 0.028$) (Table 2.3). PC1 was not affected by light or pCO_2 ($p \geq 0.269$) (Table 2.3). Biomass-normalized PC2 was positively correlated with lipids and tissue energy content ($p < 0.001$), and negatively correlated with calcification ($p = 0.015$) (Figure 2.1*b*). Hence, elevated pCO_2 conditions had significant effects on corals when skeletal and biomass energy reserve metrics were normalized to tissue biomass, and pCO_2 treatments best explained the opposing relationship of biomass quality (lipids, energy content) and calcification.

Net calcification rates, symbiont densities, and chlorophylls

pCO_2 and light treatments had no effect on net calcification rates normalized to skeletal area ($p \geq 0.605$; Figure 2.2*a*) or biomass ($p \geq 0.210$; Figure 2.2*c*) (Table 2.3; Appendix Table 2.S2, 2.S3). However, biomass-normalized calcification tended to be 15% higher at high light relative to low light conditions. Symbiont cell density cm^{-2} was not affected by treatments ($p \geq 0.124$) (Table 2.3, Figure 2.2*d*), but chlorophyll *a* and c_2 cm^{-2} declined by 28% and 25% at high light relative to low light treatments ($p < 0.001$) (Table 2.3, Figure 2.2*e*). However, photopigment concentrations per symbiont cell were not affected by treatments ($p \geq 0.109$) but tended to be lower under high light conditions (Table 2.3, Figure 2.2*f*).

Tissue energy reserves and normalization approaches

Treatments had no effect on total biomass cm^{-2} ($p \geq 0.210$) (Table 2.3, Figure 2.2*b*) or protein per gram of dry coral tissue (gdw^{-1}) ($p \geq 0.415$) (Table 2.3, Figure 2.3*a*). Carbohydrate gdw^{-1} increased 15% in corals at high light relative to low light conditions ($p = 0.040$) (Figure 2.3*b*), and corals exposed to 957 µatm pCO_2 had 15% less lipid gdw^{-1} ($p = 0.040$) (Figure 2.3*c*) and 14% less biomass energy content gdw^{-1} ($p = 0.041$) than corals at 435 µatm pCO_2 (Figure 2.3*d*) (Table 2.3; Appendix Table 2.S3).

The effects of treatments on area-normalized energy reserves differed from effects on biomass-normalized energy reserves. No effect of pCO_2, light, or their interaction was observed for carbohydrate cm^{-2}, lipid biomass cm^{-2}, or tissue energy content cm^{-2} ($p \geq 0.132$) (Table 2.3, Figure 2.4*b-d*; Appendix Table 2.S2). However, protein biomass cm^{-2} was affected by the interaction of $pCO_2 \times$ light ($p = 0.038$) and light ($p = 0.010$) but not pCO_2 alone ($p = 0.270$) (Table 2.3, Figure 2.4*a*). Mean protein (mg cm^{-2}) was 17 – 23% lower at HL–HCO_2 relative to other treatments (*post hoc*: $p \leq 0.017$) but was not significantly different from the HL–ACO_2 treatment (*post hoc*: $p = 0.157$) (Figure 2.4*a*).

Discussion

OA and light effects on calcification

Our results demonstrate calcification in *Pocillopora acuta* was not affected by pCO_2 (435 and 957 μatm) or light availability (7.5 *vs.* 15.7 mol photons m^{-2} d^{-1}). The lack of an effect of pCO_2 on calcification contrasts with the majority of studies showing OA reduces calcification rates in corals and other marine calcifiers (Kroeker et al. 2010; Chan and Connolly 2013), but is

consistent with previous work showing net calcification in *Pocillopora* spp. is insensitive to elevated pCO_2 ($\leq$ 1,970 µatm pCO_2) (Schoepf et al. 2013; Comeau et al. 2014b, 2014d) (but see [Bahr et al. 2016]). Corals from Kāne'ohe Bay experience significant diel variability in pCO_2 (Drupp et al. 2011) and have been hypothesized to exhibit varying degrees of acclimation or local adaptation to high pCO_2. However, a pan-Pacific collection (including Kāne'ohe Bay) of the congener *Pocillopora damicornis* revealed this species was resistant to elevated pCO_2 effects on calcification across geographic locations (Comeau et al. 2014b). This finding suggests pCO_2 history alone does not completely explain the resistance of *Pocillopora* spp. calcification to OA, but rather a combination of physiological and/or genetic factors may also underpin OA resistance in *P. acuta* and related pocilloporids.

The interactive effects of pCO_2 and light on coral calcification varies among coral species (Suggett et al. 2013; Enochs et al. 2014) and life-history stages (Dufault et al. 2013; Comeau et al 2013b), and may depend on the mechanism and/or rate by which species calcify (Rodolfo-Metalpa et al. 2011; Comeau et al. 2013a, 2014d) as well as their capacity to regulate internal pH (Venn et al. 2013; Allison et al. 2014; Cai et al. 2016; Comeau et al. 2017). While light-availability modulates OA effects on calcification in some corals (Dufault et al. 2013; Suggett et al. 2013; Vogel et al. 2015), meta-analysis reveals the heterogeneous response of coral calcification to declining Ω_{arag} is not well explained by light intensity (Chan and Connolly 2013). The absence of pCO_2 or light effects on *P. acuta* calcification in the current study has also been reported in other corals. For instance, *Porites rus* calcification was similarly unaffected by pCO_2 (400 *vs.* 700 μatm) at 6.2 and 28.7 mol photons m^{-2} d^{-1} (Comeau et al. 2013b), and light availability (3.5 – 30.2 mol photons m^{-2} d^{-1}) did not influence the response of *Porites compressa*

to decreasing Ω_{arag} (2.48 *vs.* 5.05) (Marubini et a. 2001) (Table 2.1). In part, the observation in some corals of light intensity mitigating OA effects on calcification may be linked to light-dependent usage of dissolved inorganic carbon substrates (e.g., HCO_3^- or CO_3^{2-}) in calcification (Comeau et al. 2013a) and/or stimulatory effects of light availability on symbiont photosynthesis, coral metabolism, ion regulation, and the synthesis of organic matrix at the calcifying surface (Muscatine et al. 1981; Gattuso et al. 1999; Muscatine et al. 2005). In the present study, the lack of pCO_2 effects on *P. acuta* calcification at both light treatments suggests beneficial effects of light availability on coral performance (Suggett et al. 2013) were realized at both light-saturating treatments (7.5 *vs.* 15.7 mol photons m^{-2} d^{-1}), or this coral species possesses mechanisms enabling it to maintain comparable rates of calcification at both 435 and 957 µatm pCO_2, potentially through pH regulation at the site of calcification (Holcomb et al. 2014).

The sensitivity of coral calcification to OA may reflect the differential capacity of coral species to up-regulate extracellular pH in the calcifying fluid at the site of calcification (Venn et al. 2011; McCulloch et al. 2012; Holcomb et al. 2014; Cai et al. 2016) Ca^{2+}/H^+ ATPases exchange ions across the calicoblastic epithelia to produce locally high pH in the calcifying fluid (ca. 0.5 – 2.0 pH units above external seawater) (Ries 2011; Venn et al. 2011; Cai et al. 2016). Alkalinization of the calcifying fluid shifts the chemical equilibrium of dissolved inorganic carbon in favor of CO_3^{2-} and facilitates the diffusion of molecular CO_2 into the calcifying fluid (Allison et al. 2014), thereby increasing [DIC] and Ω_{arag} (i.e., 15 – 22) and promoting the precipitation of aragonite (McCulloch et al. 2012; Cai et al. 2016). Under OA, a higher H^+ concentration in seawater may challenge the capacity for corals to export H^+ from tissues (Jokiel 2011), which is hypothesized to increase the metabolic costs of up-regulating calcifying fluid pH

and Ω_{arag} and cause reductions in $CaCO_3$ precipitation rates (Ries 2011). On the other hand, corals can compensate for declining Ω_{arag} in the calcifying fluid by increasing the incorporation of organic matrix proteins into the skeleton (Tambutté et al. 2015) which act to increase the nucleation of aragonite crystals (Mass et al. 2013). A more organic-rich skeleton may reduce the sensitivity of corals (and other marine calcifiers) to OA by reducing the free energy required for calcification (Spalding et al. 2017), although the synthesis of organic skeletal material requires significantly more energy than inorganic $CaCO_3$ production (Palmer 1992) and additional energy inputs may be necessary. In corals, calcification accounts for 30% of energy demand (Allemand et al. 2011). Thus, thermodynamically unfavorable conditions (low Ω_{arag}) causing greater energetic expenditures for calcifying fluid regulation and/or organic matrix synthesis (Von Euw et al. 2017) may additively influence the capacity of corals to maintain high calcification rates, or otherwise impact their energy balance, under OA.

OA and light effects on coral biomass

In agreement with previous laboratory and field studies (Wall et al. 2014; Noonan et al. 2016) (but see [Anthony et al. 2008]), elevated pCO_2 did not lead to coral bleaching or reductions in symbiont densities and/or chlorophyll concentration in low or high light treatments. Instead, corals photoacclimated (Hoogenboom et al. 2009) to increasing light levels by reducing concentrations of chlorophylls (*a* and c_2 cm^{-2}), although without appreciable loss of symbiont cells. However, exposure to 957 µatm pCO_2 altered the composition of *P. acuta* biomass relative to corals maintained at 435 µatm pCO_2 regardless of light conditions. Declining lipid biomass at high pCO_2 suggests lipid reserves were either catabolized to meet energetic demands (Vidal-Dupiol et al. 2013) and/or lipid-precursors were allocated to processes other than the formation

of lipid biomass. Under OA conditions corals may require greater energy investments in the process of calcification in order to maintain high rates of aragonite precipitation (Allemand et al. 2011; Von Euw et al. 2017). For instance, greater energy inputs from dissolved nutrients (Holcomb et al. 2010) and heterotrophic feeding (Edmunds 2011) can lessen negative effects of high pCO_2 ($\leq$ 830 μatm) on calcification in some corals. While heterotrophic food sources available to corals in the present study were restricted (<100 μm, sand-filtrated seawater), it is likely that natural nutrient sources in seawater (e.g., dissolved inorganic and organic nutrients, pico- and nanoplankton, small zooplankton) supplemented symbiont-derived nutrition (Houlbrèque and Ferrier Pagès 2009). The ability for corals to increase heterotrophic feeding in response to changes in photoautotrophic nutrition or energy demand contributes to physiological resilience (Grottoli et al. 2006), yet the capacity for many corals, including *P. acuta,* to be nutritionally flexible under normal and stressed physiological states has yet to be quantified. Recent evidence suggests some corals may increase rates of heterotrophic feeding in response to elevated pCO_2 (Towle et al. 2015). However, *in situ* elevated pCO_2 reduces the abundance of zooplankton on corals reefs (Smith et al. 2016) and may reduce heterotrophic nutrition and/or increase metabolic costs associated with prey capture. Therefore, while a combination of zooplanktivory and biomass catabolism may be employed by corals as an acclimation response to physiological stress (Grottoli et al. 2004, 2006)—including elevated pCO_2 (Towle et al. 2015)—OA effects on coral biomass (this study) and zooplankton availability (Smith et al. 2016) may negatively impact coral performance and their response to physiological challenges (Anthony 2006; Thornhill et al. 2011; Hughes and Grottoli 2013).

In corals, tissue growth is sensitive to changing resource availability and physiological stress (Stimson 1987; Fitt et al. 2000; Anthony et al. 2002). Under these conditions, skeletal growth may come at the expense of reduced tissue growth (Anthony et al. 2002) and biomass may be broken down to support metabolism (Grottoli et al. 2004). Consistent with this hypothesis are observations that low pH (7.4 – 7.7) causes an upregulation of coral genes involved in lipolysis and beta-oxidation pathways, suggesting tissue reorganization and the catabolism of fatty-acid reserves (Kaniewska et al. 2012; Vidal-Dupiol et al. 2013). Such changes in gene expression could explain the reduction in lipid biomass observed here, as well as the negative relationship between elevated pCO_2 and coral tissue biomass (*Pocillopora damicornis*, [Comeau et al. 2013c]) and lipids cm^{-2} (*Acropora millepora*, *Montipora monasteriata* [Hoadley et al. 2015]). In contrast, *Porites rus* and *Acropora pulchra* tissue biomass (Comeau et al. 2013c, 2014a) and *A. millepora* and *P. damicornis* lipids gdw^{-1} (Schoepf et al. 2013) displayed a positive parabolic relationship with elevated pCO_2. These effects may be explained by elevated [DIC] stimulating symbiont productivity and carbon translocation (Brading et al. 2011; Suggett et al. 2013; Tremblay et al. 2013) with downstream effects on biomass synthesis. Alternatively, supplemental heterotrophic feedings (Schoepf et al. 2013) may overcome OA-induced energy deficits and replenish lipid reserves (Towle et al. 2015). Together, these examples illustrate that pCO_2 is likely to have non-linear and heterogeneous effects on coral biomass, as has been noted for OA effects on calcification (Chan and Connolly 2013; Comeau et al. 2014d). Nonetheless, our finding that lipid biomass and energy content gdw^{-1} declined in *P. acuta* following one month at 957 μatm pCO_2 supports the hypothesis that OA affects energetic requirements in corals, potentially related to metabolic costs or the acquisition and allocation of resources.

At the organismal level, elevated pCO_2 (< 2,000 μatm) has negligible effects on aerobic respiration (Comeau et al. 2017), however, elevated pCO_2 can elicit compensatory changes at the cellular level that affect energy allocation, gene expression, and physiological resilience (Kanieska et al. 2012; Vidal-Dupiol et al. 2013). For instance, sea urchin larvae responded to OA with a 30% increase in the metabolic energy allocated to protein synthesis and ion transport (Pan et al. 2015). Such flexibility in energy allocation may be critical for organisms to respond to environmental stress when metabolic demands exceed metabolic capacity. In the present study, it is uncertain whether longer duration exposures to 957 μatm pCO_2 would result in further reductions (or stabilization) of *P. acuta* lipid biomass and eventually cause skeletal and biomass growth to decline. In any case, decreased biomass quality may have wide reaching effects on coral performance, including the susceptibility to post-bleaching mortality and reproduction (Anthony et al. 2002; Grottoli et al. 2004; Harii et al. 2010). Therefore, unraveling the long-term consequences of OA on biomass energetics at the organismal and cellular level should be a priority for future research.

Previous studies have observed mixed responses of total biomass to high pCO_2. For example, biomass was not affected by pCO_2 (≤ 741 μatm) in four Indo-Pacific corals (including *P. damicornis*) (Schoepf et al. 2013), and *P. rus* total biomass at two irradiances was insensitive to changes in pCO_2 (≤ 1,100 μatm) (Lenz and Edmunds 2017). However, high pCO_2 has been shown to increase total biomass in some coral species when maintained under high light conditions (Comeau et al. 2013c, 2014a). In the present study, total biomass (mg AFDW cm^{-2}) was not affected by treatments, yet area-normalized protein (a common proxy for biomass; [Edmunds and Gates 2002]) was reduced ~ 20% under 957 μatm pCO_2 and 15.7 mol photons m^{-2}

d^{-1}. Together, high light and high pCO_2 may interfere with aspects of protein metabolism (Edmunds and Wall 2014) or turnover (Pan et al. 2015) in *P. acuta* manifesting in reduced protein per skeletal surface (Edmunds et al. 2013; Hoadley et al. 2015). However, in our study the total organic fraction of *P. acuta* biomass (i.e., AFDW cm^{-2}) appears less sensitive to pCO_2 and light effects, potentially due to dynamic changes in the concentration of other tissue macromolecules aside from proteins.

Finally, the interpretation of responses to OA effects was dependent on the approach used to normalize response variables. Multivariate tests on biomass-normalized responses revealed significant effects of pCO_2 on *P. acuta* with an opposing relationship between net calcification rates and biomass quantity and quality (i.e., per cent lipid and energy content). This finding was supported by univariate tests where pCO_2 reduced biomass lipid and energy content. Conversely, pCO_2 did not affect responses normalized to skeletal area (except for protein biomass). Area- and biomass-normalizations are often used interchangeably, yet these normalizations are not equivalent due to allometric growth in corals and variability in the quality and quantity of tissue biomass over the coral skeleton (Anthony et al. 2002; Oku et al. 2002). Such factors may confound area-normalized physiological responses not directly related to skeletal area (Edmunds and Gates 2002). Indeed, the differences observed here between area- and biomass-normalized metrics suggest disparate trends in pCO_2 effects on biomass observed in other studies may in part reflect normalization approaches (Schoepf et al. 2013; Hoadley et al. 2015) and/or sampling techniques (e.g., tip subsampling *vs.* whole fragment tissues). We recommend future studies consider the significance of normalization approaches in representing physiological data (Edmunds and Gates 2002; Cunning and Baker 2014), and suggest that energy reserve-specific

metrics be normalized to biological units (i.e., living tissue biomass) so that the physiological implications of environmental change on coral tissues may be clarified without the potential confounding effects of skeletal area.

This study demonstrates that one-month exposure to OA conditions predicted for the year 2100 did not affect *Pocillopora acuta* calcification rates, but elevated pCO_2 reduce lipid biomass gdw^{-1} and energy content gdw^{-1} and interacted with high light to reduce protein cm^{-2}. Considering the significance of lipid biomass for coral performance (e.g., post-stress physiology, reproduction), reduction in lipid biomass (and biomass energy content) may negatively affect *P. acuta* and reduce its physiological resilience to rising seawater temperatures. Our findings raise a testable hypothesis for *P. acuta*: that maintenance of present-day calcification rates under OA incurs an energetic cost, which is met through catabolism of, or diversion of energy that otherwise would have been stored as, tissue lipids. Finally, we report the interpretation of pCO_2 effects on tissue biomass were dependent on whether energy reserves were normalized to tissue biomass or skeletal area. We propose data normalization to be an overlooked aspect of coral physiology that may be contributing to the observed variance in OA effects on corals.

Funding

This work was funded by grants from the Linnaean Society of New South Wales, the International Phycological Society, the Australian Wildlife Society and a Fulbright Scholarship to R.A.B.M. C.B.W. was supported by an UH Graduate Opportunity Grant, the UH Edmondson Research Fund, and Environmental Protection Agency (EPA) STAR Fellowship Assistance Agreement (FP-91779401-1). The views expressed in this publication have not been reviewed or

endorsed by the EPA and are solely those of the authors. R.C. was supported by a NSF Postdoctoral Fellowship in Biology (NSF-DBI-1400787). This is HIMB contribution number 1702, and School of Ocean and Earth Science and Technology (SOEST) contribution number 10242.

Acknowledgements

Biological collections were performed in accordance with permitting guidelines of the state of Hawai‘i Department of Land and Natural Resources Division of Aquatic Resources under Special Activity Permit 2015-8. We thank H. Putnam, A. Moran, M. Donahue, and A. Grottoli for insightful discussions, J. Davidson for laboratory and logistical support, P.J. Edmunds, E.A. Lenz, and three anonymous reviewers for comments on an earlier version of the manuscript. This manuscript is dedicated to the memory of our friend and colleague Dr. Paul Jokiel.

Table 2.1. Summary of selected works testing pCO_2 and light treatments on coral calcification using single irradiances (*top panel*) and multiple irradiances (*lower panel*)

Species	Life stage	μatm pCO_2	Daily PAR	OA effect on growth	Reference
pCO_2 effects under single light level					
Porites astreoides	recruit	480, 560, 720	0.5	50 – 78% decline skeletal extension	Albright et al. 2008
Favia fragum	recruit	421, 1311	2.7	37% decline corallite mass	Drenkard et al. 2013
Astrangia poculata	adult	390, 780	3.3	66% decline G_N	Holcomb et al. 2013
Acropora cervicornis	adult	385, 800	5.8	14% decline G_N	Towle et al. 2015
Stylophora pistillata	adult	385, 1904, 3970	7.2	18% decline G_N	Krief et al. 2010
Stylophora pistillata	adult	460, 760	15.1	26% decline G_N	Reynaud et al. 2003
Porites spp.	adult	411, 804	25.9	no effect of OA	Edmunds et al. 2012
Porites rus	adult	411, 804	25.9	28% decline G_N	Edmunds et al. 2012
pCO_2 effects under multiple light levels					
Pocillopora damicornis	recruit	490, 900	1.0, 3.5, 9.5	0%, 32%, 12% decline in G_N under OA with increasing light	Dufault et al. 2013
Acropora millepora	adult	427, 1073	1.5, 6.5	no light × pCO_2 interaction; 48% and 144% decline in G_N and G_D under OA	Vogel et al. 2015
Porites compressa	adult	336, 641	4.0, 6.0, 12.6, 23.3	0%, 44%, 27%, and 10% decline in G_N under OA with increasing light	Marubini et al. 2001
Acropora horrida	adult	390, 725	4.3, 17.3	50% (LL) and 10% (HL) decline in G_L under OA; 40% decline in G_D at LL and HL under OA	Suggett et al. 2013
Porites cylindrica	adult	390, 725	4.3, 17.3	80% (LL) and 50% (HL) decline in G_L under OA; 80% decline in G_D at LL and HL under OA	Comeau et al. 2014a
Acropora pulchra	adult	400, 750, 1100	4.3, 18.7	no effect of OA; 55% decline G_N at LL	Comeau et al. 2014a
Porites rus	adult	375, 710	6.2, 28.8	no effect of OA or PAR	Comeau et al. 2013a

OA = ocean acidification conditions of low–pH, high–pCO_2, and/or low aragonite saturation state (Ω_{arag}); PAR = photosynthetically active radiation; Daily PAR = mol photons m^{-2} d^{-1} integrated over the light period in the reference study; recruit = newly settled or post-settlement juvenile corals; adult = fragments collected from adult colonies; G_N = net calcification; G_L = calcification in light; G_D = calcification in dark; LL = low–light; HL = high–light.

Table 2.2. Summary of environmental conditions in the experimental treatment tanks between 16 December 2014 and 16 January 2015. Seawater total alkalinity (A_T), pH on the total scale (pH_T), along with seawater temperature (ca. 25 °C) and salinity (ca. 34) were used to calculate the partial pressure of carbon dioxide (pCO_2), concentrations of dissolved inorganic carbon species, and the aragonite saturation state (Ω_{arag}) using the package *seacarb* in *R*.

Treatment	PAR	pH_T	A_T (μmol kg^{-1})	pCO_2 (μatm)	HCO_3^- (μmol kg^{-1})	CO_3^{2-} (μmol kg^{-1})	Ω_{arag}
LL–ACO_2	7.5	7.99±0.01 (42)	2177±3 (42)	451±11 (42)	1733±8 (42)	179±3 (42)	2.84±0.06 (42)
LL–HCO_2	7.5	7.71±0.02 (41)	2184±4 (41)	957±39 (41)	1917±12 (41)	108±5 (41)	1.72±0.07 (41)
HL–ACO_2	15.7	8.01±0.01 (42)	2179±3 (42)	420±11 (42)	1714±9 (42)	187±4 (42)	2.97±0.06 (42)
HL–HCO_2	15.7	7.71±0.02 (28)	2184±4 (28)	957±47 (28)	1920±12 (28)	106±5 (28)	1.69±0.08 (28)

LL–ACO_2 = Low light–Ambient pCO_2; LL–HCO_2 = Low light–High pCO_2; HL–ACO_2 = High light–Ambient pCO_2; HL–HCO_2 = High light–High pCO_2; PAR = photosynthetically active radiation, integrated over 12 h (mol photons m^{-2} d^{-1}); n = 6 replicate tanks $treatment^{-1}$, except HL–HCO_2 n = 4 replicate tanks. Values are mean ± SE (n).

Table 2.3. Summary of *p*-values for pCO_2 and light effects on principal component loadings and response variables normalized to skeletal area and tissue biomass.

Response variables	*Area-normalized (cm^{-2})*			*Biomass-normalized (gdw^{-1})*		
	Effect			*Effect*		
	pCO_2	Light	pCO_2 × Light	pCO_2	Light	pCO_2 × Light
Multivariate models						
PC1	0.493	0.624	0.856	0.689	0.269	0.777
PC2	0.114	0.562	0.359	**0.028**	0.718	0.919
Univariate models						
calcification	0.605	0.793	0.861	0.586	0.277	0.879
total biomass	0.950	0.210	0.677	--	--	--
proteins	0.270	**0.010**	**0.038**	0.415	0.702	0.492
carbohydrates	0.351	0.505	0.132	0.342	**0.040**	0.297
lipids	0.145	0.751	0.683	**0.040**	0.436	0.917
energy content	0.201	0.543	0.891	**0.041**	0.445	0.952
symbiont cells	0.338	0.124	0.483	--	--	--
chlorophyll *a*	0.993	**<0.001**	0.144	--	--	--
chlorophyll c_2	0.961	**<0.001**	0.114	--	--	--
†chlorophyll *a* $cell^{-1}$	0.886	0.109	0.587	--	--	--
†chlorophyll c_2 $cell^{-1}$	0.765	0.217	0.449	--	--	--

Summarized output from linear mixed effect models; full models can be found in the electronic supplemental material. † = photopigment concentrations normalized to symbiont cell; PC = principal component; bold *p*-values represent significant effects < 0.05; dashed lines are present where responses were not measured.

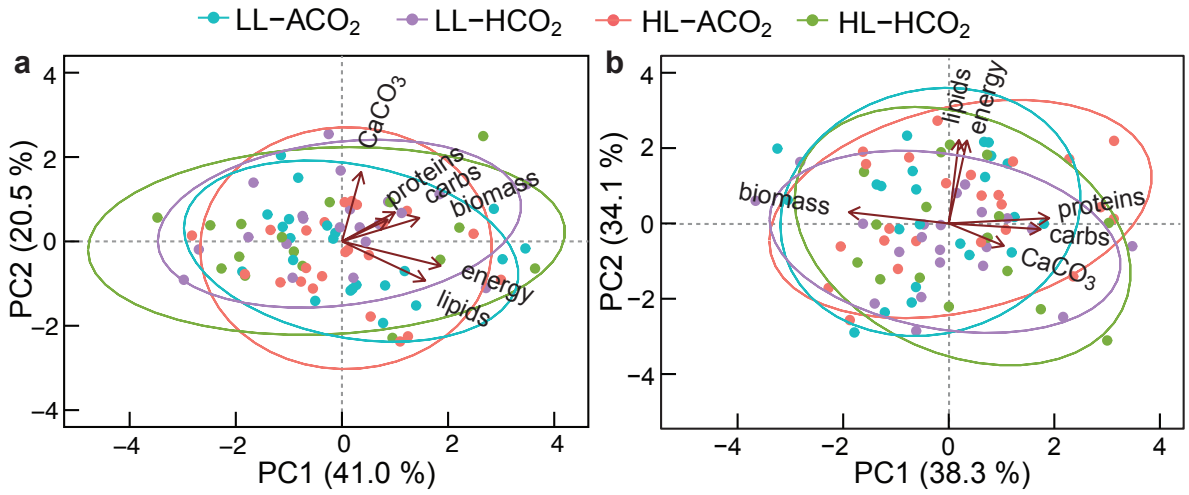

Figure 2.1. Principal component analyses (PCA) for energy reserves and net calcification normalized to (**a**) skeletal surface area (cm^{-2}) and (**b**) tissue biomass (gdw^{-1}), with total biomass (mg AFDW cm^{-2}) present in each data matrix. Axis values in parentheses represent proportion of total variance associated with the respective PC. Arrows represent correlation vectors for response variables, and ellipses represent 90% point density according to treatments. Treatment details can be found in *Table 2.2*.

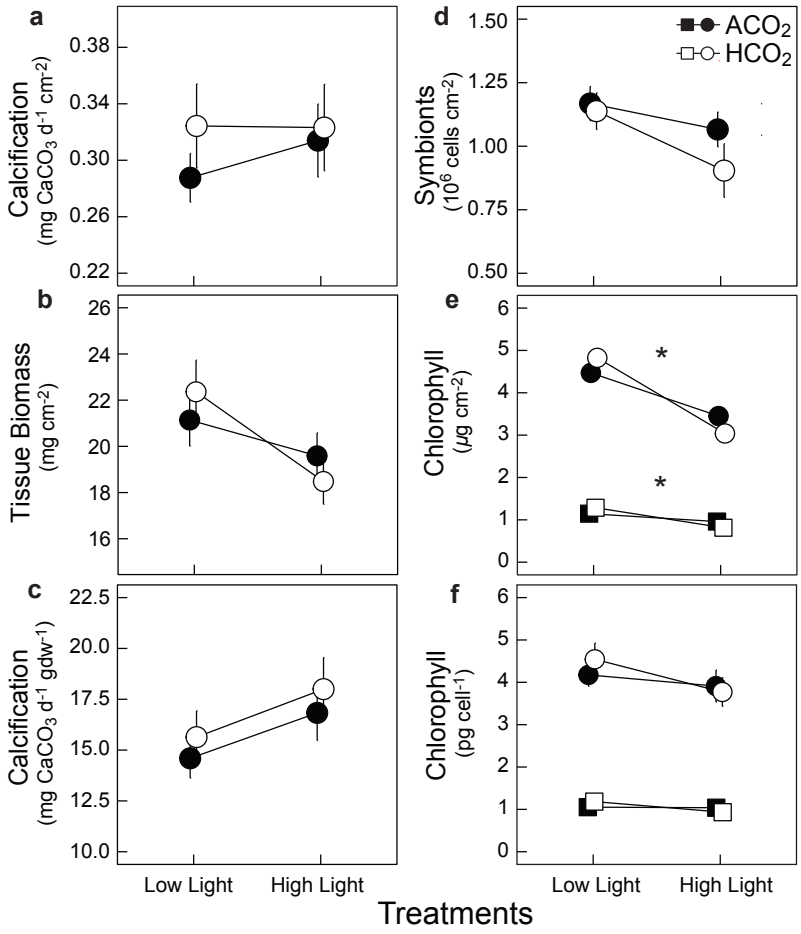

Figure 2.2. Net calcification, total biomass, photopigment concentrations, and symbiont densities in *Pocillopora acuta* corals exposed to light treatments (7.5 and 15.7 mol photons m^{-2} d^{-1}) and ambient pCO_2 (ACO_2) and high pCO_2 (HCO_2) (*Table 2.1*). (**a**) Area-normalized net calcification rates, (**b**) total tissue biomass, (**c**) biomass-normalized net calcification rates, (**d**) symbiont cell densities, and (**e**) chlorophyll *a* (*circles*) and chlorophyll c_2 (*squares*) densities normalized to skeletal area and (**f**) symbiont cells. Values displayed are means ± SE; n = 28 ($HL–HCO_2$) and n = 39 – 41 (all other treatments), except (**d**, **f**) n = 16 ($HL–HCO_2$) and n = 24 (all other treatments). Asterisks indicate a statistical difference ($p < 0.05$) between light treatments.

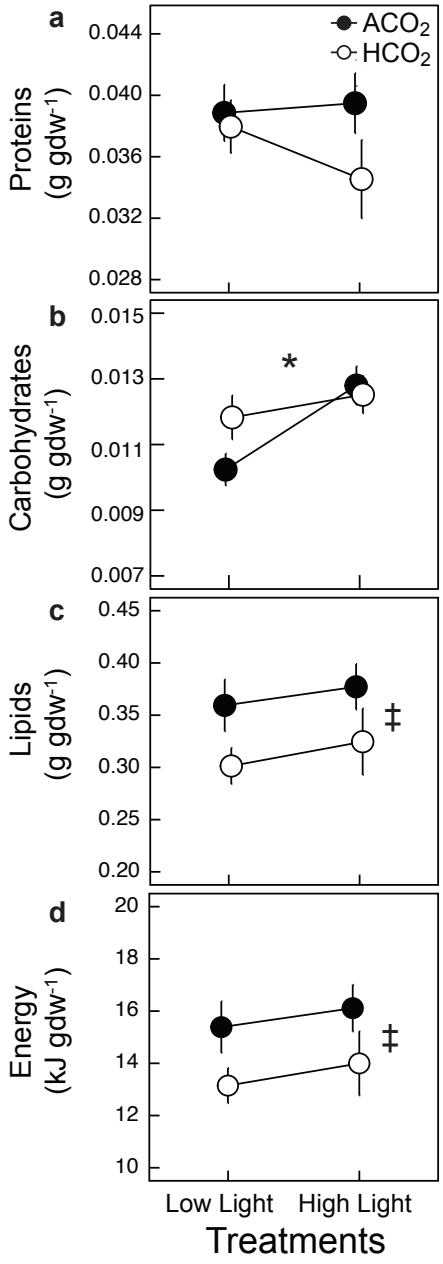

Figure 2.3. Biomass-normalized (gdw^{-1}) (**a**) proteins, (**b**) carbohydrates, (**c**) lipids, and (**d**) tissue energy content in *Pocillopora acuta* corals to light treatments (7.5 and 15.7 mol photons m^{-2} d^{-1}) and ambient pCO_2 (ACO_2) and high pCO_2 (HCO_2) (*Table 2.1*). Values displayed are means ± SE; n = 16 – 24 for lipid biomass and energy content, for other variables n = 28 (HL–HCO2) and n = 41 – 42 (all other treatments). Symbols indicate statistical differences ($p < 0.05$) between light (*) or pCO_2 (‡) treatments.

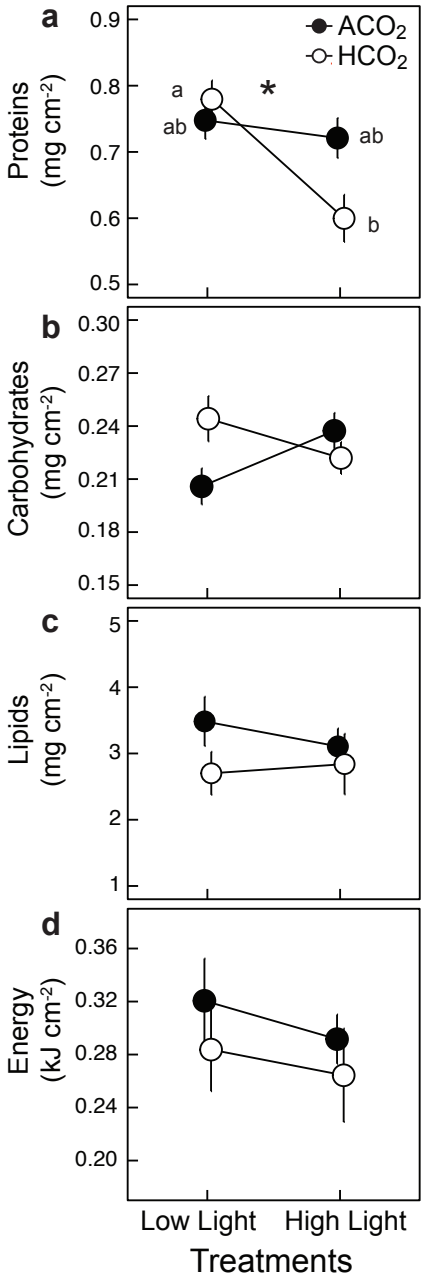

Figure 2.4. Area-normalized (cm^{-2}) (**a**) protein, (**b**) carbohydrates, (**c**) lipid biomass, and (**d**) tissue energy content in *Pocillopora acuta* corals exposed to ambient pCO_2 (ACO_2) and high pCO_2 (HCO_2) and light treatments (7.5 and 15.7 mol photons m^{-2} d^{-1}) (*Table 2.1*). Values displayed are means ± SE; n = 16 – 24 for lipid biomass and energy content, for other variables n = 28 (HL–HCO_2) and n = 41 – 42 (all other treatments). Asterisks indicate a statistical difference ($p < 0.05$) between light treatments, and *letters* indicate results of post-hoc multiple comparisons where pCO_2 × light interactions were observed.

CHAPTER 3:

SPATIAL VARIATION IN THE BIOCHEMICAL AND ISOTOPIC COMPOSITION OF CORALS DURING BLEACHING AND RECOVERY

Abstract

Ocean warming and the increased prevalence of coral bleaching events threaten coral reefs. However, the biology of corals during and following bleaching events under field conditions is poorly understood. We examined bleaching and post-bleaching recovery in *Montipora capitata* and *Porites compressa* corals that either bleached or did not bleach during a 2014 bleaching event at three reef locations in Kāneʻohe Bay, Oʻahu, Hawaiʻi. We measured changes in chlorophylls, tissue biomass, and nutritional plasticity using stable isotopes ($\delta^{13}C$, $\delta^{15}N$). Coral traits showed significant variation among periods, sites, bleaching conditions and their interactions. Bleached colonies of both species had lower chlorophyll and total biomass, and while *M. capitata* chlorophyll and biomass recovered three months later, *P. compressa* chlorophyll recovery was location-dependent and total biomass of previously bleached colonies remained low. Biomass energy reserves were not affected by bleaching, instead *M. capitata* proteins and *P. compressa* biomass energy and lipids declined over time and *P. compressa* lipids were site-specific during bleaching recovery. Stable isotope analyses did not indicate increased heterotrophic nutrition in bleached colonies of either species, during or after thermal stress. Instead, mass balance calculations revealed variations in $\delta^{13}C$ values reflect biomass compositional change (i.e., protein:lipid:carbohydrate ratios). Observed $\delta^{15}N$ values reflected spatiotemporal variability in nitrogen sources in both species, and in *P. compressa,* bleaching effects on symbiont nitrogen demand. These results highlight the dynamic responses of corals to natural bleaching and recovery and identify the need to consider the influence of biomass composition in the interpretation of isotopic values in corals.

Introduction

Scleractinian corals in association with dinoflagellate endosymbiont algae (Family: Symbiodiniaceae, formerly *Symbiodinium* spp.) (LaJeunesse et al. 2018) are important primary producers on coral reefs, which through biogenic processes create the complex calcium carbonate framework of the reef milieu. The coral-algae symbiosis can be disturbed under environmental stress, leading to the reduction of symbiotic algae in coral tissue (i.e., coral bleaching) (Weis 2008). Depending on the severity or duration of stress, bleaching causes coral mortality, although some corals survive and recover their symbionts post-bleaching (Fitt et al. 1993; Cunning et al. 2016). The strength and frequency of bleaching events has increased over the last three decades from a combination of progressive seawater warming (Heron et al. 2016) and climatic events (i.e., ENSO) (Hughes et al. 2017). It is therefore critical to advance an understanding of the environmental conditions and biological mechanisms that underpin the physiological resilience of corals to thermal stress.

The resistance and recovery of corals from bleaching stress is influenced by associations with thermally tolerant symbionts (Sampayo et al. 2008), tissue biomass abundance (Thornhill et al. 2011) and energetic quality (i.e., lipid content), and the capacity to maintain positive energy budgets through nutritional plasticity (Anthony et al. 2009). Coral nutrition is largely supported by fixed-carbon derived from endosymbiont algae, however, particle feeding (Mills et al. 2004), plankton capture (Sebens et al. 1998), and the uptake of dissolved compounds from seawater and sediments (Mills and Sebens 2004; Grover et al. 2006) (collectively, 'heterotrophy') can account for < 15 – 50% of energy demands (Porter 1976; Houlbrèque and Ferrier-Pagès 2009) and > 100% of respiratory carbon demand in bleached corals (Grottoli et al. 2006; Palardy et al. 2008;

Levas et al. 2016). Facultative shifts from autotrophic to heterotrophic nutrition are often linked to reduced symbiont photosynthesis in response to periodic light attenuation (i.e., turbidity) and/or environmental stress (Houlbrèque and Ferrier-Pagès 2009). As such, nutritional plasticity is an important acclimatization mechanism shaping the physiological niche of corals (Anthony and Fabricius 2000) and supporting the resilience of reef-building corals to changing environments and resource availability (Grottoli et al. 2006; Ferrier-Pagès et al. 2010; Connolly et al. 2012; Hughes and Grottoli 2013).

Heterotrophic nutrition is a fundamental process in the metabolism and growth of corals (Palardy et al. 2008; Houlbrèque and Ferrier-Pagès 2009; Hughes and Grottoli 2013). In some corals, thermal stress and bleaching results in an increased feeding on zooplankton (Grottoli et al. 2006; Ferrier-Pagès et al. 2010; Hughes and Grottoli 2013; Levas et al. 2013) and suspended particles (Anthony and Fabricius 2000), and stimulates coral uptake of diazotroph-derived nitrogen (Bednarz et al. 2017) and dissolved organic carbon (Levas et al. 2016). Periods of stress or resource limitation, however, do not facilitate shifts towards heterotrophic nutrition in all corals (Anthony and Fabricius 2000; Schoepf et al. 2015); instead, energetic demands are met by the catabolism of energy-rich biomass (i.e., proteins, lipids, carbohydrates) (Fitt et al. 1993; Grottoli et al. 2006; Schoepf et al. 2015). Considering the limited size of biomass reserves, corals capable of increasing the acquisition of heterotrophic energy may experience a fitness advantage during times of stress and symbiosis disruption, as well as increased rates of physiological recovery (Rodrigues and Grottoli 2007; Connolly et al. 2012; Grottoli et al. 2014).

Elevated temperature effects on corals are also mediated by co-occurring environmental factors, including: ultraviolet (UV) (Shick et al. 1996) and photosynthetically active radiation (PAR) (Coles and Jokiel 1977), the concentration (Vega-Thurber et al. 2014) and stoichiometry of dissolved nutrients (e.g., nitrogen, phosphorous) (Wiedenmann et al. 2012), and water motion (Nakamura and van Woesik 2001). For instance, elevated light levels and chronic nutrient loading can exacerbate thermal stress (Coles and Jokiel 1977; Vega-Thurber et al. 2014), while high water motion and seawater turbidity can reduce bleaching severity and mortality (Nakamura and van Woesik 2001; Anthony et al. 2007). In addition, enhanced nutrition from heterotrophic feeding preceding and following thermal stress can replenish lipid biomass (Baumann et al. 2014), reduce bleaching severity and coral mortality (Anthony et al. 2009; Ferrier-Pagès et al. 2010) and promote post-bleaching recovery of the host and symbiont (Marubini and Davies 1996; Connolly et al. 2012). Spatiotemporal variation in abiotic conditions that affect coral performance and resource availability/demand, therefore, can influence coral holobiont response trajectories and outcomes to physiological stress (Hoogenboom et al. 2011; Connolly et al. 2012; Scheufen et al. 2017). Considering reef corals may experience bleaching effects > 12 months following initial thermal stress and well beyond the return of normal tissue pigmentation (Fitt et al. 1993; Baumann et al. 2014; Grottoli et al. 2014; Levitan et al. 2014; Schoepf et al. 2015), it is important to consider the environmental effects and physiological mechanism(s) that facilitate or hinder post-bleaching recovery.

The occurrence of large-scale coral bleaching episodes has been historically rare in the Main Hawaiian Islands, being limited to 1996 (Jokiel and Brown 2004). However, coastal seawater in Hawai‘i is warming (0.02 °C y^{-1}, annual mean 1956–2014; Bahr et al. 2015) and the frequency

and severity of global bleaching events is increasing (Hughes et al. 2017). From September – October 2014, the Hawaiian Archipelago experienced a protracted period of elevated sea surface warming. Degree heating weeks (DHW) for the Main Hawaiian Islands began to accumulate on 15 September, peaking at 7 DHW on 20 October, and declining below < 7 DHW after 08 December (NOAA Coral Reef Watch 2018). Water temperatures (29 – 30.5 °C) (Bahr et al. 2015) exceeded O‘ahu mean summertime maximum temperatures (ca. 28 °C) (Jokiel and Brown 2004) and resulted in a rare coral bleaching event spanning the archipelago (Bahr et al. 2017; Couch et al. 2017) with extensive bleaching in Kāne‘ohe Bay, O‘ahu (62 – 100% of coral cover across reef habitats; Bahr et al. 2015). This event provided a rare opportunity to track the biology of bleaching resistant and susceptible corals during and after thermal stress under natural field conditions, with the potential to monitor the mechanisms of bleaching recovery among reef habitats.

In this study, the physiology underpinning two different phenotypes of bleaching response (bleached *vs.* non-bleached) were examined for two dominant Kāne‘ohe Bay coral species (*Montipora capitata* and *Porites compressa*) (Figure 3.1). *M. capitata* and *P. compressa* can differ in the physiological responses to experimental bleaching and recovery, with *M. capitata* increasing heterotrophic feeding and *P. compressa* catabolizing tissue reserves (Grottoli et al. 2006; Rodrigues and Grottoli 2007). Coral fragments were collected from bleached and non-bleached individuals of each species during peak bleaching and three months following thermal stress (Figure S1a) from three patch reefs within an environmental gradient of decreasing oceanic influence (Lowe et al. 2009) and terrigenous nutrient perturbations (Smith et al. 1981), which allowed an examination of the spatial variance and environmental influence (temperature,

light, sedimentation, dissolved nutrients) on corals after thermal stress. We tested (1) whether photopigments, coral biomass (total biomass, protein, lipid, and carbohydrate concentration and energy content), and contributions of heterotrophic nutrition ($\delta^{13}C$ and $\delta^{15}N$ values) differed among time periods, reef sites, or bleaching conditions and (2) whether environmental conditions influenced bleaching severity and mechanisms of physiological recovery.

Materials and Methods

Site description

Naturally bleached and non-bleached corals were identified from three patch reefs (Figure 3.1a): one in northern (Reef 44: 21°28'36.4" N, 157°50'01.0" W), central (Reef 25: 21°27'40.3" N, 157°49'20.1" W), and southern (Hawai'i Institute of Marine Biology (HIMB): 21°26'06.0" N, 157°47'27.9" W) Kāne'ohe Bay, O'ahu, Hawai'i (*see* Cunning et al. 2016 for more detail). Reef sites were identified for their location within the longitudinal axis of Kāne'ohe Bay, which spans a north-south hydrodynamic gradient of seawater residence times (north: < 2 d; south: 30 – 60 d) and oceanic influence (high in north, low in south) (Lowe et al. 2009).

Environmental data

Dissolved inorganic nutrients in seawater were measured on samples collected (ca. 100 ml) from surface waters (< 1 m) at each reef site once every two weeks from 04 November 2014 to 04 February 2015. In total, ten seawater samples were analyzed for each reef site over the study period. Additional samples were also collected to determine the $\delta^{15}N$ value of seawater nitrate using the bacterial denitrifier method. All seawater samples were filtered (0.7 μm) and stored in 0.1 N HCl-washed bottles and frozen at -20 °C until analyzed.

Analysis of δ^{15}N-nitrate in seawater was performed following the bacterial denitrifier method, where the bacterial strain *Pseudomonas aurofaciens* converts nitrate to nitrous oxide (N_2O) without changes in nitrogen isotopic composition (Sigman et al. 2001; McIlvin and Casciotti 2011). The nitrogen isotopic composition of N_2O was measured at the University of Hawai‘i at Mānoa Biogeochemical Stable Isotope Facility on a ThermoFinnigan Gasbench II with a Finnigan MAT 252 isotope ratio mass spectrometer. Isotope values are reported in permil (‰) relative to atmospheric N_2 standards (air). Analysis of δ^{15}N-nitrate requires sufficient concentrations of nitrate+nitrite ($NO_3^- + NO_2^-$) (i.e., N+N) in seawater, and δ^{15}N-nitrate values are not reported where N+N μmol L^{-1} was below limit for analysis.

Dissolved inorganic nutrients (ammonium [NH_4^+], nitrate + nitrite [$NO_3^- + NO_2^-$] or [N+N], phosphate [PO_4^{3-}], and silicate [$Si(OH)_4$]) in seawater were measured by the University of Hawai‘i at Mānoa SOEST Laboratory for Analytical Biogeochemistry using a Seal Analytical AA3 HR nutrient autoanalyzer and expressed as μmol L^{-1}. Photosynthetic active radiation (PAR) and temperatures data were continuously recorded at 15 min intervals at 2 m depth at each reef site. PAR was recorded using a cosine-corrected Odyssey PAR loggers (Dataflow Systems Limited, Christchurch, New Zealand) cross calibrated to a cosine quantum sensor (LI-192, Li-Cor Biosciences, Lincoln, NE) and Li-Cor quantum meter (LI-1400) (Long et al. 2012). Temperatures were recorded using Hobo Pendant UA-002-08 loggers (±0.53 °C accuracy, Onset Computer Corp., Bourne, MA) that were cross-calibrated across a range of temperatures (18 – 40 °C). PAR and temperature loggers at Reef 25 experienced mechanical errors; therefore, only data from Reef 44 and HIMB are presented. Instantaneous PAR values were used to calculate

the daily light integral (DLI) for each site (mol photons m^{-2} d^{-1}). Rates of sedimentation at each site were measured using sediment traps by weighing the mass of suspended particles falling into a polyvinylchloride tube (5 cm × 42 cm) capped at the base and held vertical to a cinder block at each reef site at a depth of 2 m. Large debris (e.g., invertebrate carapaces) was removed from collected sediments. Sediment traps were collected each month, filtered through pre-weighed commercially available coffee filters, ddH_2O rinsed, dried at 60 °C, and weighed to nearest 0.0001 g. Sedimentation rates were expressed as mg sediment d^{-1}.

Coral collection and tissue analysis

During peak bleaching in October 2014, colonies of *Montipora capitata* (Dana, 1846) and *Porites compressa* (Dana, 1846) exhibiting different bleaching conditions – tissue paling (bleached) and fully pigmented (non-bleached) (Figure 3.1b-c) – were identified and tagged (depth: <1 – 3 m) with cattle tags and zip ties. In each species, neighboring colonies of each condition (bleached and non-bleached) were selected and are referred to as conspecific colony pairs (Figure 3.1b-c). Fragments (4 cm in length) from each conspecific colony pair (5 pairs per species) were collected from the three reefs sites (detailed above) during bleaching (24 October 2014) and ca. 3 month following peak seawater temperatures during post-bleaching recovery (14 January 2015) (Figure S1). Fragments were immediately frozen in liquid nitrogen and stored at -80 °C until processing.

All biomass assays were performed on holobiont tissues (host + symbionts), following established procedures (Wall et al. 2017b). Coral tissues were removed from skeletons using an airbrush filled with filtered seawater (0.2 µm). The tissue slurry was briefly homogenized and

stored on ice. Total chlorophyll ($a+c_2$) was used as a metric of bleaching (Grottoli et al. 2006) and symbiont densities (symbiont:host cell ratio) were measured in a parallel study (Cunning et al. 2016). Chlorophylls were measured by concentrating algal symbiont cells through centrifuging the coral tissue slurry (13,000 rpm × 3 min) and subsequently extracting chlorophylls in 100% acetone for 36 h in darkness at -20 °C (Wall et al. 2017b). Extract absorbance were measured at two absorbances (λ = 630 and 663 nm) with a 750 nm internal blank on a spectrophotometer (Jeffrey & Humphrey, 1975) using a glass 96-well microtiter plate. Concentrations for chlorophyll *a* and c_2 were summed to obtain total chlorophyll (µg ml tissue slurry^{-1}) and final concentrations were standardized to coral surface area determined by the wax-dipping technique (Stimson and Kinzie 1991).

Total tissue biomass was determined from the difference of dry (60 °C) and combusted (4 h, 450 °C) masses of an aliquot of tissue extract and expressed as the ash-free dry weight (AFDW) of biomass cm^{-2}. Total protein (soluble + insoluble) was measured spectrophotometrically following the Pierce BCA Protein Assay Kit (Pierce Biotechnology, Waltham, MA) using a spectrophotometer (λ = 562 nm) against a bovine serum albumin standard curve (Smith et al. 1985). Total lipids were quantified by lyophilizing 3 ml of the tissue slurry and extracting lipids in a 2:1 chloroform:methanol solution for 1 h in darkness at -20 °C. The extracted fraction was filtered through a pre-combusted (450 °C, 4h) GF/F filter (0.7 µm), rinsed with 0.88% KCl and 100% chloroform, and evaporated under low heat (< 50 °C) in pre-combusted aluminum pans. Lipid biomass was measured gravimetrically to the nearest 0.0001 g (Schoepf et al. 2013) and normalized to total extracted tissue biomass, determined as the sum of the ash-free dry weight of debris retained on the GF/F filter during lipid extraction and the mass of extracted lipids.

Carbohydrates were measured using the phenol-sulfuric acid method using a spectrophotometer (λ = 585 nm) with glucose as a standard (Dubois et al. 1965). Finally, changes in tissue biomass reserves were assessed energetically (Lesser 2013) using compound-specific enthalpies of combustion for lipid (-39.5 kJ g^{-1}), protein (-23.9 kJ g^{-1}), and carbohydrate (-17.5 kJ g^{-1}) biomass (Gnaiger and Bitterlich 1984); tissue kJ values were summed and expressed as energy content per gram of AFDW biomass (kJ g^{-1}). Proteins, lipids, carbohydrates, and biomass kilojoules (i.e., energy content) were normalized to g AFDW of the tissue slurry.

Stable isotope analysis

An aliquot of the tissue slurry (ca. 5 ml) was filtered through a 47 mm 20 µm nylon net filter (EMD Millipore Corp., Burlington, MA) to remove inorganic carbonate and skeletal debris (Maier et al. 2010). Host and symbiont tissues were separated by centrifugation (2000 g × 3 min) and filtered seawater rinses (Muscatine et al. 1989; microscopy confirmed the efficient separation of the two tissue fractions). Tissues were filtered using a vacuum pump at low pressure onto pre-combusted 25 mm GF/F filters (450 °C, 4h), rinsed with ddH_2O to remove salts, dried at 60 °C, and packed in tin capsules. Carbon ($\delta^{13}C$) and nitrogen ($\delta^{15}N$) isotopic values and molar ratios of carbon:nitrogen (C:N) for coral host ($\delta^{13}C_H$, $\delta^{15}N_H$, $C:N_H$) and algal symbiont ($\delta^{13}C_S$, $\delta^{15}N_S$, $C:N_S$) tissues were determined using a Costech elemental combustion system coupled to a Thermo-Finnigan Delta Plus XP Isotope Ratio Mass-Spectrometer. Analytical precision of $\delta^{13}C$ and $\delta^{15}N$ values of samples was < 0.2 ‰ determined by analysis of laboratory reference material run before and after every 10 samplesIsotopic data are reported in delta values (δ) using the conventional permil (‰) notation and expressed relative to Vienna

Pee-Dee Belemnite (V-PBD) and atmospheric N_2 standards (air) for carbon and nitrogen, respectively, using the following equation:

$$\delta^{13}C \text{ or } \delta^{15}N = [(R_{sample}/R_{standard}) - 1] \times 1000$$

where R is the ratio of ^{13}C:^{12}C or ^{15}N:^{14}N in the sample and its respective standard. The relative differences in isotopic values in the host and symbiont for carbon ($\delta^{13}C_{H\text{-}S} = \delta^{13}C_H - \delta^{13}C_S$) and nitrogen ($\delta^{15}N_{H\text{-}S}$) were calculated to evaluate changes in the proportion of heterotrophic carbon to coral host nutrition (i.e., $\delta^{13}C_{H\text{-}S}$) and changes in trophic enrichment among host and symbiont (i.e., $\delta^{15}N_{H\text{-}S}$) (Rodrigues and Grottoli 2006; Reynaud et al. 2009).

An isotope mass balance was used to model the effect of changes in tissue biomass composition on holobiont (host + symbiont) $\delta^{13}C$ values during bleaching recovery, following Hayes (2001). First, the isotopic composition of the holobiont ($\delta^{13}C_{Holobiont}$) was modeled for each time period:

$$\delta^{13}C_{Holobiont} = (m_H * \delta^{13}C_H) + (m_S * \delta^{13}C_S)$$

where m is the estimated proportion of host (m_H) and symbiont (m_S) tissues in holobiont biomass (g AFDW), and $\delta^{13}C$ (defined above) are measured isotopic values of tissues. Symbiodiniaceae account for 3 – 10% of coral biomass (Muscatine et al. 1981; 1984; Porter et al. 1989; Thornhill et al. 2011); however, the influence of bleaching on this percentage is uncertain, therefore an average value of 5% total biomass was used (Thornhill et al. 2011). Second, the $\delta^{13}C$ value of biomass reflects the distribution of ^{13}C among the major classes of compounds:

$$\delta^{13}C_{biomass} \sim X_{proteins}\,\delta^{13}C_{proteins} + X_{carbohydrates}\,\delta^{13}C_{carbohydrates} + X_{lipids}\,\delta^{13}C_{lipids}$$

where X refers to the mole fraction of carbon in proteins, carbohydrates, and lipids. Therefore, biomass composition (i.e.,% of proteins, lipids, carbohydrates) and $\delta^{13}C_{Holobiont}$ values were used

to estimate compound class-specific isotopic values ($\delta^{13}C_{Compound}$) for each compound class in corals during the bleaching period of October 2014, using eqn. 5 in Hayes (2001):

$$\delta^{13}C_{carbohydrates} = \delta^{13}C_{proteins} + 1\ ‰$$

$$\delta^{13}C_{lipids} = \delta^{13}C_{carbohydrates} - 6\ ‰$$

We assume the $\delta^{13}C$ value of proteins is 1 ‰ higher that the $\delta^{13}C$ value of carbohydrates and lipids are depleted in ^{13}C by 6 ‰ relative to carbohydrates (*see* Hayes 2001 and references therein). $\delta^{13}C_{Compound}$ values for each colony were then applied to the same colonies in January 2015 using measurements of tissue composition and $\delta^{13}C_{Holobiont}$ values (i.e., observed-$\delta^{13}C_{Holobiont}$) to calculate expected-$\delta^{13}C_{Holobiont}$ values – representing the predicted value of the holobiont as a product of a fixed, colony-specific $\delta^{13}C_{Compound}$ value applied to a new biomass composition. The relationship between observed and expected $\delta^{13}C_{Holobiont}$ was evaluated using a linear regression.

Statistical analysis

A matrix of all biological response variables for *M. capitata* and *P. compressa* was first analyzed using a permutational multivariate analysis of variance (PERMANOVA) with periods (October 2014, January 2015), sites (Reef 44, Reef 25, HIMB), and colony-level physiological condition observed in October 2014 (i.e., bleached or non-bleached) as main effects. $\delta^{13}C$ values were incorporated into the data matrix by transforming to absolute values (i.e., $|\delta^{13}C|$). Sum of squares were partitioned according to Bray-Curtis dissimilarity matrix and sequential tests were applied on 1000 model permutations using *adonis2* in *R* package *vegan* (Oksanen et al. 2017; R Development Core Team 2018), with pairwise comparisons over an additional 1000 permutations in *RVAideMemoire*. Results of PERMANOVA were applied to distinguish the

hierarchy of main effects between coral species and to holistically evaluate post-bleaching recovery. Multivariate relationships between periods, sites, and bleaching conditions were visualized for each species separately using nonmetric multidimensional scaling (NMDS) plots with ellipses representing standard errors of point means. NMDS plots were used to visualize differences among reefs and bleaching conditions (i.e., site × condition), and among bleached and non-bleached corals across all sites with vectors representing significant biological responses ($p \leq 0.05$).

Environmental data (temperature, light, dissolved nutrients, sedimentation) from each reef were analyzed to test for site-specific conditions influencing bleaching and recovery responses. Environmental data was analyzed using a linear mixed effect model using *lmer* in package *lme4* (Bates et al. 2015) with reef site as a fixed effect and date of sample collection as a random effect. Biological response variables for individual species were used to test for differences among time periods, reef locations, and bleaching conditions. Physiology and isotopic data were analyzed using three-way linear mixed effect models in *lme4* with period, site, and condition as fixed effects and coral colony and colony-pairs as random effects. Model selection was performed on candidate models using a combination of AIC and likelihood ratio tests (Akaike 1978). Where significant interactions were observed, pairwise post hoc slice-tests of main effects by least-square means were performed in package *lsmeans* (Lenth 2016). Analysis of variance tables for all environmental and biological metrics were generated using type II sum of squares with Satterthwaite approximation of degrees freedom using *lmerTest* (Kuznetsova et al. 2017). Environmental data from these reefs are publically available (Ritson-Williams and Gates 2016a; 2016b; 2016c; Ritson-Williams et al. 2018). All analyses were performed in *R* version 3.4.3 (R

Development Core Team 2018); materials (data, *R* code) to reproduce tables, figures, and analyses are archived at Zenodo (Wall 2019).

Results

Environmental data

Kāneʻohe Bay reef flats sustained a maximum seawater temperatures of ca. 31 °C (Bahr et al. 2015). Peak seawater warming at HIMB spanned 15 – 24 September 2014 with temperatures ranging from 29.8 – 30.2 °C (± 0.2 °C accuracy, ± 0.1 °C resolution; NOAA 2017) (Appendix Figure 3.S1). Seawater temperatures at Reef 44 and HIMB declined from peaks in mid-October (≤ 29.2 ± 0.5 °C) declining thereafter, and seawater temperatures from October 2014 to January 2015 (mean, maximum, minimum) were comparable, with among sites differences (ca. 0.01 °C) below logger resolution (± 0.14 °C) and accuracy (± 0.53 °C) (Table 3.1). Light values integrated over 24 h (i.e., DLI mol photons m^{-2} d^{-1}) were 4.5 mol photons m^{-2} d^{-1} greater at HIMB compared to Reef 44 ($p < 0.001$) (Table 3.1; Appendix Figure 3.S1).

The concentrations of dissolved inorganic nutrients were low during most of the study, but differences among the three reefs were detected (Figure 3.2*a-d*, Table 3.1). Phosphate was lowest at Reef 25 ($p = 0.019$) although this effect was small (difference < 0.02 μmol L^{-1}). Ammonium concentrations were equivalent among reefs ($p = 0.161$) (ca. 0.5 μmol L^{-1}) but most variable at Reef 44 (transient increases of up to 2.0 μmol L^{-1}), and nitrate + nitrite concentrations at Reef 44 were two-fold higher than other sites ($p = 0.002$) (0.35 – 0.42 μmol L^{-1}). Silicate ($p = 0.724$) and short-term sedimentation rates ($p = 0.161$) (Figure 3.2e) did not differ among sites; however, silicate tended to be higher at Reef 44 and an extended monitoring of sedimentation

rates (December 2014 – January 2016) show annual sedimentation rates at Reef 44 and HIMB were greater and more variable than rates at Reef 25 ($p = 0.041$) (Figure 3.2*f*). $\delta^{15}N$ values for nitrate ranged from 3.8 to 4.9 ‰ (Table 3.2), however, low [N+N] reduced sample sizes for $\delta^{15}N$-nitrate analysis ($n = 1 – 2$ samples per site).

Coral physiology

Multivariate analysis of sixteen response variables in *Montipora capitata* and *Porites compressa* revealed significant changes in corals among time periods ($p < 0.001$), between bleached and non-bleached corals ($p \leq 0.004$) and in response to the period × condition interaction ($p \leq 0.029$) (Table 3.3). Reef sites significantly influenced *M. capitata* condition ($p = 0.006$), especially during October 2014 (Figure 3.3*a*), whereas *P. compressa* colonies were less influenced by site ($p = 0.099$) and instead predominantly affected by bleaching condition (Figure 3.4a). NMDS plots showed differences in bleached and non-bleached colonies of both species during October 2014 (*post-hoc*: $p \leq 0.008$) where bleaching correlated with reductions in chlorophyll concentration (chl) and biomass (Figure 3.3*b*, 4*b*) and lower host and symbiont C:N in *P. compressa* (Figure 3.4*b*). By January 2015, the physiological condition of previously bleached *M. capitata* (*post-hoc*: $p = 0.337$) and *P. compressa* colonies (*post-hoc*: $p = 0.125$) were indistinguishable from non-bleached conspecifics, indicating a convergence of physiological properties in corals across bleaching histories and a rapid physiological recovery from bleaching (Figures 3.3*c-d*, 3.4*c-d*). A summary of significant effects for all response variables can be found in Table 3.4.

Montipora capitata total chlorophyll ($p = 0.041$) and tissue biomass ($p = 0.011$) were affected by

the interaction of period × condition (Appendix Table 3.S3), and these responses did not vary among sites ($p \geq 0.222$). In October 2014 bleached *M. capitata* had 63% less chlorophyll and 30% less tissue biomass than non-bleached phenotypes (Figure 3.5*a*-*b*). By January 2015, however, *M. capitata* chlorophyll and tissue biomass were equivalent among bleached and non-bleached corals, having increased 255% and 95% in bleached phenotypes and 54% and 37% in non-bleached colonies, respectively, from October 2014 levels (Figure 3.5*a*-*b*). Over the recovery period, *M. capitata* protein biomass (g gdw^{-1}) declined by 20% ($p = 0.010$) but did not differ among sites ($p = 0.461$) or between bleached and non-bleached colonies ($p = 0.267$) (Figure 3.6*a*; Appendix Table 3.S3). *M. capitata* tissue lipids, carbohydrates and energy content did not differ among periods ($p \geq 0.073$), sites ($p \geq 0.065$) or between bleached and non-bleached colonies ($p \geq 0.291$) (Figure 3.6*b*-*d*).

Porites compressa chlorophyll content differed according to period × condition ($p < 0.001$) and site × condition ($p = 0.011$) interactions (Figure 3.5*c*, Appendix Table 3.S2). In October 2014, chlorophyll in bleached *P. compressa* was 84% (Reef 44), 78% (Reef 25), and 92% (HIMB) lower than non-bleached colonies. By January 2015, chlorophyll was equivalent between all *P. compressa* at Reef 25 and Reef 44, but chlorophyll recovery was suppressed in colonies at HIMB, with 25% less chlorophyll in previously bleached colonies. *P. compressa* total biomass was on average 19% higher in non-bleached relative to bleached colonies ($p = 0.025$) but did not differ among periods or sites ($p \geq 0.173$) (Figure 3.5*d*).

Porites compressa protein biomass (g gdw^{-1}) was affected by period × condition ($p = 0.011$) (Figure 3.6*e*; Appendix Table 3.S2), but in *post-hoc* tests protein was not different among

bleached and non-bleached colonies during October 2014 or January 2015. Tissue lipids and energy content were affected by the period × site interaction ($p \leq 0.008$), but not bleaching conditions ($p \geq 0.179$). At the time of bleaching in October 2014, *P. compressa* lipids and biomass energy content was equivalent among sites (Figure 3.6*f*, *h*), but by January 2015 tissue lipids and energy content declined by ca. 27% and 18%, respectively, from October 2014 levels. In particular, declining lipid biomass in recovering *P. compressa* was limited to Reef 44 and Reef 25 colonies, whereas lipids in HIMB corals remained high. Carbohydrate biomass showed no significant differences ($p \geq 0.114$) (Figure 3.6*g*).

Tissue isotopic compositions

Differences in the carbon isotopic composition of *M. capitata* host ($\delta^{13}C_H$) tissues varied according to bleaching condition ($p = 0.022$), with higher values in bleached colonies, although these differences were small (0.7 ‰) (Figure 3.7*a*; Appendix Table 3.S3). Symbiont $\delta^{13}C$ values varied over time, being lower (0.7 ‰) during bleaching in October 2014 compared to January 2015 ($p = 0.001$) (Figure 3.7b). The relative difference in *M. capitata* host and symbiont $\delta^{13}C$ values ($\delta^{13}C_{H\text{-}S}$) – a metric for greater proportion of autotrophic (positive values) and heterotrophic (negative values) derived carbon – changed over time, with higher $\delta^{13}C_{H\text{-}S}$ values in October 2014 and a decline in $\delta^{13}C_{H\text{-}S}$ values in January 2015 ($p = 0.001$) (Figure 3.7*c*); $\delta^{13}C_{H\text{-}S}$ were slightly higher in bleached colonies (0.3 ‰) ($p = 0.050$). Nitrogen isotopic composition of *M. capitata* host ($\delta^{15}N_H$) tissues differed among reef sites ($p = 0.043$), being ^{15}N-enriched (1 ‰) at HIMB (5.4 ± 0.1 ‰, mean ± SE) relative to other sites (Figure 3.7*d*). Symbiont $\delta^{15}N$ and $\delta^{15}N_{H\text{-}S}$ values showed no statistically significant effects ($p \geq 0.066$) (Figure 3.7*e-f*). *M. capitata* $C{:}N_H$ increased over time ($p < 0.001$) and was higher in bleached relative to non-

bleached colonies in January 2015 ($p = 0.046$), but differences across time and conditions were small (< 8% change). $C:N_S$ ($p \geq 0.060$) was unaffected across the study (Appendix Table 3.S3, Appendix Figure 3.S2).

Porites compressa host $\delta^{13}C$ values were comparable among all colonies in October 2014. In January 2015, effects on $\delta^{13}C_H$ values were limited to HIMB alone, where previously bleached colonies were ^{13}C-enriched (2 ‰) relative to non-bleached colonies ($p = 0.032$) (Figure 3.7*g*, Table 3.4; Appendix Table 3.S4). Similarly, symbiont $\delta^{13}C$ values in January 2015 were higher (1 ‰) in previously bleached colonies, driven largely by higher $\delta^{13}C$ values in colonies at HIMB ($p = 0.048$) (Figure 3.7*h*). *P. compressa* $\delta^{13}C_{H\text{-}S}$ values did not differ over the study ($p \geq 0.136$) (Figure 3.7*i*). *P. compressa* $\delta^{15}N_H$ values were slightly lower (0.4 ‰) in October 2014 ($p = 0.014$) but were largely spatially influenced ($p = 0.002$), being ^{15}N-enriched (1 ‰) in colonies from HIMB compared to other sites (Figure 3.7*j*). Interactive effects of period × condition on $\delta^{15}N_H$ ($p = 0.033$) were not significant in *a priori* post-hoc contrasts ($p \geq 0.078$). Similarly, *P. compressa* symbiont $\delta^{15}N$ became progressively ^{15}N-enriched (ca. 1.2 ‰) from northern Reef 44 to southern HIMB ($p = 0.024$) (Figure 3.7*k*). Additionally, $\delta^{15}N_S$ was higher (1.1 ‰) in bleached relative to non-bleached *P. compressa* in October 2014, but not January 2015 ($p = 0.009$), corresponding to lower $\delta^{15}N_{H\text{-}S}$ values ($p = 0.001$) for bleached relative to non-bleached *P. compressa* ($p = 0.001$) in October 2014 during thermal stress (Figure 3.7*l*). *P. compressa* $C:N_H$ increased over time ($p < 0.001$) and was lower (October 2014) and higher (January 2015) in bleached relative to non-bleached colonies ($p < 0.001$) (Appendix Table 3.S4), although these effects were small (< 10% change); $C:N_H$ site × condition effects ($p = 0.004$) were not significant

in *post-hoc* contrasts. $C:N_S$ showed no significant effects ($p \geq 0.085$) (Appendix Table 3.S4, Appendix Figure 3.S2).

To reconcile small changes in tissue $\delta^{13}C$ values in host and symbiont fractions across the three scales tested here (i.e., period, site, condition) an isotope mass balance was used. Measurements of total biomass and compound class concentrations (i.e., proteins, lipids, carbohydrates) (Hayes 2001) were used to estimate compound class-specific $\delta^{13}C$ values (i.e., $\delta^{13}C_{Compound}$) for all coral holobionts (i.e., $\delta^{13}C_{Holobiont}$) at the time of thermal stress in October 2014 (Appendix Figure 3.S3). Using colony-specific $\delta^{13}C_{Compound}$ estimates for corals in October 2014 and applying these estimates to the measured proportion of tissue compounds produces an expected-$\delta^{13}C_{Holobiont}$, which should explain observed-$\delta^{13}C_{Holobiont}$ if $\delta^{13}C_{Compound}$ values have not been substantially altered by the incorporation of different carbon sources or changes in residual $\delta^{13}C_{Compound}$ from metabolic effects. Expected-$\delta^{13}C_{Holobiont}$ values provided a good estimate of observed- $\delta^{13}C_{Holobiont}$, which ranged from $\delta^{13}C$ of -19 to -13 ‰ (Table 3.8). The range in $\delta^{13}C$ values is important, as it shows a considerable range in holobiont $\delta^{13}C$ from biological and environmental effects on corals and Symbiodiniaceae. The relationship between the expected-$\delta^{13}C_{Holobiont}$ and the observed-$\delta^{13}C_{Holobiont}$ values in all corals (i.e., those recovered from bleaching and non-bleached) was significant for both *M. capitata* ($R^2 = 0.88$, $p < 0.001$) and *P. compressa* ($R^2 = 0.56$, $p < 0.001$) (Figure 3.8), indicating a significant influence of protein:lipid:carbohydrate ratios in explaining variance in $\delta^{13}C$ values in both species during bleaching recovery.

Discussion

Few studies have monitored changes in coral physiology and nutritional plasticity during and after large-scale natural bleaching events (Fitt et al. 1993; Edmunds et al. 2003; Rodrigues et al. 2008; Grottoli and Rodrigues 2011) or evaluated local environmental effects on physiological conditions that shape bleaching recovery (Cunning et al. 2016). Using *Montipora capitata* and *Porites compressa* colonies from three reefs spanning 6.3 km along Kāneʻohe Bay, we observed variable tissue biomass and chlorophylls among bleaching conditions and through time, but energy reserves were unaffected by bleaching stress. Furthermore, evidence suggests relatively small changes in coral tissues composition across space and time, and not changes in heterotrophic nutrition, explain patterns in $\delta^{13}C$ values of both coral species during bleaching recovery. Taken together, these results shed light on coral physiology during and after thermal stress and identify the need to quantity tissue composition effects on isotopic values in corals, as this may provide insight into the performance of corals across a continuum of physiological conditions and ecological scales.

Environmental context, bleaching, and recovery

Seawater temperatures during and after bleaching in October 2014 were comparable among the three reefs, but light availability was lower and dissolved nutrients and sedimentation tended to be higher at Reef 44 in northern Kāneʻohe Bay (Figure 3.1a). These observations correspond with a combination of greater discharge of subterranean groundwater, watershed/stream inputs, and the unique hydrology (short seawater residence) at this location (Drupp et al. 2001; Dulai et al. 2016). While physiological stress from high light (Anthony et al. 2007) and nutrient enrichment (Wiedenmann et al. 2012) can exacerbate thermal stress, bleaching severity (assessed

from chlorophyll density) was similar among the three reef sites, and N:P ratios (range: 0.6 – 10.5) were below those reported in cases where nutrients negatively affected corals (i.e., bleaching, tissue loss) (N:P of 255:1 [Rosset et al. 2017], 22:1 and 43:1 [Wiedenmann et al. 2012]). Excess nutrient enrichment is detrimental to coral reefs (Silbiger et al. 2018 Vega-Thurber et al. 2014), yet moderate nutrient enrichment and stochastic nutrient perturbations can benefit corals by stimulating symbiont growth (Sawall et al. 2014) and increasing concentrations of dissolved organic carbon (Levas et al. 2016), suspended particles and prey (Mills and Sebens 2004; Mills et al. 2004, Selph et al. 2018) to the benefit of coral energy acquisition (Fox et al. 2018). Therefore, site-specific patterns in light and nutrient concentrations in the present study did not appear to affect bleaching responses, but may have influenced post-bleaching trajectories of physiological recovery and symbiont repopulation (*see also* Cunning et al. 2016).

Three months after a regional bleaching event (i.e., January 2015) bleached colonies had regained photopigmentation and were indistinguishable from non-bleached conspecifics, with the exception of moderately lower chlorophyll in bleached *P. compressa* at HIMB. Recovery from the 2014 bleaching event may have been hastened by seawater cooling initiated by the passage of Hurricane Ana by the Hawaiian Islands (ca. 17 – 23 October 2014; NOAA 2018) days before our sampling (24 October 2014), serving to mitigated further physiological thermal stress in October 2014 (Figure S1a) (Manzello et al. 2007). Rapid recovery rates observed here over short periods, however, do not negate possible long-term effects of bleaching. For instance, in many coral species bleaching effects can reduce long-term reproductive capacity (Levitan et al. 2014), alter tissue biochemistry (Rodrigues and Grottoli 2007; Baumann et al. 2014; Schoepf et al. 2015), and alter gene expression for several months (Pinzón et al. 2015) to a year after the onset of

thermal stress (Thomas and Palumbi 2017). Moreover, effects of repeat bleaching events can be complex and multiplicative, reducing the physiological resilience of corals in the long-term (Grottoli et al. 2014). Therefore, it is important to recognize short-term recovery of pigmentation and biomass (Figure 3.5) as one part of the bleaching condition, while acknowledging the uncertainty in long-term effects of bleaching on coral biology after symbiont repopulation.

Physiological impacts of bleaching and recovery

Bleaching sensitivity is affected by the capacity for cellular and genetic properties of Symbiodiniaceae and host genotypes to mitigate cellular damage (Weis 2008; Kenkel et al. 2013). *P. compressa* is a symbiont-specifist, hosting only one species of *Cladocopium* sp. (formerly, clade C) symbionts (ITS2 type C15) (LaJeunesse et al. 2004). *M. capitata*, however, exhibits flexible symbiont partnerships that partition across habitats (Innis et al. 2018) and influence bleaching responses (Cunning et al. 2016). In a parallel study of *M. capitata* in Kāneʻohe Bay following the 2014 bleaching event, bleached colonies were always dominated by *Cladocopium* sp. symbionts (ITS2 type C31), whereas non-bleached colonies could be dominated by *Cladocopium* sp. or *Durusdinium glynnii* (formerly, *Symbiodinium glynii* [ITS2 type D1-4-6]) (Cunning et al. 2016). Thus, symbiont communities alone cannot explain the distinct bleaching phenotypes observed in either *M. capitata* or *P. compressa* during the 2014 bleaching event, but instead point to physiological acclimatization (Kenkel and Matz 2016) or genetic mechanism(s) (Palumbi et al. 2014) on behalf of host and symbiont genotypes, or their combination as supporting holobiont thermal tolerance (Sampayo et al. 2008).

Coral host biomass quantity (i.e., total biomass), quality (i.e.,% lipids, energy content) and thickness are important determinants for stress resilience and post-bleaching survival (Loya et al. 2001; Anthony et al. 2009; Thornhill et al. 2011). In the present study, bleached colonies of both species had between 25 – 30% less biomass than non-bleached corals, and during post-bleaching recovery changes in tissue biomass were species-specific and dependent on bleaching history. In previous studies, tissue biomass (i.e., mg AFDW cm^{-2}) has been shown to decline 34 – 50% during and after thermal stress (Porter et al. 1989) as a result of tissue catabolism (Fitt et al. 1993; Grottoli et al. 2006; Rodrigues and Grottoli 2007) and/or cellular detachment during bleaching (Gates et al. 1992). Post-bleaching, *M. capitata* recovered biomass quickly (< 3 months) (Figure 3.5); in contrast, biomass in previously bleached *P. compressa* colonies remained low (17% less than non-bleached colonies) at both time periods. These results agree with laboratory experiments, where bleaching quickly reduced *M. capitata* and *P. compressa* biomass, but *P. compressa* tissues took much longer to recover (4 – 6 months post-bleaching) compared to *M. capitata* (1.5 months) (Grottoli et al. 2006; Rodrigues and Grotolli 2007). The cause for different biomass recovery rates is uncertain, but can indicate the extent of physiological stress, energetic demands, and differences in rates of tissue growth and metabolism between the two species (Coles and Jokiel 1977).

During the natural bleaching event and subsequent recovery, changes in the biomass composition were independent of bleaching history, and instead varied according to periods in both *M. capitata* (proteins) and *P. compressa* (energy content) and among sites during recovery for *P. compressa* (lipids) (Figure 3.6). Bleaching-independent changes in biomass composition and energy observed here (Figure 3.6, Figure S2) can also relate to shared physiological challenges

confronting both bleaching susceptible and resistant corals (i.e., gene regulation, stress protein synthesis) (Kenkel et al. 2013) and complex seasonal (Fitt et al. 2000) and site-specific environmental contexts (i.e., light availability) (Patton et al. 1977; Anthony 2006) juxtaposed atop bleaching stress. Indeed, while tissue composition (i.e.,% proteins, lipids, carbohydrates) did not differ among bleached and non-bleached colonies at either time point, total biomass (mg cm^{-2}) was lower in all colonies in October 2014 regardless of bleaching condition (Figure 3.5). Therefore, thermal stress may reduce the total biomass production in both bleaching susceptible and resistant corals, and tissue biomass in bleached corals may remain low for several months post-bleaching.

Nutritional plasticity and tissue isotopic composition

The isotopic values of an organism are linked to the constitutive biochemical composition of the tissues and substrates acquired through its diet and broken down in metabolism (Minagawa and Wada 1984; Hayes 2001). Isotopic inferences on nutritional plasticity in corals are also complicated by the translocation/recycling of metabolites between symbiotic partners (Reynaud et al. 2002; Einbinder et al. 2009), kinetic isotope fractionation in biological reactions (i.e., metabolic isotope effects) (Land et al. 1975), and the isotopic composition of internal and external nutrient pools (Swart et al. 2005b) which are influenced by rates of production and growth, among other processes. For instance, in Symbiodiniaceae and other microalgae, elevated rates of photosynthesis and growth produce carbon limitations (Laws et al. 1995; Swart et al. 2005a) that reduce isotopic discrimination and increase $\delta^{13}C$ values. Conversely, light attenuation and low rates of photosynthesis (Muscatine et al. 1989; Laws et al. 1995; Swart et al. 2005b; Maier et al. 2010) can decrease both $\delta^{13}C$ and $\delta^{15}N$ values in corals (but *see also*, Rost et

al. 2002). Lower $\delta^{13}C$ values can also result from greater feeding on particles (i.e., plankton, organic particles) (Levas et al. 2013; Grottoli et al. 2017) and the preferential utilization of heterotrophic nutrition in lipid biosynthesis (Alamaru et al. 2009; Baumann et al. 2014). Short-term increases in heterotrophic nutrition can be difficult to verify, however, due to uncertainty in rates of tissue turnover and changes in tissue composition, especially following physiological stress (Rodrigues and Grottoli 2006; Logan et al. 2008). For instance, the recovery of tissue biomass reserves in bleached corals is compound specific (Rodrigues and Grottoli 2007; Schoepf et al. 2015) and the nutritional inputs (i.e., autotrophy *vs*. heterotrophy) responsible for biomass growth can differ among species and according to time post-bleaching (Baumann et al. 2014).

Throughout the study *M. capitata* $\delta^{13}C_H$ values were higher in bleached corals, whereas symbiont $\delta^{13}C$ values were lower in October 2014 during bleaching relative to January 2015 during recovery (Figure 3.7a-b). *M. capitata* $\delta^{13}C_{H\text{-}S}$ values were also consistently higher in October 2014 relative to January 2015, and slightly more positive in bleached corals. Effects on *P. compressa* $\delta^{13}C$ values were limited to post-bleaching recovery in January 2015, where previously bleached colonies had higher $\delta^{13}C_S$ values at all sites and higher $\delta^{13}C_H$ values at HIMB alone, although the differences were very small (< 1 ‰). In all these cases, host and symbiont $\delta^{13}C$ and $\delta^{13}C_{H\text{-}S}$ values do not support a greater reliance on heterotrophy in bleached corals. Lower $\delta^{13}C_H$ values in non-bleached colonies (*M. capitata* overall, *P. compressa* at HIMB in January 2015) instead can be explained by changes in host biomass properties (i.e., protein:lipid:carbohydrate ratios) and not greater feeding on ^{13}C-depleted prey. In contrast, bleaching-independent effects on *M. capitata* $\delta^{13}C_S$ values related to temporal changes, perhaps from temperature effects on symbiont production and growth. Similarly, thermal effects,

seasonality, and/or symbiont repopulation may explain higher $\delta^{13}C_S$ values in previously bleached *P. compressa* in January 2015. In total, $\delta^{13}C$ values provided poor support for nutritional plasticity in both species in this study, while changes in biomass properties may offer a unifying hypothesis to explain variance in $\delta^{13}C$ values at the multiple scales within this study (period, site, condition).

Organism bulk $\delta^{13}C$ values are affected by their biochemical compositions (Logan et al. 2008; Alamaru et al. 2009). Isotope mass balance calculations show that the majority of variance in *M. capitata* and *P. compressa* $\delta^{13}C_{Holobiont}$ values (88% and 55%, respectively, Fig 8) can be explained by changes in the relative proportions of compounds (i.e., proteins, lipids, carbohydrates), despite individual compounds not differing among bleaching and non-bleached colonies of either species. However, it should be acknowledged that $\delta^{13}C$ values of compounds – particularly, lipids – in corals may change in response to physiological stress (Grottoli and Rodrigues 2011) and are shaped by biosynthesis sources and rates of tissue growth/metabolism (Alamaru et al. 2009; Baumann et al. 2014). Reef corals are considered lipid rich (ca. 30% of biomass; Patton et al. 1977), and lipids are depleted in ^{13}C relative to bulk tissues (Hayes 2001) (Figure S3). The breakdown of lipids, therefore, is expected to lead to small increases in $\delta^{13}C$ values of remaining lipid fraction and organism $\delta^{13}C$ values (DeNiro and Epstein 1977). However, corals can catabolize isotopically light lipids during bleaching, resulting in residual lipid ^{13}C-enrichment (Grottoli and Rodrigues 2011). Should tissue lipids in bleached colonies depart from predicted isotopic relationships (Hayes 2001) – being either 3 ‰ lower or higher than lipids in non-bleached colonies – the predictive power of our modeled relationship in observed- versus expected-$\delta^{13}C$ values for corals during the recovery period in January 2015 is

lessened (48 and 67% [*M. capitata*] and 27 and 36% [*P. compressa*] variance explained, respectively). Therefore, using a constant relationship of compound class-specific $\delta^{13}C$ values relative to whole tissue $\delta^{13}C$ values, we infer changes in the relative proportions of proteins, lipids, and carbohydrates and not their isotopic composition best explain patterns in the bulk $\delta^{13}C$ values of corals in this study. While few examples of compound-class or compound-specific isotope values for coral tissues exist (lipids [Alamaru et al. 2009; Grottoli and Rodrigues 2011], coral skeletal organic matrix [Muscatine 2005]), changes in biomass composition can effectively explain the patterns in $\delta^{13}C$ values of both species used in this study, albeit an understanding of baseline isotopic values for coral tissue compounds is needed to better discern effects of habitat, environment, and nutrition in reef corals.

Unlike most predator-prey relationships (Minagawa and Wada 1984), greater heterotrophic nutrition in corals does not lead to appreciable higher $\delta^{15}N$ values in coral tissue relative to its symbiont algae (Reynaud et al. 2009); instead, coral $\delta^{15}N$ values often relate to sources at the base of the food web (Heikoop et al. 2000; Dailer et al. 2010). *M. capitata* and *P. compressa* $\delta^{15}N$ values were within the range of $\delta^{15}N$-nitrate values in Kāneʻohe Bay (4 – 5 ‰) (Table 3.3) and higher at HIMB relative to other sites. Similar patterns of higher $\delta^{15}N$ values in southern Kāneʻohe Bay were also seen in juvenile brown stingray (*Dasyatis lata*) known to have a fairly constant diet (Dale et al. 2011), indicating spatial variability in the sources and isotopic values of DIN $\delta^{15}N$ values that permeate the food web of Kāneʻohe Bay (Heikoop et al 2000; Nahon et al. 2013). These spatial effects are expected to result from a combination of greater subterranean groundwater discharge in northern Kāneʻohe Bay (Dulai et al. 2016), high stream input (30% of bay total), and legacy effects of sewage dumping (1951 – 1978) in southern Kāneʻohe Bay

(Smith et al. 1981). Higher $\delta^{15}N_H$ values in all *P. compressa* in January – driven largely by corals at HIMB – may also be influenced by nitrogen acquisition deficits, as well as changes in amino-acid synthesis/deamination and nitrogen concentration of heterotrophic (Haubert et al. 2005) and autotrophic resources (Tanaka et al. 2006).

P. compressa $\delta^{15}N_S$ values differed from the host, being higher in October 2014 relative to January 2015, and in particular 2 ‰ higher in non-bleached Reef 25 *P. compressa* relative to bleached colonies in October. At the same time, the predicted +1.5 ‰ enrichment (i.e., $\delta^{15}N_{H-S}$) for consumers relative to their food source reversed and was negative for bleached *P. compressa* at Reef 25 and HIMB colonies (October 2014), suggesting disruption of nitrogen recycling (Wang and Douglas 1998) in bleached colonies and/or contributions of nitrogen not originating from animal metabolism. These low $\delta^{15}N_S$ values may indicate a greater utilization of a ^{15}N-depleted DIN source, possibly from N_2-fixation by coral-associated diazotrophs (Bednarz et al. 2017) or decreased rates of growth and nitrogen demand in non-bleached coral symbionts (Heikoop et al. 1998; Baker et al. 2013). $\delta^{15}N$ values of Symbiodiniaceae are predicted to increase when growth rates are elevated and nitrogen availability is limited (Rodrigues and Grottoli 2006), although this depends on whether rates of photosynthesis and growth are balanced (Granger et al. 2004). Increased $\delta^{15}N_S$ values in bleached *P. compressa* agrees with other studies (Rodrigues and Grottoli 2006; Bessell-Browne et al. 2014; Schoepf et al. 2015) suggesting elevated rates of mitotic cell division and photopigment synthesis post-bleaching increase symbiont nitrogen demand, thereby reduced nitrogen isotope fractionation (Heikoop et al. 1998). An increase in $\delta^{15}N_S$ values at the time of bleaching is intriguing, as this suggests symbiont repopulation proceeds rapidly following peak thermal stress. The capacity for rapid

nitrogen assimilation in symbionts post-bleaching may be an important factor in physiological resilience of corals, and may be shaped by the functional diversity of Symbiodiniaceae (Baker et al. 2013), properties of the coral host (Loya et al. 2001), and the extent of physiological stress.

Funding

Funding provided by grants from NOAA Marine Education and Training Grant (NA17NMF4520161), the University of Hawai'i at Mānoa Graduate Student Organization (19-03-15), Colonel Willys E. Lord, DVM & Sandina L. Lord Endowed Scholarhsip, and an Environmental Protection Agency (EPA) STAR Fellowship Assistance Agreement (FP-91779401-1) to CBW. The views expressed in this publication have not been reviewed or endorsed by the EPA and are solely those of the authors.

Acknowledgments

The authors thank A. Grottoli, L. Rodrigues, and J. Sparks for discussions on stable isotopes, N. Wallsgrove, C. Lyons, and W. Ko for stable isotope analyses, W. Ellis and J. Davidson for laboratory support, C. Hunter and NOAA for assistance in seawater nutrient analysis, and A. Amend, M. Donahue, A. Moran, and E. A. Lenz for constructive comments. This is SOEST contribution number 10664 and HIMB contribution number 1754.

Table 3.1. Analysis of environmental variables (dissolved inorganic nutrients, sedimentation rates, daily light availability, and temperature) at three Kāneʻohe Bay patch reefs*.

Environmental variable	*Effect*	*SS*	*df*	*F*	*p*
[a]Temperature (°C)					
daily mean	Site	0.045	1, 129	1.717	0.192
daily maximum	Site	0.738	1, 129	13.134	†**<0.001**
daily minimum	Site	0.011	1, 129	0.163	0.687
[b]Daily light integral (mol photons m^{-2} d^{-1})	Site	636.960	1, 61	130.520	**<0.001**
[c]Dissolved inorganic nutrients					
phosphate (PO_4^{3-} µmol L^{-1})	Site	0.003	2, 18	5.016	**0.019**
ammonium (NH_4^+ µmol L^{-1})	Site	0.414	2, 18	2.023	0.161
nitrate + nitrite (NO_3^- + NO_2^- µmol L^{-1})	Site	0.785	2, 18	9.314	**0.002**
silicate ($Si(OH)_4$ µmol L^{-1})	Site	10.577	2, 18	0.329	0.724
Sedimentation					
[d]*short-term* (g d^{-1})	Site	0.001	2, 2	5.221	0.161
[e]*annual* (g d^{-1})	Site	0.006	2, 24	3.667	**0.041**

*Data collected at Reef 44, Reef 25, and HIMB, except light and temperature (Reef 44 and HIMB alone). *SS* = sum of squares; *df* = degrees of freedom in numerator and denominator; bold *p* values represent significant effects ($p < 0.05$).

† Temperature difference (0.01 °C) below logger resolution (± 0.14 °C) and accuracy (± 0.53 °C)

Data collection periods are indicated by superscripts (a-e):

[a] 10 October 2014 – 17 February 2015

[b] 18 December 2014 – 17 February 2015

[c] 04 November 2014 – 04 February 2015

[d] 20 December 2014 – 17 February 2015

[e] 20 December 2014 – 14 January 2016

Table 3.2. δ^{15}N-nitrate values of seawater collected from three patch reefs in Kāneʻohe Bay, Oʻahu, Hawaiʻi.

Site	*Date*	*δ^{15}N-nitrate (‰ vs. air)*
Reef 25	28 Oct 2014	3.8
Reef 44	09 Dec 2014	4.2
HIMB	20 Jan 2015	4.6
Reef 44	20 Jan 2015	4.9

Values are means of two technical replicates. Low [NO_3^- + NO_2^-] prevented δ^{15}N-nitrate analysis of some samples.

Table 3.3. Permutational multivariate analysis of variance (PERMANOVA) of bleached and non-bleached *Montipora capitata* and *Porites compressa* at three reefs during bleaching and recovery.

Species	*Effect*	*SS*	*df*	*F*	*p*
Montipora capitata	Period	0.561	1	11.714	**<0.001**
	Site	0.221	2	2.303	**0.006**
	Condition	0.149	1	3.113	**0.004**
	Period × Site	0.088	2	0.920	0.510
	Period × Condition	0.109	1	2.271	**0.029**
	Site × Condition	0.102	2	1.060	0.352
	Period × Site × Condition	0.062	2	0.652	0.880
	Residual	2.204	46		
Porites compressa	Period	0.497	1	10.024	**<0.001**
	Site	0.141	2	1.426	0.099
	Condition	0.190	1	3.840	**<0.001**
	Period × Site	0.145	2	1.459	0.094
	Period × Condition	0.143	1	2.883	**0.007**
	Site × Condition	0.133	2	1.344	0.133
	Period × Site × Condition	0.090	2	0.912	0.573
	Residual	2.331	47		

SS = sum of squares; *df* = degrees of freedom; bold *p* values represent significant effects ($p < 0.05$).

Table 3.4. Statistical analysis of bleached and non-bleached *Montipora capitata* and *Porites compressa* at three Kāne'ohe Bay patch reefs during bleaching and recovery*.

Response variable	Species			
	Montipora capitata		*Porites compressa*	
	Oct '14: Bleaching	*Jan '15: Recovery*	*Oct '14: Bleaching*	*Jan '15: Recovery*
chlorophylls	B < NB	—	B < NB	*HIMB*: B < NB
biomass	B < NB	—	B < NB	
proteins	2014 > 2015		—	—
lipids	—		—	HIMB > R44 = R25
carbohydrates	—		—	
energy content	—		2014 > 2015	
$\delta^{13}C_H$	B > NB		—	*HIMB*: B > NB
$\delta^{13}C_S$	2014 < 2015		—	B > NB
$\delta^{13}C_{H-S}$	2014 > 2015		—	
$\delta^{15}N_H$	HIMB > R25		2014 < 2015 HIMB > R44 = R25	
$\delta^{15}N_S$	—		HIMB > R44	
			B > NB	—
$\delta^{15}N_{H-S}$	—		B < NB	—
$C:N_H$	2014 < 2015		2014 < 2015	
	—	B > NB	B < NB	B > NB
$C:N_S$	—		—	

Table information shows significant model effects and *post-hoc* comparisons ($p < 0.05$); dashed lines indicate no significant effects ($p > 0.05$). **Periods* are October 2014 bleaching and January 2015 recovery. *Sites* (north to south) are Reef 44 (R44), Reef 25 (R25) and the Hawai'i Institute of Marine Biology (HIMB). Corals are described according to their physiological condition in October 2014, being bleached (B) or non-bleached (NB); condition designators from October (i.e., B/NB) were retained in January after corals regained pigmentation. Subscripts indicate either host (H) or symbiont (S) tissues, or their relative difference (H-S).

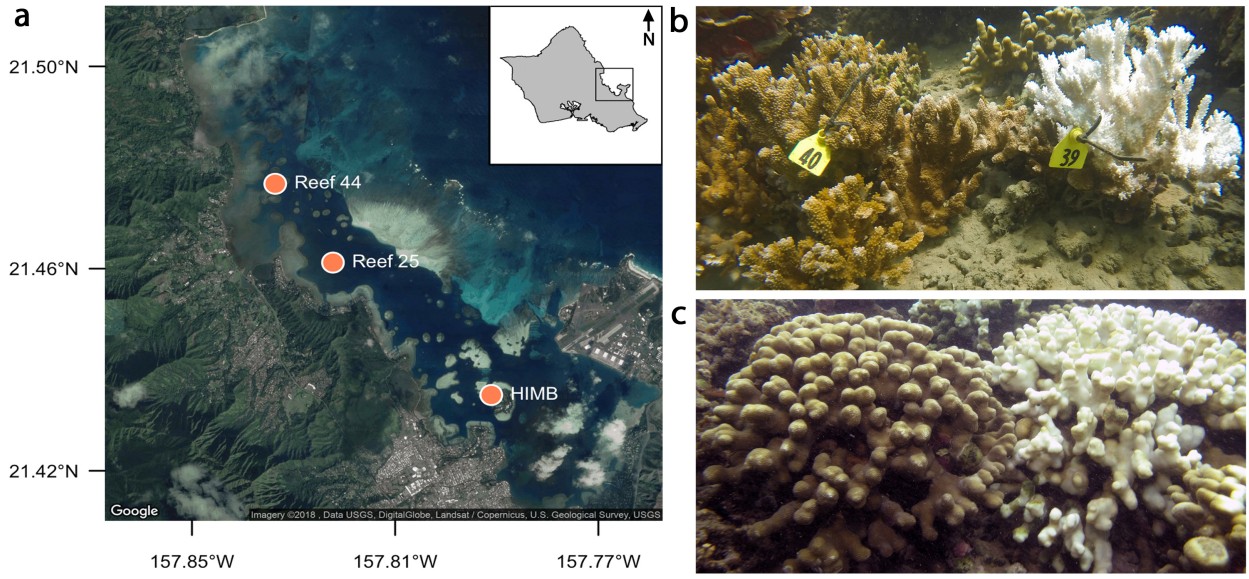

Figure 3.1. (**a**) Map of Kāneʻohe Bay on the windward side of Oʻahu, Hawaiʻi, USA, showing study sites Reef 44, Reef 25, and HIMB (Hawai'i Institute of Marine Biology). Bleached and non-bleached (**b**) *Montipora capitata* and (**c**) *Porites compressa* during a regional thermal stress event in October 2014. Photo credit (b-c): CB Wall

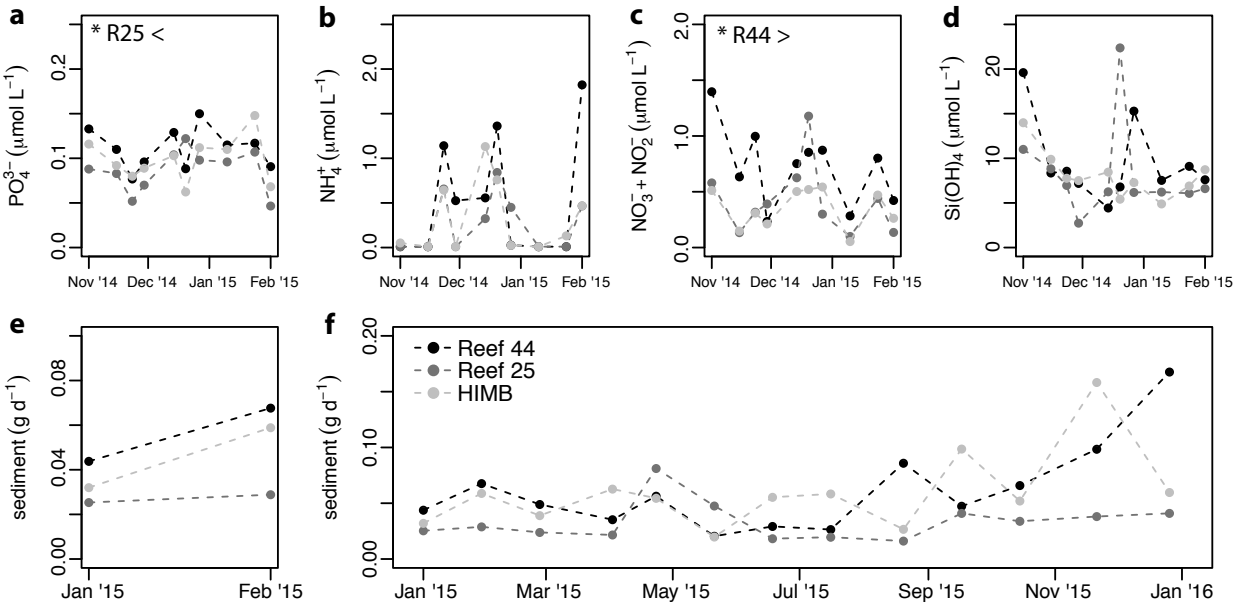

Figure 3.2. Dissolved inorganic nutrient concentrations (November 2014 – February 2015) and sedimentation rates (January 2015 – January 2016) at Reef 44, Reef 25, and HIMB in Kāneʻohe Bay. (**a**) Phosphate (PO_4^{3-}), (**b**), ammonium (NH_4^+), (**c**) nitrate + nitrite (NO_3^- + NO_2^-), and (**d**) silicate ($Si(OH)_4$) concentrations in seawater, and the (**e**) short-term and (**f**) annual sedimentation rates at the three reef sites. *Symbols* (*) indicate significant site effects ($p \leq 0.05$).

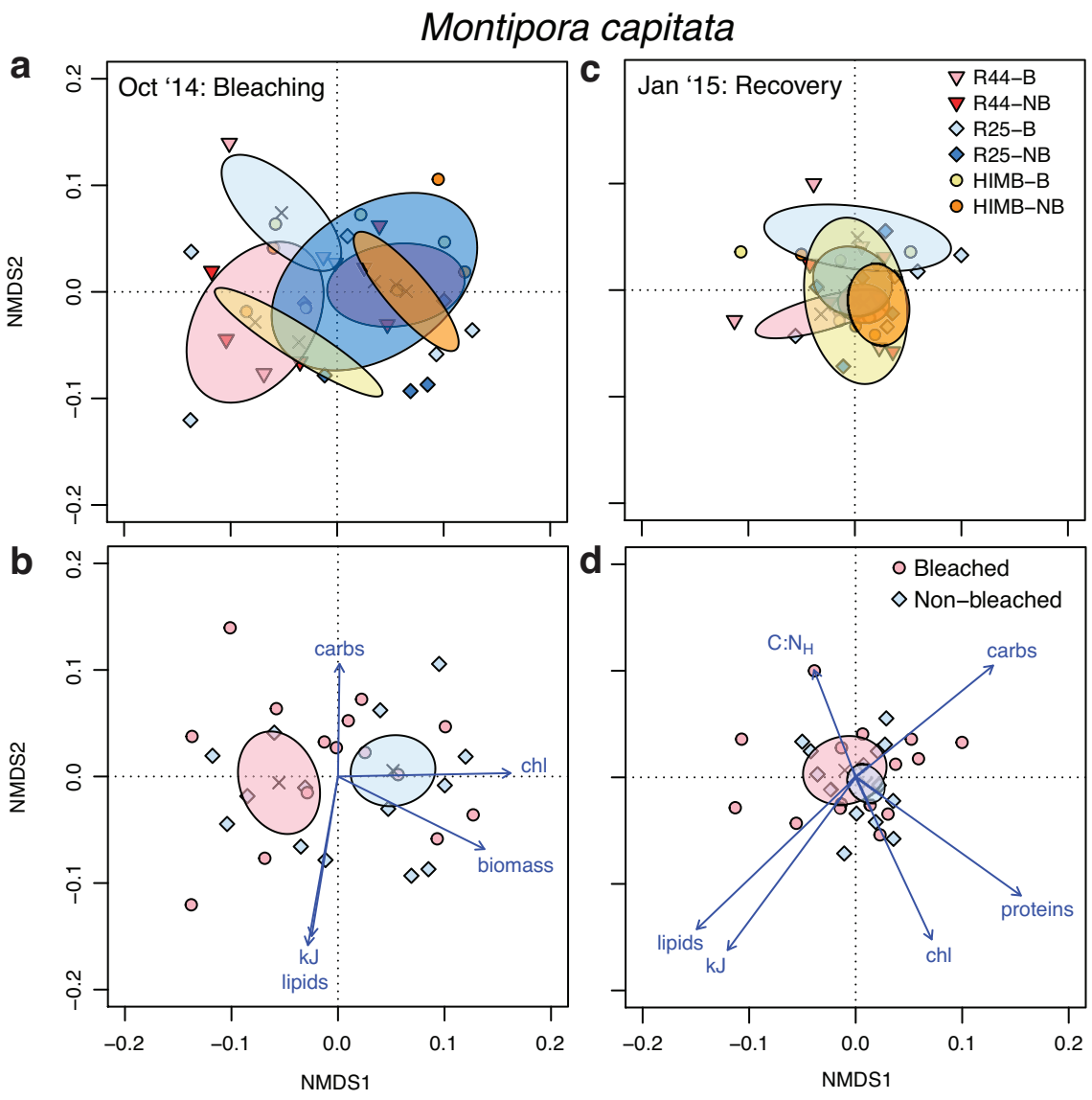

Figure 3.3. Multivariate non-metric multidimensional scaling (NMDS) plots for bleached (B) and non-bleached (NB) *Montipora capitata* at three reefs (Reef 44 [R44], Reef 25 [R25], HIMB) during bleaching (*left panel*) and recovery (*right* panel) a regional bleaching event. Polygons are standard error of point means (x *symbols*). (**a**, **c**) NMDS with site × condition effect. (**b**, **d**) NMDS with condition effect alone, with vectors showing significant responses ($p \leq 0.05$) among bleached and non-bleached corals.

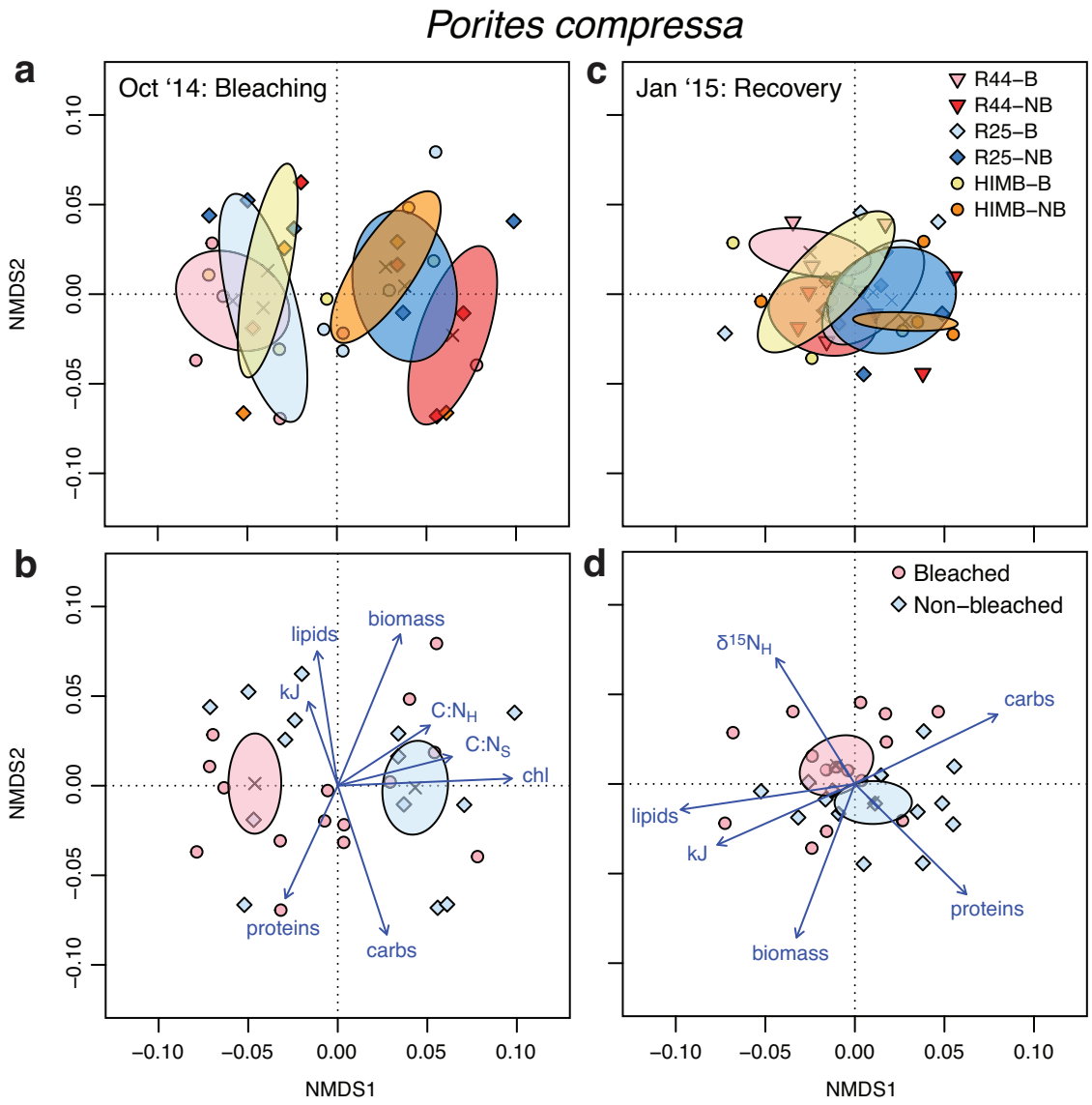

Figure 3.4. Multivariate non-metric multidimensional scaling (NMDS) plots for bleached (B) and non-bleached (NB) *Porites compressa* at three reefs (Reef 44 [R44], Reef 25 [R25], HIMB) during bleaching (*left panel*) and recovery (*right* panel) a regional bleaching event. Polygons are standard error of point means (x *symbols*). (**a**, **c**) NMDS with site × condition effect. (**b**, **d**) NMDS with condition effect alone, with vectors showing significant responses ($p \leq 0.05$) among bleached and non-bleached corals.

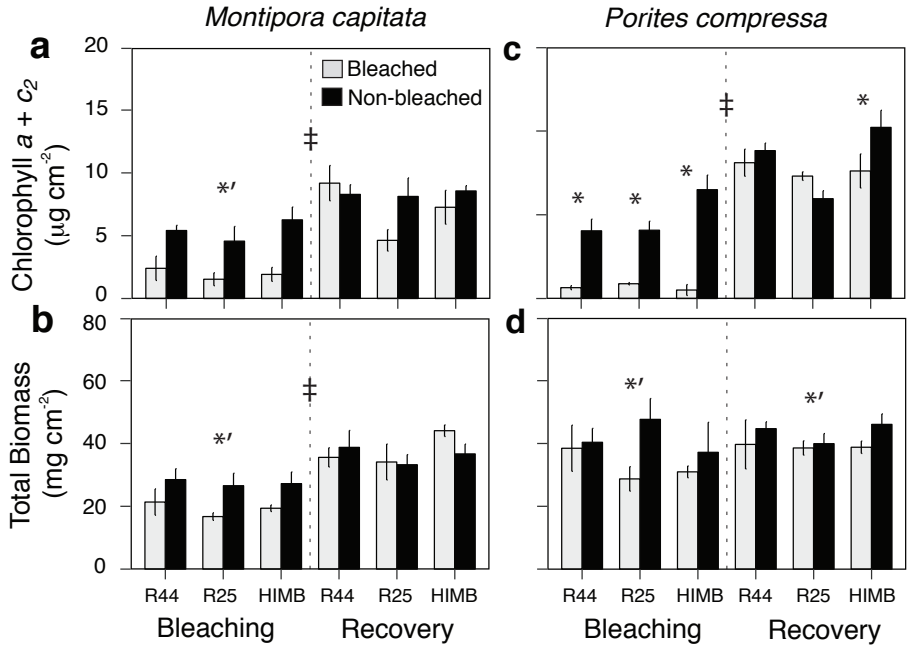

Figure 3.5. Chlorophyll and total biomass in bleached (*gray*) and non-bleached (*black*) *Montipora capitata* (*left panel*) and *Porites compressa* (*right panel*) at three reefs (Reef 44 [R44], Reef 25 [R25], HIMB) during bleaching and recovery. Area-normalized (**a**, **c**) chlorophyll ($a + c_2$) and (**b**, **d**) ash-free dry weight of tissue biomass. Values are mean ± SE ($n = 5$). *Symbols* indicate significant differences ($p \leq 0.05$) between periods (‡) and bleached and non-bleached corals within a period (*′) and within a site (*).

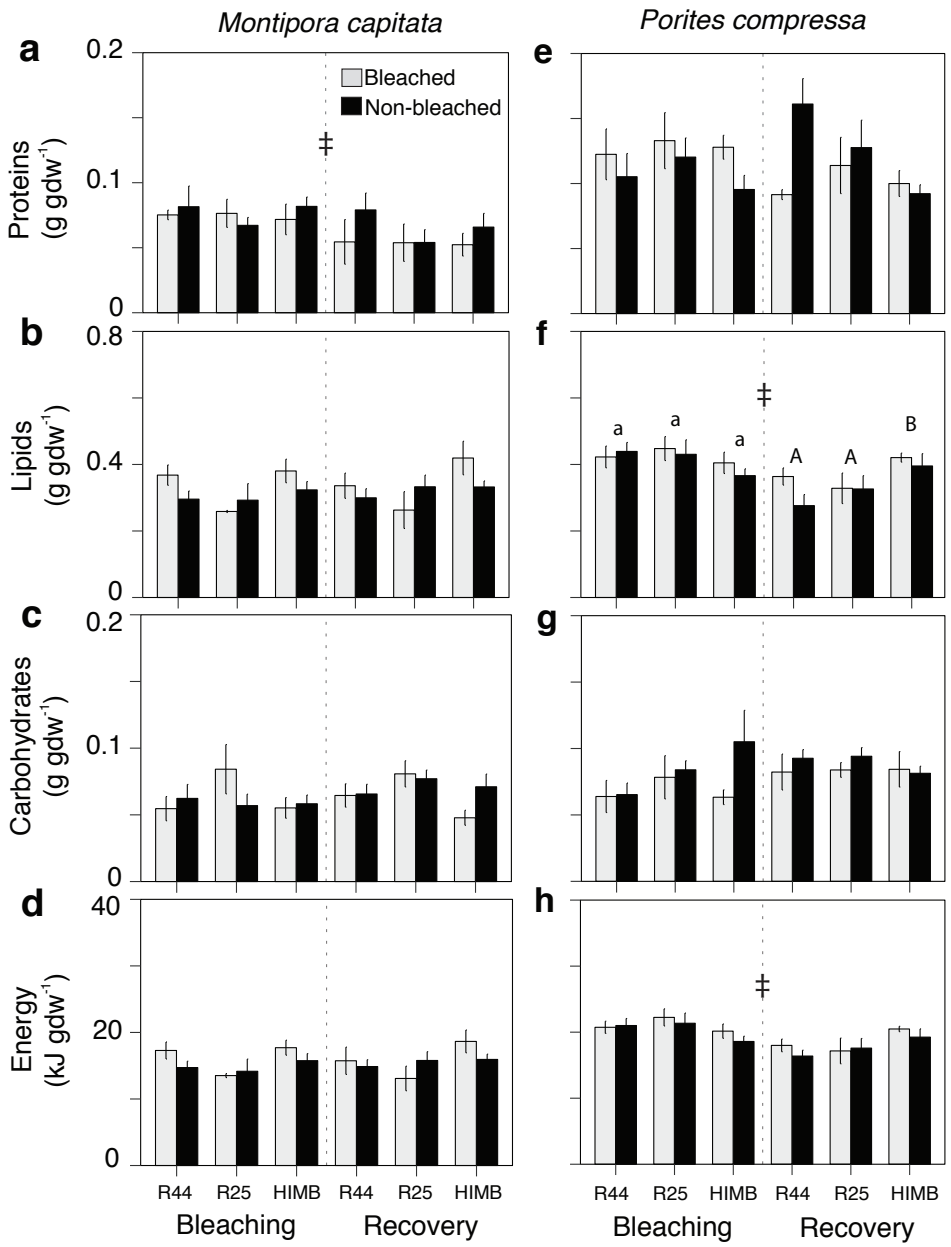

Figure 3.6. Biomass composition and energy content in bleached (*gray*) and non-bleached (*black*) *Montipora capitata* (*left panel*) and *Porites compressa* (*right panel*) at three reefs (Reef 44 [R44], Reef 25 [R25], HIMB) during bleaching and recovery. (**a**, **e**) Proteins, (**b**, **f**) lipids, (**c**, **g**) carbohydrates, (**d**, **h**) energy content (kJ) normalized to grams of ash-free dry weight (gdw^{-1}). Values are mean ± SE (n = 4 – 5). *Symbols* indicate significant ($p \leq 0.05$) period effects (‡); *letters* indicate differences between sites within periods of bleaching (*lowercase*) or recovery (*uppercase*).

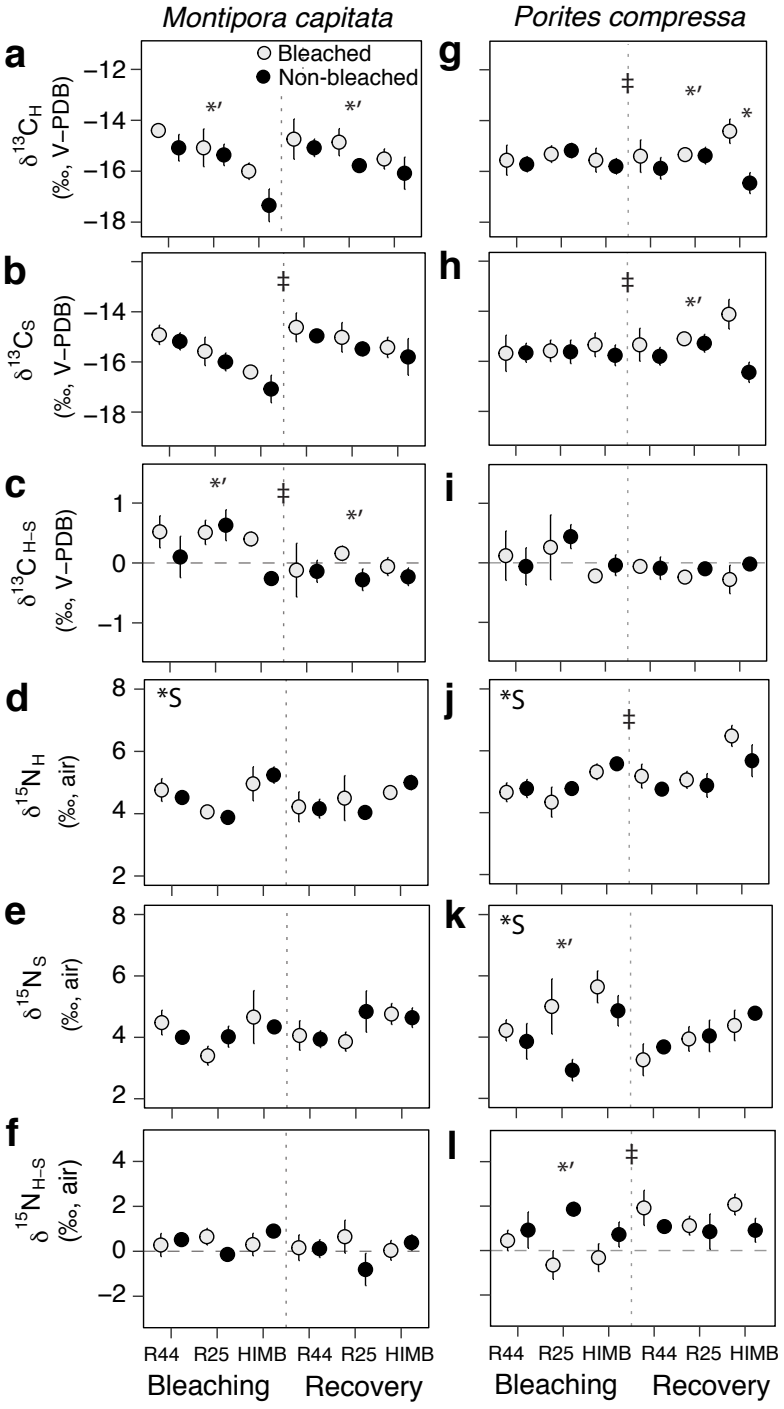

Figure 3.7. Isotopic analysis of bleached (*gray*) and non-bleached (*black*) *Montipora capitata* (*left*) and *Porites compressa* (*right*) host and symbiont tissues at three at three reefs (Reef 44 [R44], Reef 25 [R25], HIMB) during bleaching and recovery. Carbon ($\delta^{13}C$) and nitrogen ($\delta^{15}N$) isotopic values for (**a**, **g**, **d**, **j**) coral host ($\delta^{13}C_{H,}$ $\delta^{15}N_H$) (**b**, **h**, **e**, **k**) symbiont algae ($\delta^{13}C_{S,}$ $\delta^{15}N_S$) and (**c**, **i**, **f**, **l**) their relative difference ($\delta^{13}C_{H\text{-}S,}$ $\delta^{15}N_{H\text{-}S}$). Values are permil (‰) relative to standards for carbon (Vienna Pee Dee Belemnite: v-PDB) and nitrogen (air). Values are mean ± SE (n = 5); small SE may be masked by points. *Symbols* indicate significant ($p \leq 0.05$) period (‡) and site effects (*S), and differences among bleached and non-bleached corals within a period (*′) or a site (*).

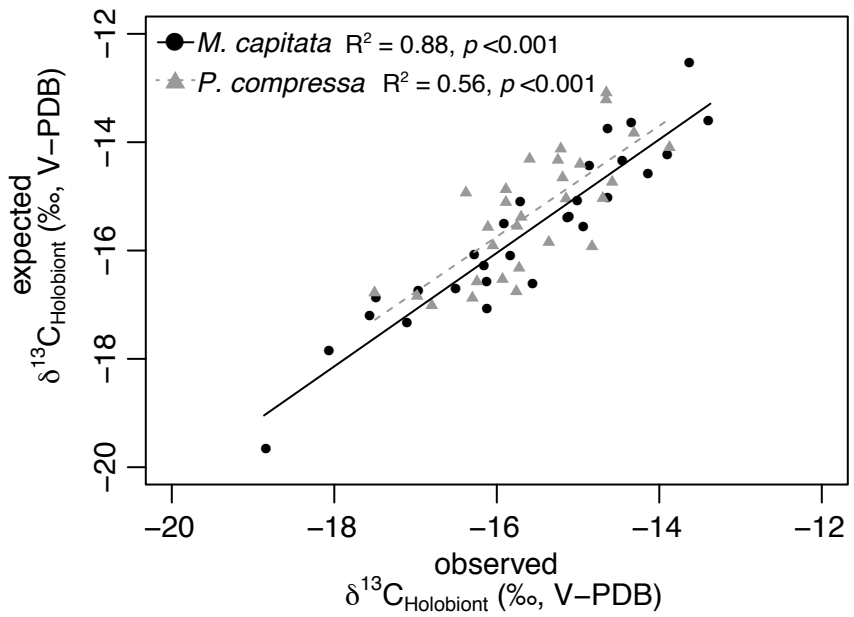

Figure 3.8. Relationship between observed and expected $\delta^{13}C_{Holobiont}$ for *Montipora capitata* (*black circles*) and *Porites compressa* (*gray triangles*) during post-bleaching recovery. Lines represent linear regression for *M. capitata* (*solid line*) and *P. compressa* (*dotted line*).

CHAPTER 4

DIVERGENT SYMBIONT COMMUNITIES DETERMINE THE PHYSIOLOGY AND ISOTOPE VALUES OF A REEF CORAL ACROSS A LIGHT AVAILABILITY GRADIENT

Abstract

Reef corals are mixotrophic organisms that meet metabolic demands through symbiont-derived photoautotrophy and the capture of particles and prey from seawater (collectively, heterotrophy). However, some symbiont genotypes (Family: Symbiodiniaceae) display environmentally mediated or genetically fixed opportunistic tendencies to the detriment of host nutrition and growth. In addition, the capacity for corals to exploit heterotrophy under normal or stressed conditions varies among species and is dependent on the composition and physiology of the symbiont community. To better understand the influence of the symbiont community on the biology and nutrition of reef corals, we sampled a single coral species (*Montipora capitata*) from a Hawaiian coral reef ecosystem (Kāneʻohe Bay) across depth (< 10 m) in two seasons, where *M. capitata* is dominated by *Durusdinium* and *Cladocopium* Symbiodiniaceae endosymbionts (hereafter, C- or D-colonies) at shallow and deeper depths, respectively. We observed symbiont community significantly influenced the physiology and $\delta^{13}C$ isotopic values of host and symbiont tissues and these effects were modulated by season and light availability across depths. D-colonies had higher symbiont densities, lower photopigments per symbiont cell and lower $\delta^{13}C$ values in host and symbiont tissues, consistent with lower carbon fixation rates and/or greater isotope fractionation. $\delta^{13}C$ values declined with depth; however, neither C- nor D-colonies showed signs of greater heterotrophy or nutritional plasticity. Changes in $\delta^{13}C$ values instead related to photoacclimation strategies that differed between symbiont communities. Together, these results reveal that the genetic composition and physiological properties of a coral's symbiont community influences holobiont $\delta^{13}C$ values and agree with laboratory studies suggesting *Durusdinium* symbionts being opportunists with reduced autotrophic potential.

Introduction

Nutrient exchanges between scleractinian corals and dinoflagellate symbionts (Symbiodiniaceae, formerly *Symbiodinium* spp.) (LaJeunesse et al. 2018) underpin the success of hermatypic reef corals as habitat engineers and energy transformers in coral reef ecosystems (Wild et al. 2011). Reef corals are reliant on the translocation of symbiont-derived compounds (i.e., glucose, amino acids, organic acids, free fatty acids) (Muscatine and Cernichiari 1969; Papina et al. 2003) to support respiratory demands (> 90%, Muscatine et al. 1984), skeletal growth (Gattuso et al. 1999) and the storage of high-energy compounds (i.e., lipids) (Baumann et al. 2014). In exchange, symbiont algae residing within host cells receive metabolic waste products (i.e., CO_2, NH_4^+) required for growth and photosynthesis (Rahav et al. 1989). However, climate change and local stressors can destabilize the coral-algae symbiosis, contributing to the decline of reef corals and the degradation of coral reef habitats (Vega-Thurber et al. 2014; Hughes et al. 2017). The persistence of reef corals into the future will depend on the capacity for corals and their symbionts to prevent symbiosis disruption and maintain energy acquisition under changing resource availability and stressful environmental conditions. Associations with stress tolerant symbiont genotypes may impart stressor resistance; however, the nutritional and energetic consequences of alternative host-symbiont associations in reef corals are not fully understood.

The genetic and functional diversity of Symbiodiniaceae shapes the energy balance and stress tolerance of reef corals. Molecular advances in the study of Symbiodiniaceae (Sampayo et al. 2009; Pochon et al. 2014) have revealed distinct symbiont genera and species (formerly clades and subclades) (LaJeunesse et al. 2018) each with different capacities to support coral nutrition (Stat et al. 2008; Pernice et al. 2014) and tolerate environmental stress (Baker 2003). For

instance, *Durusdinium* (formerly clade D) symbionts observed in human-impacted and/or thermally stressed reefs (Glynn et al. 2001; van Oppen et al. 2001; Baker et al. 2003; Stat et al. 2013) and *Symbiodinium* (formerly clade A) common on shallow reef zones of Red Sea and Caribbean (Ezzat et al. 2017; Baker et al. 2018) are tolerant of light and temperature stress but are generalist endosymbionts, assimilating and transferring less nutrition (carbon and nitrogen) to their coral hosts compared to common specialist endosymbionts, *Cladocopium* and *Brevolium* (formerly clade C and B, respectively) (Stat et al. 2008; Baker et al. 2013; Pernice et al. 2014; Ezzat et al. 2017; Matthews et al. 2017). As a consequence, opportunistic symbionts reduce coral tissue and skeletal growth and reproductive output compared to mutualistic symbionts (i.e., *Cladocopium* and *Brevolium*) (Cantin et al. 2009; Jones and Berkelmans 2010, 2011; Cunning et al. 2015). In order to cope with less autotrophic nutrition, coral's may require greater particle feeding to meet metabolic needs, as has been observed in corals under thermal stress (Grottoli et al. 2006) and high turbidity (Anthony 2006). Tradeoffs associated with harboring opportunistic symbionts, however, can be environmentally mediated and diminished under conditions of thermal stress (Baker et al. 2013; Cunning et al. 2015) or high light (Cooper et al. 2011c; Ezzat et al. 2017). Moreover, ecological selection and niche partitioning of Symbiodiniaceae and coral hosts among reef habitats (Sampayo et al. 2007; Bongaerts et al. 2010) can optimize coral performance despite symbioses dominated by less mutualistic symbionts (Cooper et al. 2011b, 2011c; Ezzat et al. 2017).

Environmental factors such as light availability/depth (Sampayo et al. 2007; Cooper et al. 2011c; Innis et al. 2018), water quality (Cooper et al. 2011a), temperature (Oliver and Palumbi 2011) and bleaching history (Jones et al. 2008; Lewis et al. 2019) play an important role in shaping

intraspecific changes in symbiont communities. The ability for corals to adapt to changes in photosynthetically active radiation (PAR, hereafter 'light') influence the ecological niche of reef corals (Hoogenboom et al. 2009), and many coral species exhibit shallow-to-deep transitions in symbiont communities. For example, shallow colonies of *Seriatopora hystrix* in Western Australia (Cooper et al. 2011b) and *Montipora capitata* in Kāne'ohe Bay, Hawai'i (Innis et al. 2018) are dominated by *Durusdinium* symbionts, whereas deeper colonies are more often dominated by *Cladocopium* symbionts; similar shallow-to-deep transitions from *Symbiodinium* (shallow) to *Cladocopium* (deep) have also been observed for *Stylophora pistillata* (Ezzat et al. 2017) in the Red Sea and Caribbean *Orbicella faveolata* (Baker et al. 2018). Where depth and turbidity attenuates light, corals can rely on the photoacclimatization potential of their endosymbionts (Cooper et al. 2011b) and/or particle feeding (collectively, 'heterotrophy') to meet metabolic demands (Anthony 1999, 2006). Stable isotope analyses are a useful tool in assessing the trophic ecology and nutrient fluxes in mutualistic symbiosis, such as reef corals (Ferrier-Pagès and Leal 2018). Carbon stable isotopes have shown a trend for greater heterotrophic capacity in some corals with increasing depth (Muscatine et al. 1989); however, the capacity for nutritional plasticity depends on the coral host (Alamaru et al. 2009) and the symbiont genotypes residing in tissues (Leal et al. 2015; Ezzat et al. 2017). The influence of symbiont community composition on the biology and nutrition of corals across natural environmental gradients has rarely been tested (but see Cooper et al. 2011b, 2011c), but is central to the understanding of the response of the coral holobiont to changing resource conditions.

Here, we examine the changes in the physiology and heterotrophic capacity of a Hawaiian reef coral (*Montipora capitata*) dominated by *Cladocopium* spp. or *Durusdinium glynnii* (Wham et al. 2017) symbionts (hereafter, C- and D-colonies) across a light-resource gradient (< 10 m) during summer and winter seasons. *M. capitata* shows depth-dependent shifts in symbiont communities (Innis et al. 2018), stress-induced changes in nutritional modes (Grottoli et al. 2006), and environmental stress resilience (Cunning et al. 2016; Wall et al. 2019); therefore, we predicted greater heterotrophic feeding would occur in this coral at environmental extremes (e.g., high- and low-light environments) or in response to opportunistic symbiont associations (i.e., *Durusdinium*). We observed distinct traits of symbionts in C- and D-colonies, which impacted carbon isotopic values but did not indicate changes in nutrition in either holobiont across space or time. These results are first evidence of *in situ* interactions of environmental and symbiont community composition effects on the physiology and isotope values in a single coral species over a small spatial gradients.

Materials and Methods

Site information

Montipora capitata (Dana, 1846) colonies were sampled from four reefs in the northern and southern lagoon of Kāneʻohe Bay on the windward side of the island of Oʻahu, Hawaiʻi, USA; one patch reef in the lagoon and one fringing reef adjacent to the shoreline were sampled in both the northern and southern regions of the bay (Figure 1). Reef locations were in northwest (NW) (21°28'46.5"N, 157°50'08.7"W), northeast (NE) (21°28'36.5"N, 157°49'33.1"W), southwest (SW) (21°26'40.3"N, 157°48'21.6"W), and southeast (SE) (21°26'14.9"N, 157°47'21.3"W) at Moku o Loʻe and the Hawaiian Institute of Marine Biology (Figure 4.1). Inshore Kāneʻohe Bay

is shallow (< 15 m) with high coral cover on near shore reef fringes and lagoon patch reefs (Bahr et al. 2015; Neilson et al. 2018). However, coral colonies are rare at >6 m in most locations and the as the benthos becomes dominated by fine-silt/mud (Smith et al. 1981).

Sampling periods were defined as "summer" and "winter", historically corresponding to periods of low and high seasonal rainfall (PACIOOS 2018). Summer coral samples were pooled from coral collections made in 2016 by Innis and colleagues (June 8, July 11 and 29, August 3 and 9), which have been previously used in describing the ecology of *M. capitata* symbiont community composition (Innis et al. 2018); winter samples were collected on December 19, 2016. While seawater temperatures in 2014 and 2015 were unseasonably warm due to El Niño conditions, causing bleaching across the Hawaiian archipelago (Bahr et al. 2017; Couch et al. 2017), seawater temperatures in 2016 did not deviate from historical averages (PACIOOS 2018) and bleaching was not observed in Kāneʻohe Bay.

Environmental conditions

To describe the light environments across the four locations photosynthetic active radiation (PAR) light loggers (Odyssey, Dataflow Systems Limited, Christchurch, New Zealand) were deployed at each of the four collection locations at 2 m depth from 10 June 2016 – 11 January 2016 recording every 15 min. Loggers were cross-calibrated using a LI-1400 quantum meter (Li-Cor, Lincoln, Nebraska, USA) attached to a cosine LI-192 underwater quantum sensor.

To compare light availability across depth, additional PAR loggers were deployed at three depth (< 1 m, 2 m, 8 m) during two deployment periods (9 – 17 October 2016 and 9 – 19 November

2016). These data were used to calculate attenuation coefficients (kd_x) and to estimate daily light integrals (DLI) at each site across colony depth ranges. At each site, light (DLI) and depth for logger at < 1 m and 8 m was relativized to the logger at 2 m (i.e., $\Delta DLI = DLI_{2m} - DLI_d$ and $\Delta depth = depth_{2m} - depth_d$). The log(ΔDLI) was analyzed in a no-intercept linear model with the predictor Δdepth as a continuous numeric variable. Model coefficients were saved and represent site-specific kd_x. We estimated the seasonal DLI for each sampled colony by calculating the mean DLI at 2m for summer months (June, July, August) and winter months (November, December, January), and then adjusting for colony-specific depth using the site-specific attenuation coeffeicient following a modified Beer-Lambert equation for light attenuation in water:

$$Ez_d = Ez_{2m}^{-kd_x*(\Delta depth)}$$

where Ez_d is DLI in mol photons m^{-2} d^{-1} at depth d in meters, Ez_{2m} is the mean seasonal DLI at 2 m depth, kd_x is the site-specific attenuation coefficient, and $\Delta depth$ is the difference in depth at 2 m and depth d.

Dissolved inorganic nutrients and SPM for isotope analysis

An analysis of seawater dissolved inorganic nutrients and the isotope values of plankton food sources (i.e., isotope end-members) were performed to account for site and/or seasonal differences in nutrient loading and heterotrophic food sources among reefs and between seasons. Seawater (ca. 25 L) was collected at each site on 10 August and 19 December 2016 to analyze dissolved inorganic nutrient concentrations. For nutrient analysis, 100 ml of seawater was immediately filtered (0.7 μm) through an acid-washed (0.1 N HCl) syringe into acid-washed Nalgene bottles. Samples were kept on ice and then frozen at -20 °C until analyzed. Molar

concentrations (μmol L^{-1}) of ammonium (NH_4^+), nitrate+nitrite (NO_3^- + NO_2^- or N+N), phosphate (PO_4^{3-}) and silicate ($Si(OH)_4$) were analyzed using a Seal Analytical AA3 HR nutrient autoanalyzer at the University of Hawai‘i at Mānoa SOEST Lab for Analytical Biochemistry.

Plankton sampling was performed at the four locations where corals were collected (detailed above), as well as two locations where corals were not collected in central Kāne‘ohe Bay (21°27'28.7"N, 157°49'37.5"W, and 21°27'35.2"N, 157°49'23.7"W) to increase spatial resolution of suspended particulates and sample sizes. At each location, plankton was sampled by pooling a vertical tow (< 10 m) and surface horizontal tows (63 μm mesh), visible debris or plant materials were removed, and plankton were size-fractioned with nylon mesh in two size classes: 100 – 243 μm and > 243 μm. Seawater samples (10 L) collected at 3 m depth were fractioned with nylon mesh into three size classes: < 10 μm, 10 – 100 μm, < 243 μm. All samples were filtered onto GF/F filters (0.7 μm) using a vacuum pump at low pressure, rinsed with ddH_2O, and dried at 60 °C overnight. Plankton samples were removed from filters and ground to a powder with mortar and pestle; seawater fractioned materials were left on the GF/F filter, which was subsampled for isotope analysis (detailed below). Samples were not acidified prior to analysis as this alters nitrogen isotope values (Schlacher and Connolly 2014).

Coral sampling and tissue analysis

In summer and winter, branch tip fragments (4 cm^2) were collected from *Montipora capitata* colonies at each reef locations chosen at random within three depth strata (< 2, 2 – 5, >5 m) that spanned the depth gradient where colonies were observed, with ca. 5 fragments per depth stratum (n = 15 samples $site^{-1}$). Depth and time of day were recorded for each colony with a submersible

depth gauge, and final depths were corrected to mean seawater height using NOAA tide data at 6-min intervals for Moku o Lo‘e (Station ID: 1612480) from CO-OPS API in a custom *R* code (Innis et al. 2018). Immediately after collection, corals were flash frozen in liquid nitrogen, transported to HIMB, and stored at -80 °C until processed for tissue analysis and DNA extraction.

Coral tissues were removed from the skeleton using an airbrushed connected to a SCUBA tank and supplied with filtered seawater (0.7 µm). The coral slurry was briefly homogenized, and aliquots were taken for physiology and isotopic analysis. Concentrations of symbiont cells were determined by microscopy using replicate counts ($n = 4 – 8$) of the tissue slurry on a haemocytometer. Photopigments chlorophyll *a* and c_2 were quantified by centrifuging an aliquot of the tissue slurry to isolate symbiont cells (13,000 rpm × 3 min), re-suspending the pellet in 100 % acetone, and extracting pigments at -4 °C for 24 h in darkness (Fitt et al. 2000). Chlorophyll concentrations were measured on a spectrophotometer using a glass 96-well plate at 630 nm and 663 nm on a spectrophotometer, and chlorophyll *a* concentrations quantified using equations for dinoflagellates (Jeffrey and Humphrey 1975). Total biomass of the holobiont tissue slurry was quantified as the difference between the dried (60 °C, 24 h) and combusted (450 °C, 4 h) masses, and quantified as the ash-free dry weight (AFDW) of coral biomass (Wall et al. 2019). All physiological metrics (cell densities, chlorophyll concentration, total biomass) were standardized to the surface area of the coral skeleton, measured using the wax-dipping technique (Stimson and Kinzie 1991), and chlorophyll was additionally normalized to symbiont cell abundance.

Stable isotope analysis

Stable isotope analysis was performed on suspended particles and plankton (collection methods detailed above), coral and symbiont tissues, and coral skeleton material were analyzed to examine the trophic ecology and nutrient exchanges between host and symbiont. To separate coral host and symbiont tissues, an aliquot of tissue slurry was filtered to remove carbonates (20 μm nylon mesh) (Maier et al. 2010) and then separated by centrifugation (2000 g × 3 min) with sequential filtered seawater (0.2 μm) rinses (Muscatine et al. 1989). Separated tissue fractions were lyophilized, ground with a mortar and pestle, and packed in tin capsules for analysis. Isotope values for carbon ($\delta^{13}C$) and nitrogen ($\delta^{15}N$) and tissue molar C:N ratio for coral host ($\delta^{13}C_H$, $\delta^{15}N_H$, $C:N_H$) and algal symbiont ($\delta^{13}C_S$, $\delta^{15}N_S$, $C:N_S$) were determined with a Costech elemental combustion system coupled to a Thermo-Finnigan Delta Plus XP Isotope Ratio Mass Spectrometer (IRMS) at the University of Hawai‘i at Mānoa SOEST Biochemical Stable Isotope Facility. Sample analytical precision of $\delta^{13}C$ and $\delta^{15}N$ was < 0.2 ‰ as determined by analysis of laboratory reference material run before and after every 10 samples, with coral/algae technical replicates deviating by < 0.1 ‰.

Coral skeleton samples were collected by shaving the uppermost layers of the coral skeleton (ca. 1 mm) using a Dremel tool equipped with a diamond-tip and ground to a powder with a mortar and pestle (Rodrigues and Grottoli 2006). Collected skeletal material (2 g) was stored in pre-cleaned and weighed glass vials with teflon lids; samples were not pre-treated in bleach prior to analysis (Grottoli et al. 2005). The carbon isotope values of coral skeletal carbonates ($\delta^{13}C_{Sk}$) in ca. 80 μg of skeletal material was acidified (100 % orthophosphoric acid) under vacuum at 90 °C in a common acid bath system where released CO_2 from reaction vessels analyzed by a GVI

Optima Stable Isotope Ratio Mass Spectrometer; carbonate analyses were performed by the University of California at Davis Stable Isotope Laboratory. Laboratory carbonate reference materials and technical replicates of coral skeleton deviated by 0.02 ‰ and < 0.2 ‰ for oxygen and carbon isotope values, respectively. To examine metabolic and kinetic isotope effects (KIE) on skeletal carbonates estimates for carbon and oxygen isotope equilibrium ($\delta^{13}C_{eq}$ and $\delta^{18}O_{eq}$, respectively) for skeletal aragonite were estimated using values from Schoepf et al. (2014), which calculated average Kāne'ohe Bay seawater $\delta^{13}C_{eq}$ values of +2.82 ‰ ($\delta^{13}C_{DIC}$ values of +0.12 ‰ [analyzed 2006 and 2007]) and estimated an average $\delta^{18}O_{eq}$ value of -1.24 ‰ for the range of temperature seen in Kāne'ohe Bay (23.0 – 28.0 °C) ($\delta^{13}C_{seawater}$ estimated at +0.4 ‰ [SMOW]) (Schoepf et al. 2014). A 0.33 slope was applied to isotope equilibrium to plot the KIE line, reflecting the simultaneous depletion in heavy isotopes of oxygen and carbon during kinetic and metabolic isotope effects, respectively (McConnaughey 2003). Carbon and nitrogen stable isotope ratios are reported using delta values (δ) in permil (‰) notation relative Vienna Pee-Dee Belemnite [V-PBD]) and atmospheric N_2 (air) for carbon and nitrogen, respectively. The relative differences of host and symbiont carbon ($\delta^{13}C_{H\text{-}S}$) and nitrogen ($\delta^{15}N_{H\text{-}S}$) isotope values were calculated as metrics for heterotrophic capacity (i.e., $\delta^{13}C_{H\text{-}S}$) and changes in trophic enrichment (i.e., $\delta^{15}N_{H\text{-}S}$) (Rodrigues and Grottoli 2006; Reynaud et al. 2009).

DNA extraction and symbiont community analysis

Symbiont communities in *M. capitata* were quantified by extracting DNA from whole corals or tissue slurry using DNA buffer (0.4 M NaCl, 0.05 M EDTA) with 1 or 2 % (w/v) sodium dodecyl sulfate, following a modified CTAB-chloroform protocol (Cunning et al. 2016; dx.doi.org/10.17504/protocols.io.dyq7vv). qPCR of extracted DNA consisted of quantifying

specific actin genes corresponding to internal transcribed spacer (ITS2) region of rDNA for *Cladocopium* spp. (ITS2 type C31) and *Durusdinium glynnii* (ITS2 type D1-4-6) (Wham et al. 2017), which are numerically dominant in Kāneʻohe Bay *M. capitata* (Cunning et al. 2016). *Symbiodinium* ITS2 and actin gene sequencing have previously validated the specificity of these symbiont-specific primers to the genera level (Cunning and Baker 2013). Two qPCR reactions (10 µl) were run for each coral sample using a StepOnePlus platform (Applied Biosystems) set to 40 cycles, internal cycle baseline of 3 – 15, and a relative fluorescence (ΔR_n) threshold of 0.01. Symbiont genera present in only one technical replicate were considered absent. In each sample, relative symbiont abundance (i.e., C:D ratio) was determined from amplification threshold cycles (C_T) for *Cladocopium* and *Durusdinium* (i.e., C_T^C, C_T^D) according to the formula C:D = 2^(C_T^C - C_T^D). Gene locus copy number and fluorescence intensity were used to normalize symbiont-specific C_T values (Cunning et al. 2016). *Cladocopium*- or *Durusdinium*-dominated symbiont communities were determined for each colony (i.e., C- or D-colonies) based on the numerical abundance of Symbiodiniaceae measured in qPCR (threshold: symbiont proportion > 0.5) (Innis et al. 2018).

Statistical analysis

Discrete environmental data (dissolved inorganic nutrient analysis, plankton) were analyzed with a linear model with reef locations and seasons as fixed effects. Due to seasonal changes in solar insolation and to compare previous reports of Symbiodiniaceae depth distribution in *M. capitata* (Innis et al. 2018) a generalized linear model (GLM) with a binomial distribution and logit link function was used with colony depth, season, and location treated as main effects. Best-fit GLMs were selected by AIC (Akaike 1978) and effects evaluated using Chi-square tests.

Biological response variables (physiology and isotope values) were analyzed in three-way linear mixed effect (LME) model (lmer in package *lme4* [Bates et al. 2018]) with season (winter *vs*. summer), light at depth (continuous variable), and dominant symbiont (*Cladocopium*- *vs*. *Durusdinium*-dominance) as fixed effects; reef location was treated as a random effect. Pairwise post hoc slice-tests of main effects were performed using estimated marginal means (EMMs) in package *emmeans* (Lenth 2019). Analysis of variance tables were generated using type II sum of squares for linear models in the package *car* (Fox and Weisberg 2011) and LME models in the package *lmerTest* (Kuznetsova et al 2017). Principal components analyses (PCA) of a scaled and centered correlation matrix was performed to examine the larger relationships of physiological and isotope response metrics and their clustering among spatiotemporal factors (i.e., season, location, colony depth-bins) and symbiont community. All statistical analyses were performed in *R* version 3.5.2 (R Core Team 2018). Data and scripts to reproduce analyses and figures are available at Github (github.com/cbwall/Coral-isotopes-across-space-and-time).

Results

Environmental conditions

Light availability—expressed as the daily light integral (DLI) at 2 m—from June – August 2016 (mean ± SE, n = 66 – 82) was highest in locations away from shore (NE and SE) and lowest at SW location (Figure 4.2). DLI from November 2016 – January 2017 was reduced compared to summer, but winter DLI values were similar among the four locations except for SW where light values were low. Using light attenuation coefficients for June 2016 – January 2017, estimated DLI values for < 1 m ranged from 17.3 – 21.3 ± 0.6 mol photons m^{-2} d^{-1} at all locations, except at

SW (9.8 ± 0.5 mol photons m^{-2} d^{-1}) and was attenuated by 61 % and 82 % at 2 m and 8 m, respectively (Figure 4.2).

Phosphate, N+N, and ammonium concentrations at all locations were higher in winter sampling (December 2016) compared to summer sampling (August 2016) ($p \leq 0.046$) (Table S1, Figure S2); silicate concentration showed no significant effects ($p > 0.323$). N+N was consistently higher in northern Kāneʻohe Bay (NW, NE) ($p < 0.001$), and in the winter phosphate increased at NE and NW locations.

Carbon and nitrogen isotope values of suspended particles and plankton did not differ between locations ($p \geq 0.146$) and seasonal effects were negligible ($\delta^{15}N$ enriched by 0.3 ‰ in winter relative to summer) ($p \geq 0.049$) (Table S1). Therefore, isotope values were pooled among the locations and seasons to generate isotope end member plots (Figure S3). Particle size fraction influenced both carbon and nitrogen isotope values ($p < 0.001$). Mean $\delta^{13}C$ value were similar for all samples (-21.1 to -20.4 ‰) but were 2 ‰ higher in the 10 – 100 μm fraction (-18.1 ‰). Mean $\delta^{15}N$ values were lowest in < 10 μm (5.3 ‰), intermediate in 100 – 243 μm (6.5 ‰), and highest in 10 – 100 μm fractions (7.4 ‰). In pooled fractions, small particles (< 243 μm) were ca. 1 ‰ depleted in ^{15}N relative to large particles (> 243 μm) (5.9 and 6.8 ‰, respectively).

Symbiont community, physiology, and isotope measurements

Corals were collected over comparable depth ranges in summer (0.2 – 9.4 m) and winter (0.2 – 7.7 m) (Figure S4). The distribution of dominant Symbiodiniaceae genera in *Montipora capitata* (C- *vs*. D-colonies) was depth-dependent in both seasons ($p < 0.001$), with a greater number of

D-colonies at shallow depths and greater C-colonies with increasing depth (Figure 4.3). Colonies with *Durusdinium* dominated symbiont communities ranged from 0.4 – 3.3 m depth (summer) but occasionally deeper (7.7 m, winter), although at lower frequencies (Figure 4.3). *Durusdinium* was also observed as a background symbiont member (proportion ≤ 0.35) across depths in summer (0.8 – 7.8 m) and winter (0.2 – 6.5 m).

A summary of physiology and isotope model effects can be found in Table 4.1. Total biomass (mg cm^{-2}) did not vary between seasons, across light environments, or between corals C- or D-colonies ($p \geq 0.109$) (Figure 4.4*a*). Symbiont densities (cells cm^{-2}) were lower in C-colonies relative to D-colonies ($p < 0.001$). Symbiont densities increased with light availability ($p = 0.013$) and were influenced by the season × light interaction ($p = 0.005$), where the positive relationship between light and symbiont density was lessened in the summer relative to the winter (Figure 4.4*b*). Total chlorophyll (μg $a + c_2$) was higher in winter ($p < 0.001$) and increased as light availability decreased ($p = 0.004$) (Figure 4.4*c*). C-colonies had more chlorophyll than those D-colonies ($p < 0.001$), although this effect varied by season × symbiont ($p = 0.022$). Chlorophyll concentrations were equivalent between C- and D-colonies in the summer; in winter months chlorophyll concentrations increased in C-colonies but not D-colonies (Figure 4.4*c*). Chlorophyll *a* per symbiont cell (pg $cell^{-1}$) did not differ significantly between seasons ($p = 0.098$), but decreased in response to high DLI ($p < 0.001$) and was higher in C-colonies ($p < 0.001$) (Figure 4.4*d*). As a random effect, location was a significant factor in models of physiological responses, accounting for 9 – 32 % of model variance (Figure 4.S5).

The carbon isotope composition of *M. capitata* tissues became progressively ^{13}C-enriched with increasing light availability for both coral host ($\delta^{13}C_H$) and the symbiont algae ($\delta^{13}C_S$) ($p < 0.001$) (Figure 4.5*a*-*b*). Host and symbiont $\delta^{13}C$ values in C-colonies were ^{13}C-enriched relative to D-colonies ($p < 0.001$), and these effects were seasonally dependent ($p \leq 0.031$). In host tissues, $\delta^{13}C$ values were 1.6 ‰ higher (summer) and 0.8 ‰ higher (winter) in C-colonies relative to D-colonies (Figure 4.5*a*). Similarly, $\delta^{13}C_S$ values were 1.5 ‰ higher in C-colonies in summer, but no difference was detected between C- or D-colonies in the winter (Figure 4.5*b*). The difference in host and symbiont carbon isotope values ($\delta^{13}C_{H\text{-}S}$) did not differ between C- or D-colonies (average ±0.2‰) and showed no interaction with light in summer. However, in winter $\delta^{13}C_{H\text{-}S}$ progressively increased as light decreased ($p = 0.040$) and was lower in D-colonies ($p = 0.037$) (Figure 4.5*c*). Carbon isotope values of coral skeletal carbonates ($\delta^{13}C_{Sk}$) were not affected by light availability ($p = 0.736$) but were affected by season ($p = 0.009$), being 0.4 ‰ enriched in the winter relative to summer (Figure 4.S6). Location accounted for 17 – 27 % of carbon isotope model variance (Figure 4.S5).

Host and symbiont $\delta^{13}C$ values were closely matched (Figure 4.5*c*) and attributes of the symbiont (i.e., symbiont densities and photopigments) showed the clearest statistical effects. Therefore, we examined the relationship between symbiont physiology and carbon isotope values (Figure 4.S7*a*-*c*). $\delta^{13}C_S$ values were positively related to symbiont densities in the winter, but not summer, for both C-colonies ($p < 0.001$, $R^2 = 0.360$) and D-colonies ($p = 0.007$, $R^2 = 0.708$). All colonies showed no relationship between $\delta^{13}C_S$ values and areal-chlorophyll concentrations in either season ($p \geq 0.414$); however, $\delta^{13}C_S$ values in C-colonies became ^{13}C-enriched (higher) as chlorophylls per symbiont cell declined in both summer ($p = 0.004$, $R^2 = 0.173$) and winter ($p =$

0.030, $R^2 = 0.115$). $\delta^{13}C_H$ values for C- and D-colonies exhibited identical effects as observed for $\delta^{13}C_S$ (data not shown). $\delta^{13}C_{H-S}$ values were only influenced by symbiont densities and became more positive with declining symbiont densities in summer D-colonies ($p = 0.004$, $R^2 = 0.478$) and in both C-colonies ($p = 0.014$, $R^2 = 0.145$) and D-colonies in winter ($p = 0.007$, $R^2 = 0.361$) (Figure 4.S8).

The nitrogen isotope composition of the coral host ($\delta^{15}N_H$) decreased with increasing light availability ($p = 0.045$) and did not change in response to seasons or symbiont communities ($p \geq 0.293$) (Figure 4.S9). Symbiont algae $\delta^{15}N_S$ values in C- and D-colonies were equivalent in summer, but marginally increased (0.3 ‰) in D-colonies relative to C-colonies in the winter months ($p = 0.017$) (Figure 4.S9). The difference between host and symbiont nitrogen isotope values ($\delta^{15}N_{H-S}$) was lowest in colonies under high light conditions and $\delta^{15}N_{H-S}$ increased as light declined ($p = 0.018$). $\delta^{15}N_{H-S}$ was equivalent among all colonies during summer but $\delta^{15}N_{H-S}$ increased (C-colonies) and decreased (D-colonies) in winter according to symbiont community ($p < 0.001$) (Figure 4.S9). Molar ratios of carbon:nitrogen (C:N) in host and symbionts showed no significant effects ($p \geq 0.134$) (Figure 4.S10). Location explained a large portion of variance for $\delta^{15}N_H$ (75 %) and $\delta^{15}N_S$ (80 %) models but less (< 20 %) in $\delta^{15}N_{H-S}$ and C:N models (Figure 4.S5).

Principal component analysis of biological responses

Data clustering revealed spatiotemporal trends in coral data among seasons, locations, symbiont communities, and colony depths (Figure 4.6) with two principal components (PCs) explaining 56 % of the variance in response metrics. Overall, PC1 separates corals with higher tissue $\delta^{13}C$

values from corals with high $\delta^{15}N$ values, and PC2 separates corals with high tissue biomass and symbiont density from those with high chlorophylls. Seasonal effects on colony responses were similar; however, greater shifts in chlorophylls and nitrogen isotope values were observed in the winter compared to the summer (Figure 4.6*a*). Corals showed limited clustering by location, with the exception of the NE location, which had higher PC1 values associated with $\delta^{13}C$ values (Figure 4.6*b*). Symbiont clustering reflected relationships along PC2 with D-colonies being associated with high symbiont densities and coral biomass and C-colonies having greater chlorophylls concentrations (total and per symbiont cell) (Figure 4.6*c*). Vertical zonation across depths showed corals at < 2 m depth were most distinct from other depths, and this mirrored effects of symbiont community in addition to a positive correlation with PC1 and $\delta^{13}C$ values (Figure 4.6*d*). In addition, there was less variation between corals with increasing depth, indicated by reduced ellipse area in deeper colonies relative to those at the surface.

Discussion

The combination of light stress at reef pinnacles and rapid attenuation of light with increasing depth contributes to the structure of Symbiodiniaceae and *Montipora capitata* in Kāne‘ohe Bay (Innis et al. 2018). The functional significance of these different symbiont communities has implications for symbiont niche partitioning, nutrient exchange in the holobiont (Ezzat et al. 2017), and thermal stress sensitivity (Cunning et al. 2016).

Environmental contexts

Light attenuation was rapid across the narrow depth gradient (0.5 – 8 m); the maximum PAR at 8 m in summer (100 – 350 μmol photons m^{-2} s^{-1}) and winter (50 – 200 μmol photons m^{-2} s^{-1}) in

Kāne‘ohe Bay was equivalent to the maximum PAR observed at 40 – 70 m in coral reefs of the Red Sea (Mass et al. 2007) and 20 – 40 m in Caribbean (Frade et al. 2007). This rapid light attenuation can in part be explained by the fine-grained particles that dominate inshore Kāne‘ohe Bay reefs (Smith et al. 1981), which settle slowly and are easily re-suspended, resulting in significant magnitude and duration of light attenuation (Storlazzi et al. 2015). Lower light intensities in winter relate to solar insolation and cloud cover; however, proximity to shoreline and stream runoff may also influence the overall lower light intensities at the SE location compared to other sites. Changes in nutrient concentrations were relatively small (< 0.5 – 1.0 μmol nutrients L^{-1}) and our sampling did not reveal large changes in nutrient enrichment among sites or seasons. Nevertheless, model results of reef location indicated a significant effect of location on response metrics, explaining between 9 – 32 % (physiology) and 17 – 80 % (isotope values) of model variation, indicating a degree of site-specific influence in our analyses, particularly for $\delta^{15}N$ values (discussed below). The limited replication at the reef scale ($n = 4$) limits our inference in interpreting spatial effects (i.e., reef type, bay region, proximity to shore), yet these factors are relevant and may be particularly important in considering effects of coastal biogeochemistry on corals in future studies.

Symbiont community effects on physiology and isotope composition

Symbiont communities in *M. capitata* were depth-dependent, and in both summer and winter months *Durusdinium* was the dominant symbiont in shallow *M. capitata* (< 2 m), with greater probability of *Cladocopium*-dominance with increasing depth. However, *Durusdinium* was not solely restricted to shallow depths and was observed as a dominant (at low frequency) and as a background symbiont (< 1 – 35 % of community) in corals down to 8 m depth. Intraspecific

shifts in symbiont communities generally occur over large depth ranges, for instance, *Stylophora pistillata* transitions from *Symbiodinium microadriaticum* (ITS2: A1) (< 10 m) to *Cladocopium* spp. (> 40 m) in the Red Sea (Ezzat et al. 2017), and *Seriatopora hystrix* transitions from *Durusdinium* spp. (< 23 m) to *Cladocopium* spp. (> 23 m) in western Australia (Cooper et al. 2001c). At the genus level, symbiont-specificity also occurs among closely related coral hosts, and this drives vertical zonation in symbiont genotypes (i.e., formerly subclades) over 10s of meters (Frade et al. 2007). However, rapid light attenuation and high turbidity along Kāne‘ohe Bay’s inshore reefs, has compressed a vertical zonation in *M. capitata* symbiont communities to within a few meters (< 2 m) of the surface (Innis et al. 2018; this study).

Globally, the prevalence of *Durusdinium* increases in corals from human-impacted reefs, including locations that experience higher temperatures and/or recent thermal stress, as well as high levels of sedimentation (reviewed in, Stat and Gates 2011). The high probability of shallow (ca. < 3 m) *M. capitata* being dominated by *Durusdinium* in Kāne‘ohe Bay likely reflects the greater capacity for *Durusdinium* to tolerate environmental stress, including high temperatures (Cunning et al. 2016), high light (Cooper et al. 2011c), poor water quality and high sedimentation compared to *Cladocopium* (Cooper et al. 2011a). The rarity of D-colonies at depth may also be explained by niche partitioning and poor performance of *Durusdinium* to under broad conditions of light intensity and quality (Mass et al. 2007, 2010). However, considering *M. capitata* symbionts are vertically transmitted, post-settlement selection of host-symbiont genotypes and their influence on holobiont population structure (Bongaerts et al. 2010) may also support spatial distribution of *Durusdinium* in Kāne‘ohe Bay *M. capitata* colonies.

Changes in symbiont densities and photopigmentation therefore are important to light-use efficiency and photoacclimation in reef corals. Across our study the density of *M. capitata* symbionts increased with light availability, whereas areal and cell-specific chlorophylls concentrations declined as light increased. Light effects on symbiont density were influenced by the high abundance of shallow colonies harboring *Durusdinium*, which had 54 – 58 % greater symbiont densities compared to C-colonies. Lower symbiont densities in C-colonies were matched with nearly double the concentration of chlorophylls per-symbiont-cell compared to D-colonies, which showed limited potential to regulate both areal and cell-specific chlorophyll concentrations in response to changing environmental conditions between seasons.

The inverse relationship between symbiont densities and chlorophylls (per cell) is indicative of photoacclimation driven by dynamic regulation of symbiont photomachinery (i.e., number of photosynthetic units [PSUs], photosystem II [PSII] turnover time, PSII functional absorption cross-section) (Falkowski and Raven 2007) that maximize light capture while mitigating photodamage through photoprotective mechanisms (i.e., nonphotochemical quenching). The increase in photopigmentation (areal and per cell) at low DLI/depth did not drive bleaching responses, which are observed in corals at extreme light limitations (Bessel-Browne et al. 2017). In Western Australia, shallow (< 23 m) *Seriatopora hystrix* harboring *Durusdinium* spp. also showed high symbiont densities with low chlorophyll $cell^{-1}$ compared to deeper colonies (> 23 m) harboring *Cladocopium* (Cooper et al. 2011c). Therefore, differences in symbiont community composition produce distinct holobiont traits that relate to symbiont-driven mechanisms for photoacclimation under contrasting light regimes.

Photoacclimation to periodic and annual changes in light availability is integral to maintaining positive energy budgets in photoautotrophs, especially in turbid near shore environments where light conditions can change dramatically over short periods. The kinetics of photoacclimation in response to changing light can be swift (5 – 10 d) (Anthony and Hoegh-Guldberg 2003a) and can buffer changes in photosynthesis in response to variable light conditions. Ultimately, the regulation of symbiont photopigments and cells optimizes photochemical efficiency at a given light environment. Therefore, the very high symbiont abundance in shallow *M. capitata* with *Durusdinium* symbionts is intriguing. While differences in symbiont densities could be a result of different sizes of algal cell, the range in coccoid cell sizes in described *Cladocopium* and *Durusdinium* species overlap (LaJeunesse et al. 2018) and attributing individual cell sizes to genotypes in mixed symbiont communities *in hospite* is problematic. Regulating symbiont abundance is important for many aspects of coral performance, including photosynthetic performance (Dennison and Barnes 1988) and stress responses. For instance, high densities of opportunistic symbionts correspond to greater respiratory costs that reduce overall photosynthesis:respiration and nutritional potential (Starzak et al. 2014). In addition, corals with high symbiont densities are more sensitive to stressful conditions that lead to symbiosis collapse (Cunning and Baker 2014) from a greater production of reactive chemical species (Weis 2008). High *Durusdinium* densities in *M. capitata* hosts, therefore, may relate to the photophysiology of this symbiont and its ability to avoid cellular mechanisms of symbiont expulsion relative to *Cladocopium*, although this may come at the expense of net productivity and autotrophic nutrition.

Alternatively, differences in symbiont densities may be driven by Symbiodiniaceae growth rates and/or responses to nutrient availability (Bayliss et al. 2019). The host controls symbiont population densities by limiting symbiont access to nitrogen (Falkowski et al. 1993), and excess nutrient availability in seawater (Ezzat et al. 2015) or from metabolism (i.e., heterotrophic feeding) increases symbiont densities (Houlbrèque et al. 2003). High *Durusdinium* densities may then also be attributed to changes in host metabolism, possibly stimulating ammonium production in the urea cycle and increasing nitrogen available to the symbiont (Matthews et al. 2018). For example, *Aiptasia* anemones infected with *Durusdinium trenchii* symbionts exhibited high rates of translocated products and/or derivatives being shuttled to the host's urea cycle, whereas this urea cycle feedback was not seen in anemones in symbiosis with *Brevolium minutum* (Matthews et al. 2018). *Durusdinium* does not appear more competitive for carbon or nitrogen assimilation compared to *Cladocopium* (Baker et al. 2013), and indeed shows reduced contribution of assimilated compounds to host growth and nutrition (Cantin et al., 2009; Pernice et al. 2014). Therefore, the retention of nutrients by *Durusdinium* in support of symbiont energy demands provides a testable hypothesis to explain high symbiont stocking in this coral-*Durusdinium* holobionts. Such metabolic tradeoffs with hosting opportunistic symbionts require further study, but may prove to be unexplored mechanism by which these symbiont benefit while imparting a metabolic cost to the coral host.

Stable isotope analysis

Coral trophic plasticity, or increases in heterotrophic derived nutrition, relate to periods of attenuated photoautotrophic nutrition as a result of environmental change, light availability, or physiological stress (Muscatine et al. 1989; Anthony and Fabricius 2000; Grottoli et al. 2006).

The isotopic composition of an organism's tissues reflects their food source and the discrimination of isotopically enriched compounds in metabolic reactions. We did not observe substantial variance in host or symbiont carbon isotope values that indicate heterotrophic plasticity over seasons, light environments, or symbiont community (discussed below). However, substantial and persistent effects of symbiont community on isotope values were observed, which in conjunction with physiological responses of holobionts, reveals unique differences among *Cladocopium* and *Durusdinium* harboring corals. We hypothesize that these differences correspond to the functional diversity and biology of and their influence on the coral host.

Our analyses of isotope values of *M. capitata* tissues (host, symbionts, skeleton) showed a decline in host and symbiont $\delta^{13}C$ with low-light/depth, in agreement with increased carbon isotope fractionation (i.e., reduced metabolic isotope effects) and reduced rates of carbon fixation in deep or low-light environments (Muscatine et al. 1989; Maier et al. 2010). Spatiotemporal changes in $\delta^{13}C$ values were reflected in both the host and symbiont, resulting in limited relative differences in carbon isotope values (i.e., $\delta^{13}C_{H\text{-}S}$)—a commonly applied metric for greater heterotrophy ($\delta^{13}C_{H\text{-}S}$ values < 0) relative to autotrophy ($\delta^{13}C_{H\text{-}S}$ values > 0) (Muscatine et al. 1989; Rodrigues and Grottoli 2006; Fox et al. 2018). Moreover, $\delta^{13}C_{H\text{-}S}$ values were generally positive in low-light corals (except for two C-colonies in summer) and became more positive with low-light in winter months. In addition, isotope analyses did not support the hypothesis that *M. capitata* responds to energetic consequences of hosting more opportunistic *Durusdinium* symbionts with greater heterotrophic nutrition. Furthermore, *M. capitata* did not show signs of changes its nutrition or trophic ecology as a response to changing light conditions or seasons, and

instead photoacclimatory mechanisms maintained autotrophic nutrition in corals, although these mechanisms appeared to be differ between symbiont communities. In Mo‘orea, French Polynesia, a similar lack of nutritional plasticity was observed in ten coral species among habitats of ranging human impacts in wet and dry seasons (Nahon et al. 2013). In Mo‘orea and Kāne‘ohe Bay, changes in host and symbiont $\delta^{13}C$ values appear related to differences in rates of isotopic fractionation and/or isotopic values of inorganic carbon sources used by symbionts in photosynthesis and not greater heterotrophic feeding (Nahon et al. 2013, this study).

Skeletal carbonate $\delta^{13}C$ values (i.e., $\delta^{13}C_{Sk}$) varied by 4 ‰ across all samples (-4 to -0.4 ‰), and this may reflect a combination of changes in light and nutrition (Grottoli and Wellington 1999), changing photosynthesis to respiration ratios (Maier et al. 2003), or dissolve inorganic carbon sources (Swart et al. 1996). However, the range and average $\delta^{13}C_{Sk}$ values (ca. -2.5 ‰) were consistent among seasons (< 0.5 ‰ among seasons) and did not decline with reduced DLI. Lower $\delta^{13}C_{Sk}$ values might be expected under conditions with declining symbiont productivity and greater metabolic fractionation and/or contributions of respiratory-derived ^{13}C-depleted carbon to the internal carbon pool used in biomineralization (Grottoli and Wellington 1999). Nevertheless, the relatively small differences in coral skeletal carbonates and $\delta^{13}C_{H\text{-}S}$ values across light environments and seasons suggest continued nutrient recycling among symbiotic partners, where photosynthesis dominated energy acquisition and autotrophy remained a principle source of coral nutrition even under extreme low-light conditions. Our analyses of *M. capitata*, therefore, reinforce the conclusion that facultative shifts in heterotrophic nutrition are species-specific (Palardy et al. 2005) and limited to extreme physiological conditions (i.e.,

bleaching [Grottoli et al. 2006], particle loading [Anthony and Fabricius 2000]) or geographic locations favoring mixotrophy (i.e., high near-shore productivity [Fox et al. 2018]).

Symbiont community determined $\delta^{13}C$ values in both the host and the symbiont tissues. In both C- and D-colonies, symbiont and host tissues became ^{13}C-depleted as light availability declined and symbiont community effects were seasonally dependent. $\delta^{13}C$ values in D-colonies values were on average 1.5 ‰ lower in summer ($\delta^{13}C_H$ and $\delta^{13}C_S$) and 0.8 ‰ lower ($\delta^{13}C_H$) in winter relative to C-colonies. Ultimately, these effects drove significant differences in $\delta^{13}C_{H\text{-}S}$ among C- and D-colonies in winter months, although responses to changing light availability were conserved in both holobionts and seasonally dependent. The significantly lower carbon isotope values in D-colonies may be the result of greater isotope fractionation and/or lower rates of growth and/or photosynthesis (Laws et al. 1995) in *Durusdinium* symbionts. For example, symbiont communities influence holobiont metabolism and production (Starzak et al. 2014). In laboratory experiments opportunistic symbionts such as *Durusdinium* and *Symbiodinium* had reduced carbon and nitrogen assimilation rates compared to *Cladocopium* (Stat et al. 2008; Pernice et al. 2014). Lower rates of nutrient assimilation and transfer may provide greater isotope discrimination and increase the incorporation of ^{12}C relative to ^{13}C during photosynthesis that are preserved during translocation where isotope effects are absent. In addition, symbiont communities influence metabolic processing of translocated products (Loram et al. 2007), and distinct metabolite profiles relating to organic carbon production and lipid metabolism have been reported for corals and anemones hosting different symbiont genotypes (Sogin et al. 2017; Matthews et al. 2018). Therefore, differences the functional diversity of symbiont genotypes

influences the production and biochemical processing of nutrition in corals that may have carry over effects on tissue isotope values.

Differences in coral tissue composition also contribute to changes in carbon isotope values (Tolosa et al. 2011). The isotopic composition of an organism relates to the relative proportion of lipids:proteins:saccharides and higher lipid-content relative to other compounds lead to lower tissue $\delta^{13}C$ values, and lipids are ^{13}C-depleted relative to other proteins and saccharides due to fractionation during lipid synthesis (Hayes 2001). We did not observe changes in the total biomass of *M. capitata* tissue or molar ratios of C:N in host or symbionts among symbiont communities, seasons or in response to light availability. However, the composition of coral tissue may have changed over time in response to changing resources (Anthony 2006; Leuzinger et al. 2011), stress and recovery (Rodrigues and Grottoli 2007; Wall et al. 2019), and symbiont community (Cooper et al. 2011c) along habitat gradients (Alamaru et al. 2009). In a flexible symbiont partnership, shallow *Pachyseris speciosa* harboring *Durusdinium* symbionts had double the concentration of storage lipid relative to structural lipids compared to deep colonies in symbiosis with *Cladocopium* (Cooper et al. 2011c). Also, changes in the contribution of autotrophic or heterotrophic carbon to lipid production change in response to symbiotic instability or depth (Alamaru et al. 2009; Baumann et al. 2014) that in turn influence tissue isotope values. Therefore, greater lipid biomass and/or heterotrophic carbon sources for lipid production may influence lower $\delta^{13}C$ values with decreasing light and these effects may be more pronounced in D-colonies relative to C-colonies. Conversely, the breakdown of ^{13}C depleted lipids (low $\delta^{13}C$ values) would increase the $\delta^{13}C$ values of residual tissues. Swart and colleagues (2005b) evaluated the temporal variability in $\delta^{13}C$ of respired CO_2 in *M. faveolata* over twelve

months and reported seasonality in $\delta^{13}C$ values of respired CO_2, ranging from high $\delta^{13}C$ values (ca. -9 ‰) in late spring (May – June) and low $\delta^{13}C$ values (ca. -17 ‰) in autumn (September – December), suggesting greater lipid catabolism in autumn months. Therefore, seasonally dependent isotopic enrichment in host tissues may be an effect of changes in energy reserve storage and catabolism. It is also possible that seasonal changes in metabolism relate to both dominant and background symbionts. This may be particularly true for D-colonies, which often have background *Cladocopium* symbionts in low abundance and also exhibited greater change in $\delta^{13}C$ values among seasons. Symbiont communities and metabolism are central to the physiological ecology and resilience of reef corals, however, these questions are often explored using gene expression and metabolomics approached (Matthews et al. 2018; Helmkampf et al. 2019). Identifying symbiont-driven effects on coral metabolism, energy storage and nutriton at the physiological level (Cooper et al. 2011a) are needed to supplement "–omics" approaches in order better understand and identify tradeoffs in host-symbiont interactions.

Nitrogen isotope values in the host and symbiont showed limited statistical effects relative to carbon. Where significant effects were observed for $\delta^{15}N$ values, effect sizes were small (< 0.5 ‰). Overall, slight increases in $\delta^{15}N_H$ values were observed as light-availability declined, and winter C-colonies had lower $\delta^{15}N_S$ and higher $\delta^{15}N_{H-S}$. $\delta^{15}N$ values showed a large range but were similar in both symbiotic partners (ca. 2.7 – 6.0), and the pattern in trophic enrichment followed predictions of greater ^{15}N-enrichment in the host compared to its symbiont, although this is well below the 1.5 – 3.0 ‰ enrichment seen non-symbiotic food webs (Minagawa and Wada 1984). The absence of clear effects of light or symbiont community on $\delta^{15}N$ values can indicate high rates of photosynthesis and nitrogen-limitations in the holobiont (Maier et al.

2010). However, light effects on $\delta^{15}N$ values in corals in the lab and field are variable and inconsistent (Heikoop et al. 1998; Reynaud et al. 2009), and we observed poor relationships between $\delta^{15}N$ values and physiological metrics related to photosynthesis and photoacclimation. Photoacclimation, however, had a clear influence on *M. capitata* host and symbiont $\delta^{13}C$ values, which showed significant negative relationships with photopigmentation (pg cell^{-1}) and to a lesser extent a positive relationships to symbiont densities (Figure 4.3; Figure 4.S7), and these effects were more pronounced in C-colonies. Light-dependent fractionation predicts shared expression of ^{13}C and ^{15}N discrimination (i.e., greater fractionation) as photosynthesis becomes light-limitations (Granger et al. 2004); thus, trends in ^{13}C and ^{15}N depletion in host and symbiont are expected with increasing depth (Muscatine and Kaplan 1994; Heikoop et al. 1998). Yet, we observed the opposite: when light was abundant $\delta^{15}N$ values were low when $\delta^{13}C$ values were high. In other words, when photosynthesis was high and carbon isotopic fraction reduced, nitrogen isotope fractionation appeared minimal. The cause for this trend in carbon and nitrogen isotope values and light-independent patterns in $\delta^{15}N$ values is unclear, but may relate to changes in internal or external nitrogen pools as a result of photoacclimation-driven processes, increased nitrogen recycling during high rates of photosynthesis/growth (and $\delta^{13}C$ value high), or greater utilization of ^{15}N-enriched nitrogen sources under conditions where $\delta^{13}C$ values (and photosynthesis rates) are low.

An additional explanation for the large range in $\delta^{15}N$ values is linked to spatiotemporal variability in the nitrogen sources available to corals. For instance, reef location explained 75 – 80 % of $\delta^{15}N_H$ and $\delta^{15}N_S$ model variance, and differing proximities to terrigenous nutrient sources (i.e., shoreline, watersheds, subterranean groundwater discharge) relative to oceanic

inputs (Dailer et al. 2010), and the removal (denitrificaiton) and addition (fixation) of isotopically light nitrogen to the dissolved nitrogen pool influence $\delta^{15}N$ values at the base of the food web (Sigman and Casciotti 2001). The average nitrogen isotope values in plankton and suspended particles ranged by 2 ‰ (5.5 – 7.5 ‰) and average $\delta^{15}N$-nitrate values in Kāne‘ohe Bay (winter 2014) range from 3.8 – 4.9 ‰ (Wall et al. 2019). While our limited sampling of the carbon and nitrogen isotope values did not reveal substantial spatiotemporal effects on size-fractioned plankton/suspended particles, spatial effects on $\delta^{15}N$ values have been previously reported in corals (Wall et al. 2019) and stingrays (Dale et al. 2008) within Kāne‘ohe Bay in relation to oceanic and terrestrial nutrient inputs. Considering the values of heterotrophic sources in seawater, corals and their symbionts most resemble the $\delta^{15}N$ isotopic composition of dissolved inorganic nitrogen (DIN), which through the coral-symbiont nitrogen cycle is assimilated by the symbiont and transferred to the coral host (Kopp et al. 2013) to be metabolized and excreted into the internal nitrogen pool once more available to the symbiont. This forward- and back-translocation of nitrogen products among symbiotic partners and the diverse nitrogen end members available for corals (Houlbrèque and Ferrier-Pagès 2009) minimizes trophic enrichment and complicates nutritional inferences based on coral $\delta^{15}N$ values (Reynaud et al. 2009).

The genetic and functional diversity of Symbiodiniaceae genotypes influences the energetics and performance of reef corals. Environmental pressures (e.g., light, temperature, sedimentation) can lead to shifts in coral-Symbodiniaceae communities that allow for opportunistic, symbiont generalists to persist in coral populations with consequences for stress tolerance, nutrient exchanges, and holobiont physiology. Environmental effects on coral metabolism and nutrition

have been widely studied using stable isotope, but rarely have these studies accounted for symbiont community effects *in situ*. Discounting or ignoring the diversity in symbiont communities and their influence on the holobiont, therefore, has the potential to confound isotopic inferences in reef corals. Our results show substantial effects of symbiont community on the physiology and isotope values ($\delta^{13}C$) in a single coral species that occurs over narrow habitat range across a light/depth gradients. Importantly, we show symbiont communities (C vs. D-colonies) produced distinct patterns in the cell densities and chlorophylls per symbiont cell and these properties of the symbiont predicted changes in $\delta^{13}C$, but not $\delta^{15}N$, isotope values. These results indicate environmental and symbiont community effects on photoacclimation and symbiont standing stock are driving changes in $\delta^{13}C$ values in the holobiont. However, neither environment nor symbiont communities indicated greater reliance on heterotrophic nutrition. Together, these findings show symbiont diversity and function (i.e., photoacclimation, nutrient transfer) produce discrete patterns in stable isotope values in reef corals, and these patterns relate to niche partitioning in response to environmental pressure. Finally, we identify symbiont community effects as an important, yet often overlooked, component to isotopic investigations into coral physiological ecology. There is a need to unravel ecological implications of symbiont functional diversity on coral nutritional plasticity, host-symbiont nutrient exchanges, and coral biomass properties (i.e., tissue composition) in order to accurately quantify costs and benefits of symbiont communities now and into the future.

Funding

CBW was supported by funds from the Colonel Willys E. Lord & Sandina L. Lord Endowed Scholarship, UH Mānoa SOEST/HIGP Denise B. Evans Fellowship in Oceanographic Research,

and an Environmental Protection Agency (EPA) STAR Fellowship Assistance Agreement (FP-91779401-1). The views expressed in this publication have not been reviewed or endorsed by the EPA and are solely those of the authors.

Acknowledgements

All corals were collected under State of Hawai‘i Division of Aquatic Resources Special Activity Permit 2016-55 and 2018-03. We thank R. Cunning, T. Innis, R. Ritson-Williams, A. Huffmyer for field assistance, S. Matsuda, E. Lenz, A. Amend, A. Moran, C. Sabine for comments and fruitful discussion, and W. Ko, N. Wallsgrove, and H. Spero for stable isotope analyses. We dedicate this publication to the memory of our dear friend, colleague, and mentor Dr. Ruth Gates.

Table 4.1. Statistical analysis of *Montipora capitata* host and symbiont physiology and tissue isotope values from four locations in Kāneʻohe Bay along a depth gradient in summer and winter.

Response variable	*Effects*				
	Season	Light	Symbiont	Season × Light	Season × Symbiont
biomass	--	--	--	--	--
symbionts	--	0.010	<0.001	0.004	--
total chlorophylls	<0.001	0.004	<0.001	--	0.022
chlorophyll per cell	--	<0.001	<0.001	--	--
$\delta^{13}C_H$	--	<0.001	<0.001	--	0.031
$\delta^{13}C_S$	--	<0.001	<0.001	--	0.001
$\delta^{13}C_{H-S}$	0.002	--	<0.001	0.040	0.037
$\delta^{13}C_{Sk}$	0.009	--	--	--	--
$\delta^{15}N_H$	--	0.040	--	--	--
$\delta^{15}N_S$	--	--	0.008	--	0.017
$\delta^{15}N_{H-S}$	--	0.018	0.002	--	<0.001
$C:N_H$	--	--	--	--	--
$C:N_S$	--	--	--	--	--

Table information shows significant model effects ($p < 0.05$); dashed lines indicate no significant effects ($p > 0.05$). *Season* = summer or winter, *Light* = light at depth of collection, *Symbiont* = *Cladocopium* spp. (formerly clade C) or *Durusdinium glynnii* (formerly clade D)-dominated symbiont community. Subscripts indicate either host (H) or symbiont (S) tissues, or their relative difference (H-S), and skeletal carbonates (Sk).

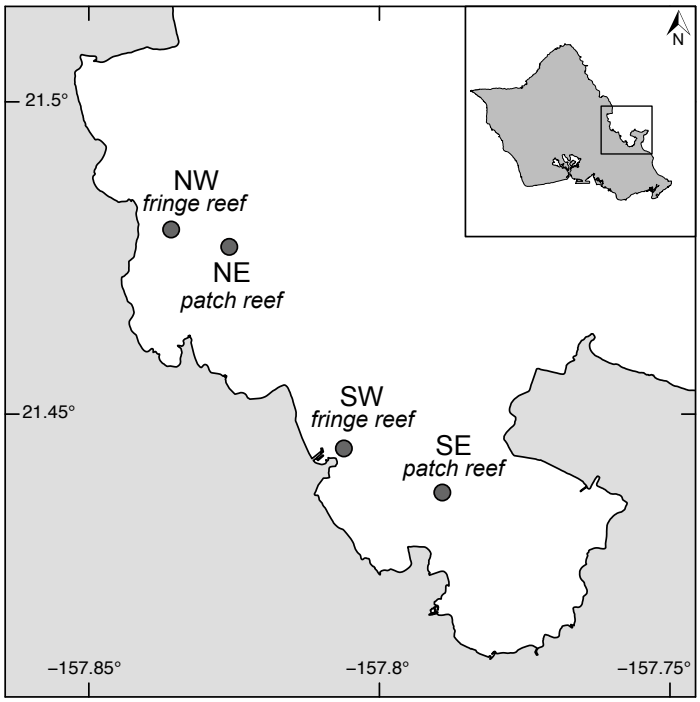

Figure 4.1. Map of Kāneʻohe Bay on the windward side of Oʻahu, Hawaiʻi. *Circles* indicate the two fringing reef and two patch reef where corals were collected: the Northwest (NW), Northeast (NE), Southwest (SW) and Southeast (SE) locations.

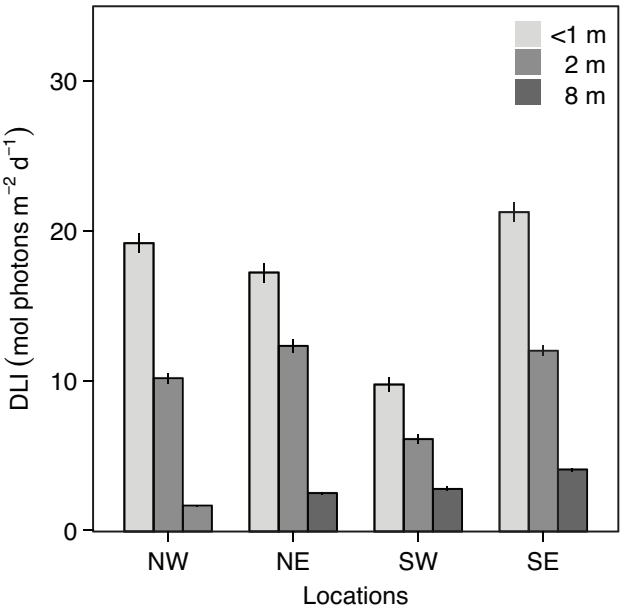

Figure 4.2. Daily Light Integral (DLI) at four reef locations where corals were collected, averaged over the study period (10 June 2016 – 12 January 2017) at <1 m, 2 m and 8 m depth. Values are mean ± SE (n = 163 – 202).

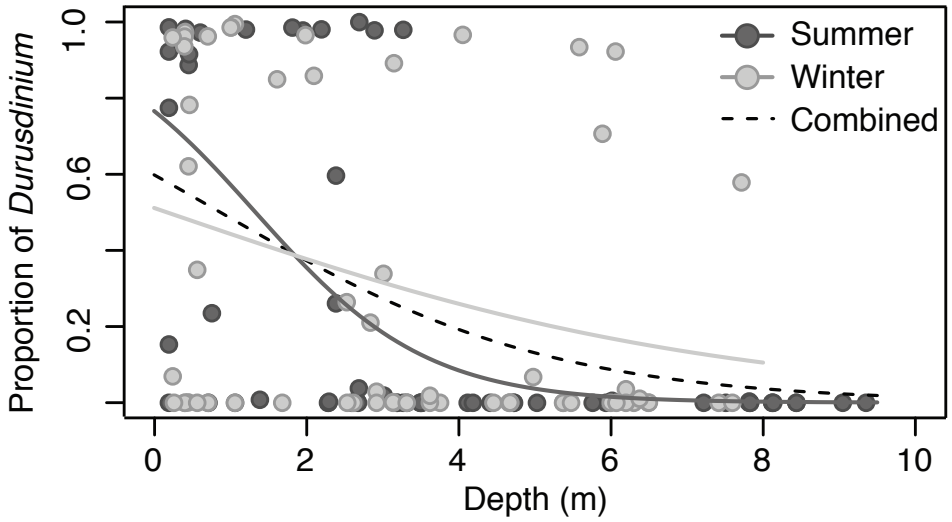

Figure 4.3. Symbiont community in *Montipora capitata* colonies collected in summer (dark gray) and winter (light gray) as a function of the proportion of *Durusdinium* relative to *Cladocopium* across (**a**) depth of collection and (**b**) light availability, represented as the daily light integral (DLI). Lines represent logistic regression models by each season (*solid* lines) and the combined summer plus winter dataset (*dotted* line).

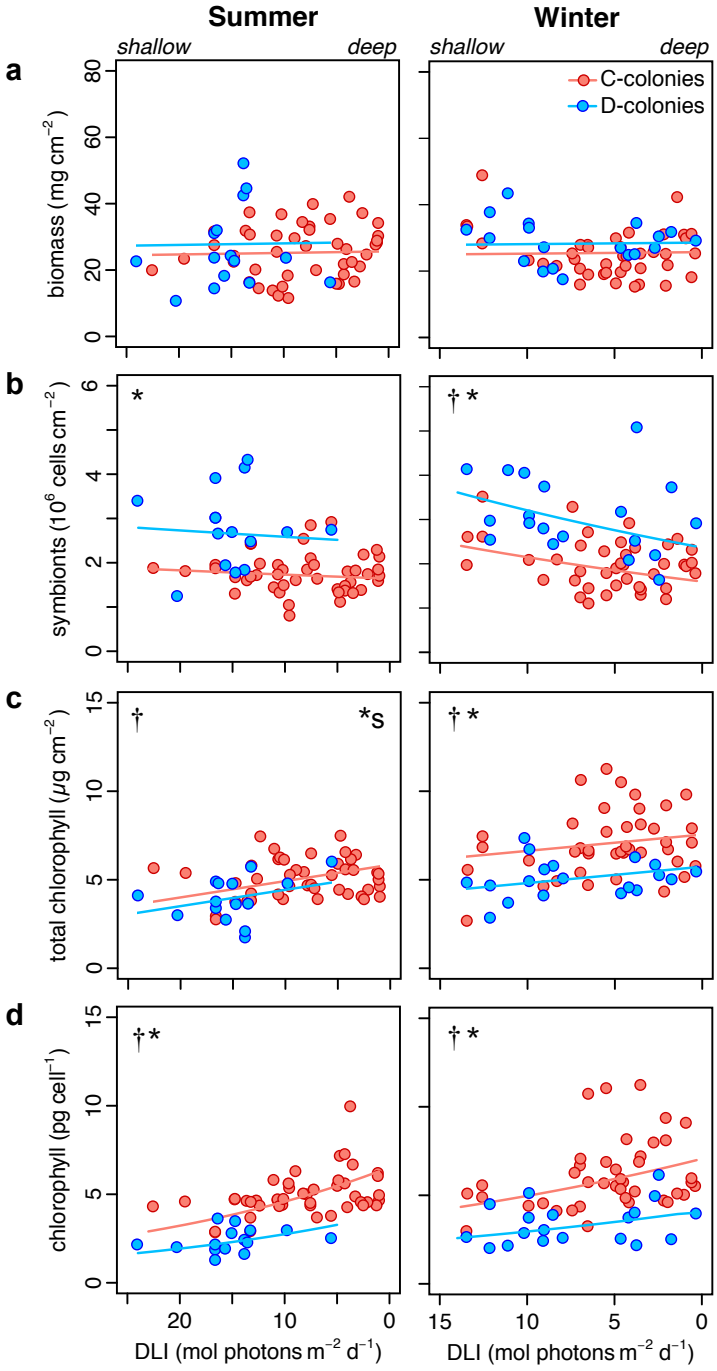

Figure 4.4. Physiological metrics for *Montipora capitata* colonies dominated by C (*Cladocopium* spp.) or D (*Durusdinium* spp.) symbionts. Colonies were collected from four Kāne'ohe Bay reef locations in summer (*left*) and winter (*right*) spanning a light availability gradient across <1 m – 9 m depth. Area-normalized (**a**) total tissue biomass, (**b**) symbiont cell densities, (**c**) total chlorophylls ($a + c_2$), and (**d**) chlorophylls per symbiont cell. Solid lines represent linear mixed effect model fits. *Symbols* indicate significant differences ($p < 0.05$) between symbiont communities (*), in response to light (†), and between seasons (*s).

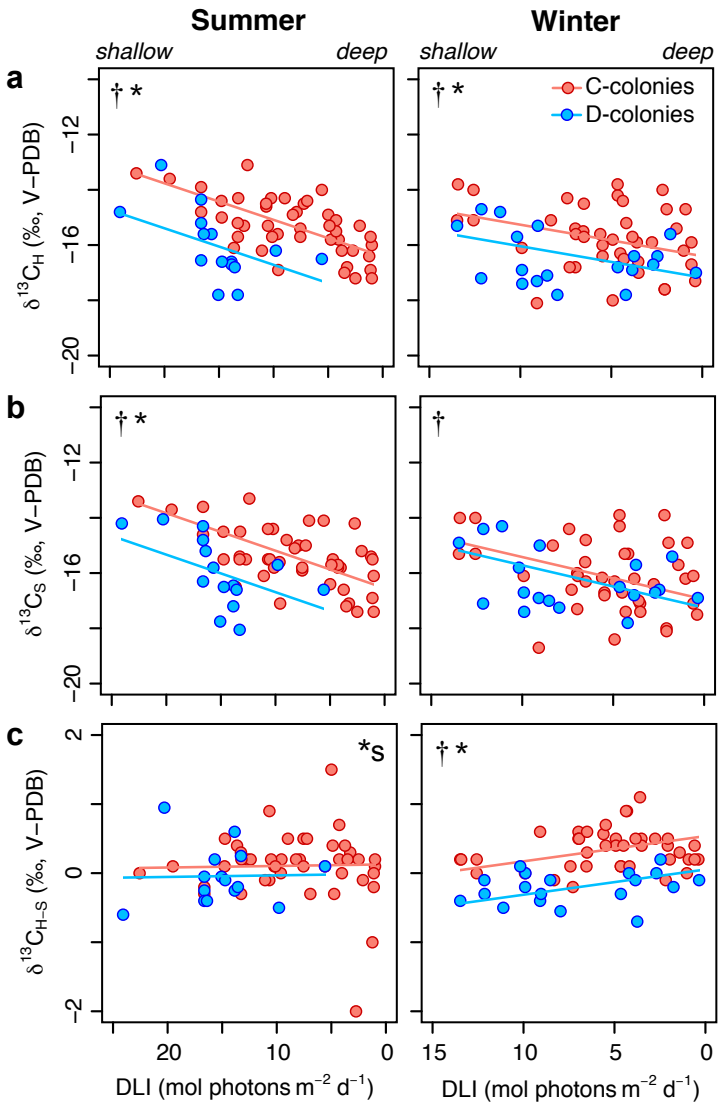

Figure 4.5. Carbon stable isotope values for *Montipora capitata* colonies dominated by C (*Cladocopium* spp.) or D (*Durusdinium* spp.) symbionts. Colonies were collected from four Kāneʻohe Bay reef locations in summer (*left*) and winter (*right*) spanning a light availability gradient across <1 m – 9 m depth. Values are for (**a**) coral host ($\delta^{13}C_H$) (**b**) symbiont algae ($\delta^{13}C_S$) and (**c**) their relative difference ($\delta^{13}C_{H\text{-}S}$) in permil (‰) relative to carbon standards (Vienna Pee Dee Belemnite: V-PDB) and nitrogen (air). Solid lines represent linear mixed effect model fits. *Symbols* indicate significant differences ($p < 0.05$) between symbiont communities (*), in response to light (†), and between seasons (**s*).

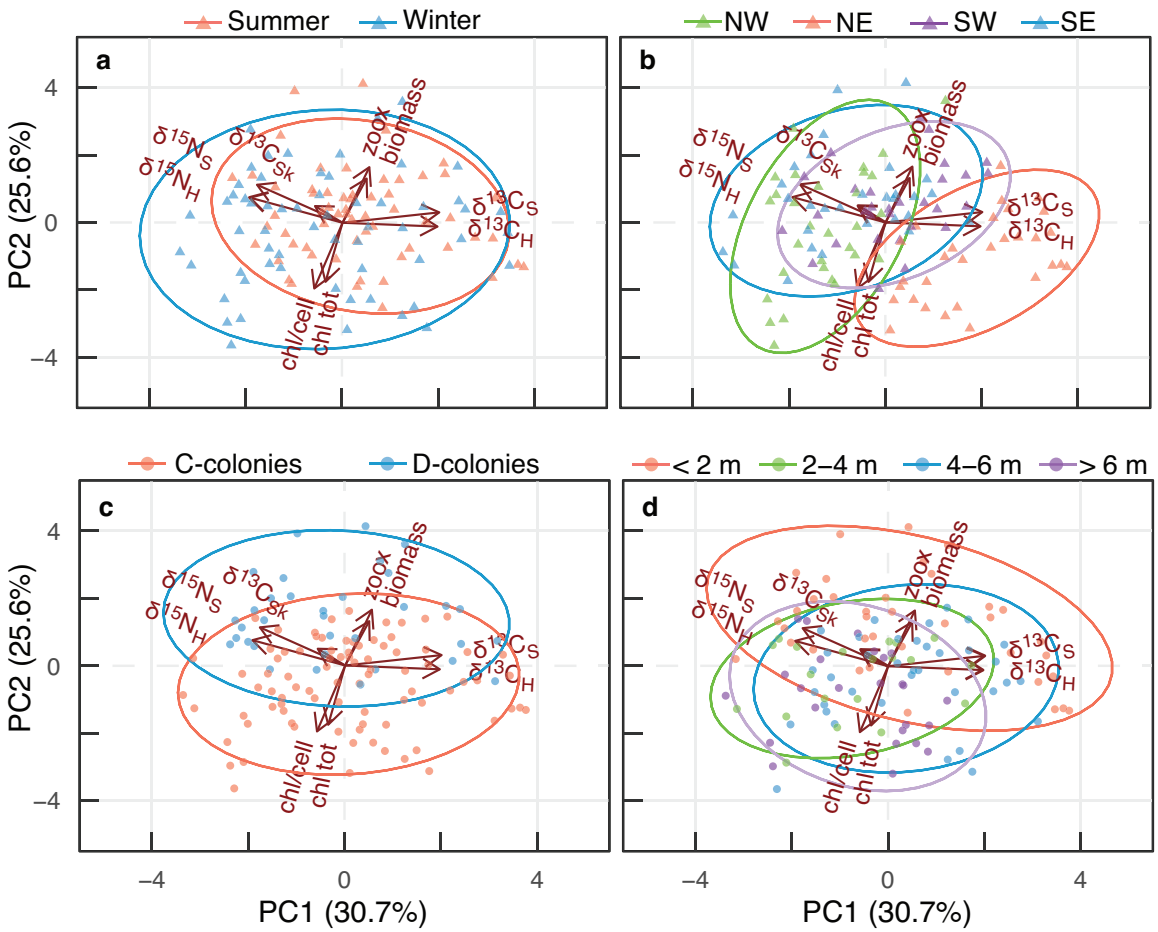

Figure 4.6. Principal component analyses (PCA) on a matrix of physiological responses and isotope values in the coral *Montipora capitata* evaluating the influence of (**a**) season, (**b**) location, (**c**) symbiont community, and (**d**) depth bin. Axis values in parentheses represent proportion of total variance associated with the respective PC. Arrows represent correlation vectors for response variables, and ellipses represent 90% point density according to treatments. See *Table 1* for response metric details.

CHAPTER 5

CONCLUSION

Conclusion

Climate change is an existential threat to the survival of reef corals and their dominance on coral reefs (Hoegh-Guldberg et al. 2017). However, the responses of reef corals to local and global environmental change—including ocean acidification and warming—are not uniform, suggesting some coral holobionts (i.e., coral animal, endosymbiont Symbiodiniaceae, and associated microbes) are capable of withstanding current and near-future environmental change (Strahl et al. 2015). However, stress tolerance may come at a cost to overall coral performance and the capacity for coral reefs ecosystems to provide essential services in the forms of fisheries, coastal protection, and net accretion (Pandolfi et al. 2011; Wild et al. 2011; Eyre et al. 2018).

The role of tissue abundance and composition has wide ranging implications for the function and biology of reef corals. Soft tissues are energetic stores that represent sources of autotrophic and heterotrophic nutrition (Baumann et al. 2014), and are important in the reproduction and post-stress survival of corals (Ward et al. 1995; Grottoli et al. 2004; Leuzinger et al. 2012). In the context of environmental change, coral tissues respond to changes in light availability, pCO_2 and temperature, and nutritional states such as greater feeding on plankton (Houlbrèque et al. 2003; Anthon et al. 2007; Schoepf et al. 2013). Importantly, it is not only the quantity of tissues but also tissue quality (e.g., energy content and lipid composition) that can change in response to environmental contexts and physiological conditions (Anthony et al. 2009). As energy stores, changes in the abundance and composition of tissues shift energetic landscapes for metabolism and the potential for physiological resilience.

Energetic approaches to physiological challenges may hold the key to understanding climate change effects on marine organisms and the implication of these effects at ecosystem scales (Anthony et al. 2009; Kroeker et al., 2012; Lesser 2013; Pan et al. 2015). In reef corals, the symbiosis between cnidarian host and endosymbiont Symbiodiniaceae algae is underpinned by nutritional exchanges, which support metabolism and the growth in both partners. Climate change in the form of ocean acidification (OA) and rising ocean temperatures will disrupt the coral-Symbiodiniaceae and may alter the function of reef corals by influencing the acquisition and allocation of resources to meet metabolic demands. However, flexibility in nutrition, energy allocation, and symbiotic partnerships can contribute to the capacity for corals to withstand a range of environmental stressors, including those occurring from anthropogenic climate change (Anthony et al. 2009). Resistance to OA effects may originate from energetic investments in the regulation of pH and dissolved organic carbon (DIC) species at the site of calcification (Holcomb et al. 2014), possibly through changes in metabolism, lipid biosynthesis, and gene regulation (Vidal-Dupiol et al. 2013) or greater nutrient availability (Holcomb et al. 2010; Edmunds 2011). Similarly, corals with greater tissue biomass are less likely to suffer mortality from bleaching (Thornhill et al. 2011), and the use of tissue energy reserves (primarily lipids and proteins) or heterotrophy are important determinates of coral physiological recovery from bleaching (Anthony et al. 2009). These examples identify the existence of energetic bases of OA and bleaching effects on corals. Although, mechanisms for these effects may differ among species and in concert with other factors (i.e., light, water motion), and therefore require further clarification.

In my results, I show the coral *Pocillopora acuta* experiences changes in coral biomass-normalized lipids and energy content and area-normalized proteins when exposed to elevated pCO_2 under two saturated irradiance treatments. However, *P. acuta* did not show signs of reduced skeletal growth in response to OA. Therefore, our results point to changes in resource allocation in favor of skeletal growth at the expense of tissue energy and composition as a mechanism for coral calcification resistance to OA. However, the catabolism of tissues and/or the shuttling of energy to maintain skeletal growth instead of tissue growth may not be observed in all corals and may be subject to unidentified tradeoffs, dependent on morphological traits, environmental conditions, and site-specific histories (Comeau et al. 2014; Strahl et al. 2015; Bahr et al. 2016). For instance, fast growing corals like *P. acuta* may be more sensitive to OA effects on calcification (Comeau et al. 2014d); however, *P. acuta* in Kāneʻohe Bay may experience end-of-century pCO_2 values (RCP 6.0 ca. 850 µatm pCO_2 [Moss et al. 2010]) on a daily basis due to a combined action of reef metabolism and seawater residence (Drupp et al. 2011, 2013). Therefore, this coral species may be acclimatized and/or locally adapted to changes in pCO_2 and possess mechanisms to attenuate OA effects on skeletal growth not expressed in all coral taxa (Schoepf et al. 2013; Comeau et al. 2014b; Drenkard et al. 2018).

Putative energetic mechanisms for dealing with OA effect may be characterized by tipping points. Under this framework, elevated pCO_2 first solicits changes in resource allocation, but as pCO_2 rises to an ultimate threshold concentration further increases in pCO_2 result in soft tissues losses and/or increased feeding efforts are unsustainable and physiological function declines. Clearly, a knowledge gap exists in the understanding of pCO_2 effects on the tissues and energy investments in corals and other organisms (Edmunds et al. 2013; Pan et al. 2015; Spalding et al.

2017), and understanding how energetic consequences OA propagate through individuals and influence community processes (Kroeker et al. 2012) should be a priority of future research.

In contrast to effects of pCO_2 on *P. acuta*, the tissue composition bleached and non-bleached colonies of *Montipora capitata* and *Porites compressa* did not change during or after thermal stress *in situ*. Instead, bleaching reduced total tissue biomass and spatiotemporal factors (i.e., seasons, sites, and their interactions) influenced biomass composition—specifically lipids and proteins. These findings support other studies that have identified an important role of tissue biomass in coral physiology and in determining post-bleaching survival (Thornhill et al. 2011), but also that tissue biomass composition responds to changes in environmental conditions that occur among reef habitats and across seasons (Anthony 2006; Hoogenboom et al. 2011). Interestingly, we also observed a pattern of lower tissue biomass in all colonies of both species regardless of bleaching responses following peak thermal stress compared to three months of recovery when waters had cooled. It is possible that regardless of symbiont expulsion that coral colonies sensitive and resistant to thermal stress undergo tissue loss during bleaching, and this may relate to the balance of energy availability and metabolic costs/demands, including changes in the production and composition of coral mucus (Wright et al. 2019). Wholesale losses of coral tissue, however, may not result in large changes in tissue composition among bleached and non-bleached colonies, as has been reported in some corals. However, the onset of changes in tissue quantity and composition can proceed at different rates and may manifest at different periods post bleaching (Rodrigues and Grottoli 2007).

The contrasting patterns of elevated pCO_2 effects on *P. acuta* biomass composition and the effects of thermal bleaching and recovery on *M. capitata* and *P. compressa* tissue quantity indicate opposing forces responsible for shaping coral tissues. For instance, OA does not appear to disrupt the function of the coral holobiont to the point where symbiont photosynthesis, host respiration, or total tissue biomass changes and corals do not undergo appreciable losses in symbiont abundance or photopigmentation (Wall et al. 2014; Comeau et al. 2017, but see Anthony et al 2008; Noonan and Fabricus 2016). Tissue biomass stores, such as lipids and proteins are useful in maintaining coral function during periodic energy deficits (Rodrigues and Grottoli 2007) and may be particularly important under chronic stressors that proceed gradually, such as OA or seasonal changes. Indeed, my results showed *P. acuta* lipids, tissue energy, and proteins to all changed in response to pCO_2, while *M. capitata* (protein) and *P. compressa* (lipids and energy) responded to spatiotemporal effects but not bleaching. In each case tissue compositions changed in response to gradual changes in environmental conditions that affect coral function but are not drivers of coral mortality and did not lead to changes in total coral biomass. In contrast, the high temperature anomaly experienced by Hawaiian corals in 2014 lead to extensive disruption of the coral-Symbiodiniaceae mutualism causing bleaching (Bahr et al. 2017), symbiont and tissue losses, and coral mortality but no consistent effects on coral tissue composition. These findings reveal the importance of coral tissues in shaping stress effects on coral performance, albeit how tissues energy is mobilized and allocated may depend on stressor duration, magnitude, and type.

Despite the significance of biomass composition in organism performance, the role of compound classes (i.e., lipids, carbohydrates, proteins) has received limited attention in the interpretation

and understanding of tissue $\delta^{13}C$ analysis. Relatively small changes in the ratios of lipids:carbohydrates:proteins can influence carbon stable isotope values of bulk tissues, which is fundamentally a product of the biochemical pathways from which compounds originate and the relative proportion of compounds in tissues (Hayes 2001). In my results, I show that considering the role of compound-class specific isotope values and lipids:carbohydrates:proteins in tissues can use useful in disentangling effects of tissue level changes from changes in nutrition. Accounting for changes in tissue composition—but also changes in specific compounds—is an important consideration in the inferences from carbon isotope data, as changes in relative proportions of compound classes and the composition of each compound pool (i.e., lipid classes) affects bulk isotope values and can influence inferences on coral nutritional modes and plasticity. While there are limited examples in the coral literature where isotope values have been measured in specific compounds or in classes of compounds (i.e., lipids, carbohydrates, and proteins), advancing this understanding is vital in reducing uncertainty in stable isotope studies.

The analysis of carbon and nitrogen stable isotopes in tissues has contributed to our understanding of the physiological ecology and nutrition of reef corals. However, fundamental questions remain in our understanding of the mechanisms governing patterns of stable isotope values in the corals-Symbiodiniaceae symbiosis among coral species and across environmental conditions. For this reason, greater attention should be devoted to identifying the influence of tissue composition, tissues turnover rates, and the role of cryptic symbiotic partners (i.e., nitrogen fixers, endolithic algae) and alternative Symbiodiniaceae communities on coral host and symbiont algae. Pairing of tissue isotope analysis with biochemical and physiological assays has also proven useful in contextualizing changes in coral isotope values (Rodrigues and Grottoli

2006) and niche partitioning of Symbiodiniaceae (Ezzat et al. 2018), as well as determining the mechanisms, tipping points, and processes that lead to changes in isotope values across spatial scales and environmental regimes (Maier et al. 2010; Fox et al. 2018; Radice et al. 2019). For instance, my findings on C- and D-dominated *M. capitata* show that Symbiodiniaceae diversity has a considerable influence on carbon isotope values, but corals of either symbiont community showed no change in heterotrophic feeding, tissue C:N, or nitrogen values despite considerable changes in light availability and seasonal effects. Despite knowledge of functional differences in the carbon fixation and thermal tolerance of Symbiodiniaceae species, the influence of symbiont genetic diversity on coral nutrition and baseline physiological processes has been much less explored. Distinctions symbioses attributes (i.e., cell densities, photopigments, fixation/translocation rates) have clear implications for coral energy budgets and tissue isotope values. Yet, paired analyses of coral genetics, physiology, and isotope values are rare and dominated by laboratory studies. My *in situ* analyses of isotope values in *M. capitata* emphasize the need for greater attention to *in situ* variance in isotope values among corals with different symbiont communities and highlight the need to better understand how symbiont community and environment affect the trophic ecology and nutritional exchanges in the coral-Symbiodiniaceae symbiosis.

A path forward in using stable isotopes to disentangle biological changes in an organism's nutrition (or metabolism) from unconstrained variance in the form of fractionation-mediated effects may be in the development of compound specific isotope analyses (CSIA). CSIA are analyses of individual compounds and their propagation through food webs/organisms and include such compounds as fatty acids (FA) and amino acids (AA) (see review by Ferrier-Pagès

and Leal 2018). CSIA approaches have advanced in recent years and their application in ecological studies (particularly in food webs) is increasing. The acceptance of CSIA techniques—despite their significantly greater investments in costs and labor—is due to the greater resolution these technique afford, along with the capacity for these tools to simultaneously provide information on dietary food sources, nutrition, and physiology of an organism (Whiteman et al. 2019). While limited, the analysis of FA-CSIA in reef corals has been applied to determine the source of FA in the diets different corals among reef locations (Teece et al. 2011). Similarly, the application of CSIA of carbon and nitrogen in individual AA may be useful in clarifying the origin and cycling of AA in mixotrophic mutualistic symbiosis (Ferrier-Pagès and Leal 2018), and examples of these tools in the study of reef corals are forthcoming.

Identifying the traits and mechanism of coral physiological resilience are vital to coral conservation. Energetics provides a framework to understand how reef corals and other diverse marine species cope with changing energetic demands and disrupted symbiotic states. My research identifies unique pathways by which corals may survive and maintain important functions during physiological challenges, while also identifying unique attributes between distinct symbiont communities within a single coral species. While technological advances have been made in understanding the consequences of climate change on individual organisms, future challenges will be integrating these findings into ecological theory in order to gain an ecosystem perspective of climate change effects (Gaylord et al. 2015). In this undertaking, there is an expanding niche for stable isotope ecology and the application of bulk and compound-specific biomass analyses to understand organism and ecosystems. Stable isotope tools may provide

unique perspectives that supplement physiology, genetic and –omic approaches in quantifying the consequences of changing environments on species-species interaction (including competition and symbioses) and mechanisms underlying biological processes (i.e., calcifying fluid pH, resource allocation). Together, embracing new approaches in the study of earth's biodiversity may provide actionable evidence to aid conservation and restoration efforts, providing near-term lifelines to coral reefs in the face of humanity's reluctance to address the climate crisis.

MANUSCRIPT PUBLICATION AND OTHER ACKNOWLEDGEMENTS

CHAPTER 2

Published in *Royal Society Open Science*

Authors: Robert A.B. Mason, William R. Ellis, Ross Cunning, Ruth D. Gates

Citation: Wall CB, Mason RAB, Ellis WR, Cunning R, Gates RD (2017) Elevated pCO_2 affects tissue biomass composition, but not calcification, in a reef coral under two light regimes. R Soc Open Sci 4:170683

Chapter 2 Data: Wall CB, Mason RAB, Ellis WR, Cunning R, Gates RD (2017) Data from: Elevated pCO_2 affects tissue biomass composition, but not calcification, in a reef coral under two light regimes. Dryad Digital Repository. https://doi.org/10.5061/dryad.5vg70.3

CHAPTER 3

Published in *Limnology and Oceanography*

Authors: Raphael Ritson-Willaims, Brian N Popp, Ruth D. Gates

Citation: Wall CB, Ritson-Williams R, Popp BN, and Gates RD (2019) Spatial variation in the biochemical and isotopic composition of corals during bleaching and recovery. Limnol Oceanogr http://doi.org/10.1002/lno.11166

Chapter 3 Data: Wall C (2019) cbwall/Energetics-and-isotopes-in-bleached-and-recovering-corals: Physiology and isotopes values of bleached and recovering corals (Version v1.0-pub). Zenodo. http://doi.org/10.5281/zenodo.2587467

CHAPTER 4

In preparation for submission to *ISME Journal*

Authors: Mario Kaluhiokalani, Brian N Popp, Megan Donahue

Chapter 4 Data: Data and scripts to reproduce analyses and figures are available at Github (github.com/cbwall/Coral-isotopes-across-space-and-time).

Appendix Table 2.S1. Principal component loadings with eigenvalues > 1.0 analyzed in linear mixed effect models.

	Effect	*SS*	*df*	*F*	*p*
Area-normalized					
PC1 (41.0%)	pCO_2	1.004	1,21	0.488	0.493
	Light	0.510	1,21	0.248	0.624
	pCO_2 × Light	0.070	1,21	0.034	0.856
PC2 (20.5%)	pCO_2	2.899	1,22	2.704	0.114
	Light	0.372	1,22	0.347	0.562
	pCO_2 × Light	0.940	1,22	0.877	0.359
Biomass-normalized					
PC1 (38.3%)	pCO_2	0.279	1,23	0.164	0.689
	Light	2.185	1.22	1.285	0.269
	pCO_2 × Light	0.139	1,22	0.082	0.777
PC2 (34.1%)	pCO_2	9.726	1,22	5.502	**0.028**
	Light	0.236	1,22	0.133	0.718
	pCO_2 × Light	0.019	1,22	0.011	0.919

Values in parentheses represent percentage of variation explained for each principal component (PC). *SS* = sum of squares; *df* = degrees of freedom in numerator and denominator; bold values represent significant effects ($p < 0.05$).

Appendix Table 2.S2. Statistical analysis of pCO_2 and light effects on area-normalized net calcification, biomass energy reserves, symbiont cell density, and photopigment concentrations of the reef coral *Pocillopora acuta*.

Dependent variable	*Effect*	*SS*	*df*	*F*	*p*
calcification	pCO_2	0.004	1, 22	0.275	0.605
mg $CaCO_3$ cm^{-2} d^{-1}	Light	0.001	1, 22	0.070	0.793
	pCO_2 × Light	4.808×10^{-4}	1, 22	0.031	0.861
biomass mg cm^{-2}	pCO_2	0.030×10^{-4}	1, 22	0.004	0.950
	Light	0.001	1, 22	1.667	0.210
	pCO_2 × Light	1.316×10^{-4}	1, 22	0.178	0.677
proteins mg cm^{-2}	pCO_2	0.004	1, 22	1.279	0.270
	Light	0.024	1, 22	7.940	**0.010**
	pCO_2 × Light	0.015	1, 22	4.850	**0.038**
carbohydrates mg cm^{-2}	pCO_2	0.002	1, 22	0.909	0.351
	Light	0.001	1, 22	0.459	0.505
	pCO_2 × Light	0.005	1, 22	2.453	0.132
lipids mg cm^{-2}	pCO_2	0.402	1, 22	2.283	0.145
	Light	0.018	1, 22	0.104	0.751
	pCO_2 × Light	0.030	1, 22	0.171	0.683
energy content kJ cm^{-2}	pCO_2	0.010	1, 22	1.740	0.201
	Light	0.002	1, 22	0.382	0.543
	pCO_2 × Light	1.072×10^{-4}	1, 22	0.019	0.891
symbiont cells cm^{-2}	pCO_2	1.798×10^{4}	1, 22	0.962	0.338
	Light	4.791×10^{4}	1, 22	2.563	0.124
	pCO_2 × Light	0.953×10^{4}	1, 22	0.510	0.483
chlorophyll *a* cm^{-2}	pCO_2	1.000×10^{-4}	1, 21	1.000×10^{-4}	0.993
	Light	25.085	1, 21	31.055	**<0.001**
	pCO_2 × Light	1.860	1, 21	2.302	0.144
chlorophyll c_2 cm^{-2}	pCO_2	0.130×10^{-4}	1, 22	0.002	0.961
	Light	0.104	1, 22	18.894	**<0.001**
	pCO_2 × Light	0.015	1, 22	2.711	0.114
chlorophyll *a* $cell^{-1}$	pCO_2	0.755×10^{-4}	1, 22	0.021	0.886
	Light	0.010	1, 22	2.786	0.109
	pCO_2 × Light	0.001	1, 22	0.305	0.587
chlorophyll c_2 $cell^{-1}$	pCO_2	4.362×10^{-4}	1, 22	0.092	0.765
	Light	0.008	1, 22	1.618	0.217
	pCO_2 × Light	0.003	1, 22	0.594	0.449

SS = sum of squares; *df* = degrees of freedom in numerator and denominator; bold *P* values represent significant effects ($p < 0.05$)

Appendix Table 2.S3. Statistical analysis of pCO_2 and light effects on biomass-normalized net calcification and biomass energy reserves of the reef coral *Pocillopora acuta*.

Dependent variable	*Effect*	*SS*	*df*	*F*	*p*
calcification	pCO_2	0.235	1, 22	0.306	0.586
mg $CaCO_3$ gdw^{-1} d^{-1}	Light	0.958	1, 22	1.243	0.277
	pCO_2 × Light	0.018	1, 22	0.024	0.879
proteins g gdw^{-1}	pCO_2	0.680×10^{-4}	1, 22	0.692	0.415
	Light	0.148×10^{-4}	1, 22	0.150	0.702
	pCO_2 × Light	0.480×10^{-4}	1, 22	0.488	0.492
carbohydrates g gdw^{-1}	pCO_2	1.993×10^{-4}	1, 22	0.943	0.342
	Light	0.001	1, 22	4.747	**0.040**
	pCO_2 × Light	2.411×10^{-4}	1, 22	1.141	0.297
lipids g gdw^{-1}	pCO_2	0.051	1, 22	4.762	**0.040**
	Light	0.007	1, 22	0.630	0.436
	pCO_2 × Light	1.200×10^{-4}	1, 22	0.011	0.917
energy content kJ gdw^{-1}	pCO_2	80.984	1, 22	4.721	**0.041**
	Light	10.385	1, 22	0.605	0.445
	pCO_2 × Light	0.062	1, 22	0.004	0.952

SS = sum of squares; *df* = degrees of freedom in numerator and denominator; bold *P* values represent significant effects ($p < 0.05$).

Appendix Table 3.S1. Statistical analysis of bleached and non-bleached *Montipora capitata* at three reefs during bleaching and recovery.

Dependent variable	*Effect*	*SS*	*df*	*F*	*p*
chlorophyll ($a + c_2$) (μg cm^{-2})	Period	235.380	1, 28	65.245	**<0.001**
	Site	12.354	2, 12	1.712	0.222
	Condition	54.080	1, 14	14.990	**0.002**
	Period × Condition	16.541	1, 28	4.585	**0.041**
biomass (mg cm^{-2})	Period	2912.240	1, 28	55.484	**<0.001**
	Site	145.006	2, 26	1.381	0.270
	Condition	103.915	1, 26	1.980	0.171
	Period × Condition	394.610	1, 28	7.518	**0.011**
proteins (g gdw^{-1})	Period	0.003	1, 28	7.689	**0.010**
	Site	0.001	2, 26	0.798	0.461
	Condition	0.001	1, 26	1.289	0.267
lipids (g gdw^{-1})	Period	0.001	1, 27	0.163	0.690
	Site	0.021	2, 25	2.611	0.093
	Condition	0.005	1, 25	1.163	0.291
carbohydrates (g gdw^{-1})	Period	0.003	1, 28	3.481	0.073
	Site	0.003	2, 26	2.021	0.153
	Condition	1.583×10^{-4}	1, 26	0.195	0.662
energy content (kJ gdw^{-1})	Period	0.039	1, 27	0.006	0.937
	Site	37.867	2, 25	3.059	0.065
	Condition	5.666	1, 25	0.916	0.348

SS = sum of squares; *df* = degrees of freedom in numerator and denominator; bold *p* values represent significant effects ($p < 0.05$).

Appendix Table 3.S2. Statistical analysis of bleached and non-bleached *Porites compressa* at three reefs during bleaching and recovery.

Dependent variable	*Effect*	*SS*	*df*	*F*	*p*
chlorophyll ($a + c_2$) (μg cm^{-2})	Period	1641.570	1, 24	258.386	**<0.001**
	Site	61.579	2, 12	4.846	**0.029**
	Condition	257.599	1, 12	40.547	**<0.001**
	Period × Site	39.845	2, 24	3.136	0.062
	Period × Condition	187.462	1, 24	29.507	**<0.001**
	Site × Condition	86.012	2, 12	6.769	**0.011**
	Period × Site × Condition	8.942	2, 24	0.704	0.505
biomass (mg cm^{-2})	Period	248.036	1, 55	1.910	0.173
	Site	74.351	2, 55	0.286	0.752
	Condition	691.067	1, 55	5.321	**0.025**
proteins (g gdw^{-1})	Period	0.891×10^{-4}	1, 28	0.086	0.772
	Site	0.003	2, 26	1.422	0.259
	Condition	0.761×10^{-4}	1, 26	0.073	0.789
	Period × Condition	0.008	1, 28	7.378	**0.011**
lipids (g gdw^{-1})	Period	0.064	1, 52	12.184	**<0.001**
	Site	0.005	2, 52	0.451	0.639
	Condition	0.010	1, 52	1.856	0.179
	Period × Site	0.059	2, 52	5.620	**0.006**
carbohydrates (g gdw^{-1})	Period	0.001	1, 29	2.653	0.114
	Site	0.001	2, 26	0.593	0.560
	Condition	0.001	1, 26	2.344	0.138
energy content (kJ gdw^{-1})	Period	92.140	1, 52	14.071	**<0.001**
	Site	4.004	2, 52	0.306	0.738
	Condition	8.596	1, 52	1.313	0.257
	Period × Site	69.078	2, 52	5.275	**0.008**

SS = sum of squares; *df* = degrees of freedom in numerator and denominator; bold *p* values represent significant effects ($p < 0.05$).

Appendix Table 3.S3. Statistical analysis of bleached and non-bleached *Montipora capitata* at three reefs during bleaching and recovery.

Dependent variable	*Effect*	*SS*	*df*	*F*	*p*
$\delta^{13}C_H$	Period	0.600	1, 29	1.108	0.301
	Site	3.547	2, 12	3.276	0.073
	Condition	3.561	1, 14	6.578	**0.022**
$\delta^{13}C_S$	Period	6.208	1, 29	14.169	**<0.001**
	Site	2.723	2, 12	3.108	0.082
	Condition	1.641	1, 24	3.745	0.073
$\delta^{13}C_{H-S}$	Period	2.752	1, 29	12.705	**0.001**
	Site	0.452	1, 12	1.044	0.381
	Condition	0.996	1, 14	4.598	0.050
$\delta^{15}N_H$	Period	0.002	1, 29	0.753	0.393
	Site	0.025	2, 12	4.150	**0.043**
	Condition	0.204×10^{-4}	1, 14	0.007	0.935
$\delta^{15}N_S$	Period	0.005	1, 43	0.785	0.381
	Site	0.027	2, 12	2.283	0.145
	Condition	0.002	1, 43	0.379	0.541
$\delta^{15}N_{H-S}$	Period	1.601	1, 29	1.774	0.193
	Site	0.809	2, 24	0.448	0.644
	Condition	0.395	1, 24	0.438	0.514
	Site × Condition	5.492	2, 24	3.044	0.066
$C:N_H$	Period	3.194	1, 26	24.610	**<0.001**
	Site	0.375	2, 12	1.445	0.274
	Condition	0.471	1, 14	3.627	0.078
	Period × Site	0.854	2, 26	3.288	0.053
	Period × Condition	0.568	1, 26	4.377	**0.046**
$C:N_S$	Period	0.053	1, 43	3.724	0.060
	Site	0.048	2, 12	1.658	0.231
	Condition	0.014	1, 43	0.982	0.327

SS = sum of squares; *df* = degrees of freedom in numerator and denominator; bold *p* values represent significant effects ($p < 0.05$). *Subscripts* indicate coral host (H), symbiont algae (S), or the differences between host and symbiont (H-S) isotopic values.

Appendix Table 3.S4. Statistical analysis of bleached and non-bleached *Porites compressa* at three reefs during bleaching and recovery.

Dependent variable	*Effect*	*SS*	*df*	*F*	*p*
$\delta^{13}C_H$	Period	0.028	1, 24	0.111	0.742
	Site	0.136	2, 12	0.269	0.769
	Condition	1.291	1, 12	5.091	**0.043**
	Period × Site	0.320	2, 24	0.631	0.540
	Period × Condition	2.204	1, 24	8.689	**0.007**
	Site × Condition	1.446	2, 12	2.849	0.097
	Period × Site × Condition	2.014	2, 24	3.970	**0.032**
$\delta^{13}C_S$	Period	1.014	1, 28	1.632	0.212
	Site	0.180	2, 12	0.145	0.867
	Condition	2.294	1, 14	3.691	0.075
	Period × Condition	2.646	2, 28	4.258	**0.048**
$\delta^{13}C_{H-S}$	Period	0.693	1, 54	2.287	0.136
	Site	0.529	2, 54	0.872	0.424
	Condition	0.126	1, 54	0.416	0.522
	Period × Condition	0.015	1, 54	0.050	0.825
$\delta^{15}N_H$	Period	2.774	1, 28	6.795	**0.014**
	Site	8.481	2, 12	10.390	**0.002**
	Condition	0.099	1, 14	0.241	0.631
	Period × Condition	2.054	1, 28	5.031	**0.033**
$\delta^{15}N_S$	Period	2.440	1, 28	2.655	0.114
	Site	9.459	2, 12	5.145	**0.024**
	Condition	1.452	1, 14	1.579	0.229
	Period × Condition	7.142	1, 28	7.770	**0.009**
$\delta^{15}N_{H-S}$	Period	10.292	1, 28	7.844	**0.009**
	Site	0.606	2, 12	0.231	0.797
	Condition	0.876	1, 14	0.668	0.428
	Period × Condition	16.485	1, 28	12.564	**0.001**
$C:N_H$	Period	5.874	1, 26	33.869	**<0.001**
	Site	0.150	2, 12	0.433	0.658
	Condition	0.040	1, 14	0.228	0.640
	Period × Site	2.324	2, 26	6.702	**0.004**
	Period × Condition	3.470	1, 26	20.007	**<0.001**
$C:N_S$	Period	3.203	1, 42	2.589	0.115
	Site	0.209	2, 12	0.085	0.919
	Condition	3.847	1, 42	3.110	0.085
	Period × Condition	2.010	1, 42	1.625	0.209

SS = sum of squares; *df* = degrees of freedom in numerator and denominator; bold *p* values represent significant effects ($p < 0.05$). *Subscripts* indicate isotopic values of coral host (H), symbiont algae (S), and their relative difference (H-S).

Appendix Table 4.S1. Model analysis of environmental variables (daily light availability, dissolved inorganic nutrients, suspended particulate matter, and isotopic values of size fractioned plankton and particles) at four reefs in Kāne‘ohe Bay*.

Environmental variable	*Effect*	*SS*	*df*	*F*	*p*
[a]Daily light integral (DLI)†	Location	4378.754	3,530	134.674	**<0.001**
(mol photons m^{-2} d^{-1})	Season	1040.907	1,210	96.043	**<0.001**
	Location × Season	490.862	3,531	15.097	**<0.001**
[b]Dissolved inorganic nutrients					
phosphate	Location	0.005	4	1.218	0.426
(PO_4^{3-} µmol L^{-1})	Season	0.009	1	8.182	**0.046**
	Residual	0.004	4		
ammonium	Location	0.090	4	5.696	0.060
(NH_4^+ µmol L^{-1})	Season	1.325	1	336.712	**<0.001**
	Residual	0.018	4		
nitrate + nitrite	Location	0.488	4	294.012	**<0.001**
(NO_3^- + NO_2^- µmol L^{-1})	Season	0.067	1	162.024	**<0.001**
	Residual	0.002	4		
silicate	Location	21.495	4	1.629	0.324
($Si(OH)_4$ µmol L^{-1})	Season	3.612	1	1.095	0.354
	Residual	13.194	4		
[b]Size fractioned plankton and particles					
carbon isotope values ($\delta^{13}C$)	Location	17.926	5	1.342	0.263
	Season	7.921	1	2.965	0.914
	Size fraction	76.419	4	7.150	**0.001**
	Residual	130.920	49		
nitrogen isotope values ($\delta^{15}N$)	Location	2.326	5	1.729	0.146
	Season	1.094	1	4.065	**0.049**
	Size fraction	30.377	4	28.234	**<0.001**
	Residual	13.180	49		

* Model outputs are linear models with Type II analysis of variance tables, except for †, where model outputs is linear mixed effect model with Date as a random effect. *SS* = sum of squares; *df* = degrees of freedom; for † *df* is degrees of freedom in numerator and denominator; bold *p* values represent significant effects ($p < 0.05$).
Data collection periods are indicated by superscripts (a-c):
[a] 10 June 2016 – 12 January 2017
[b] 20 August 2016 and 19 December 2016

Appendix Table 4.S2. Statistical analysis of *Montipora capitata* physiology from four locations in Kāneʻohe Bay along a depth gradient in summer and winter.

Dependent variable	*Effect*	*SS*	*df*	*F*	*p*
biomass (mg cm^{-2})	Season	0.159	1,116	0.003	0.959
	Light	4.358	1,108	0.072	0.789
	Symbiont	162.958	1,116	2.690	0.104
symbionts (cells cm^{-2})	Season	0.008	1,112	0.133	0.716
	Light	0.392	1,115	6.866	**0.010**
	Symbiont	3.133	1,113	54.830	**<0.001**
	Season × Light	0.481	1,113	8.411	**0.004**
total chlorophyll ($a + c_2$ μg cm^{-2})	Season	45.581	1,114	25.545	**<0.001**
	Light	16.042	1,110	8.990	**0.004**
	Symbiont	31.622	1,115	17.721	**<0.001**
	Season × Symbiont	9.718	1,113	5.411	**0.022**
chlorophyll per cell ($a + c_2$ pg symbiont $cell^{-1}$)	Season	0.147	1,114	2.825	0.096
	Light	2.387	1,116	43.977	**<0.001**
	Symbiont	5.125	1,114	98.716	**<0.001**

Season = summer or winter, *Light* = light at depth of collection, *Symbiont* = *Cladocopium* spp. (formerly clade C) or *Durusdinium glynnii* (formerly clade D)-dominated symbiont community. *SS* = sum of squares; *df* = degrees of freedom in the numerator and denominator; bold *p* values represent significant effects ($p < 0.05$).

Appendix Table 4.S3. Statistical analysis of *Montipora capitata* tissue isotope composition from four locations in Kāne‘ohe Bay along a depth gradient in summer and winter.

Dependent variable	*Effect*	*SS*	*df*	*F*	*p*
$\delta^{13}C_H$	Season	1.032	1,111	1.398	0.240
	Light	23.638	1.114	32.005	**<0.001**
	Symbiont	27.456	1.112	37.174	**<0.001**
	Season × Light	0.170	1,112	0.231	0.632
	Season × Symbiont	3.523	1,112	4.770	**0.031**
$\delta^{13}C_S$	Season	0.002	1,113	0.002	0.962
	Light	35.816	1,115	44.529	**<0.001**
	Symbiont	12.375	1,113	15.386	**<0.001**
	Season × Symbiont	8.757	1,113	10.887	**0.001**
$\delta^{13}C_{H-S}$	Season	1.320	1,111	9.931	**0.002**
	Light	0.360	1,113	2.712	0.102
	Symbiont	2.291	1,113	17.243	**<0.001**
	Season × Light	0.574	1,113	4.322	**0.040**
	Season × Symbiont	0.590	1,112	4.441	**0.037**
$\delta^{13}C_{Skel}$	Season	4.888	1,115	6.961	**0.009**
	Light	0.155	1,115	0.221	0.639
	Symbiont	0.002	1,115	0.003	0.953
$\delta^{15}N_H$	Season	0.109	1,113	1.132	0.290
	Light	0.418	1,114	4.327	**0.040**
	Symbiont	0.038	1,113	0.392	0.532
$\delta^{15}N_S$	Season	0.001	1,112	0.014	0.907
	Light	0.002	1,113	0.022	0.882
	Symbiont	0.790	1,112	7.241	**0.008**
	Season × Symbiont	0.644	1,112	5.903	**0.017**
$\delta^{15}N_{H-S}$	Season	0.104	1,114	1.849	0.177
	Light	0.323	1,115	5.767	**0.018**
	Symbiont	0.538	1,114	9.588	**0.002**
	Season × Symbiont	0.963	1,113	17.173	**<0.001**
$C:N_H$	Season	0.369×10^{-3}	1,115	0.070	0.792
	Light	0.004	1,114	0.703	0.403
	Symbiont	0.001	1,115	0.155	0.695
$C:N_S$	Season	0.021	1,115	2.281	0.134
	Light	0.344×10^{-3}	1,115	0.037	0.847
	Symbiont	0.016×10^{-3}	1,115	0.002	0.967

Season = summer or winter, *Light* = light at depth of collection, *Symbiont* = *Cladocopium* spp. (formerly clade C) or *Durusdinium glynnii* (formerly clade D)-dominated symbiont community. *SS* = sum of squares; *df* = degrees of freedom in numerator and denominator; bold *p* values represent significant effects ($p < 0.05$). *Subscripts* indicate coral host (H), symbiont algae (S), or their relative difference (H-S), and skeletal carbonates (Sk).

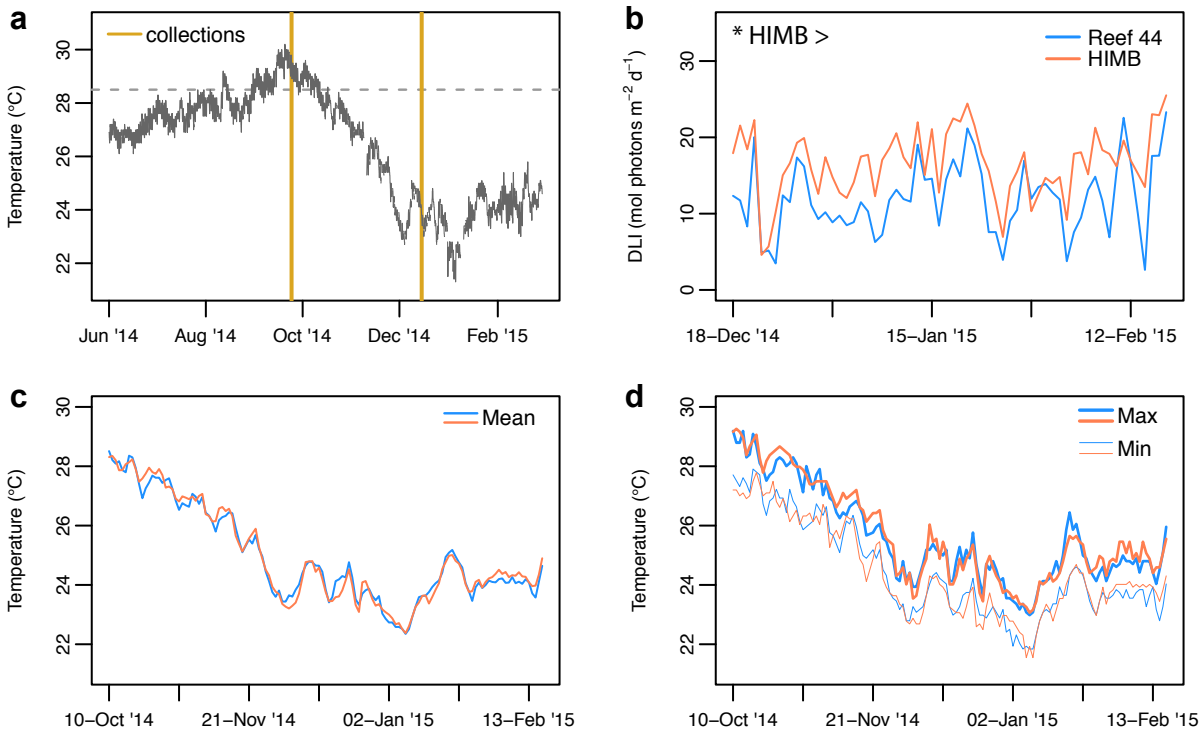

Appendix Figure 3.S1. (**a**) Seawater temperature at the NOAA Moku o Loʻe weather station located at the Hawaiʻi Institute of Marine Biology. *Horizontal* dashed line indicates bleaching threshold for reef corals in Hawaiʻi (28.5 °C); *vertical* yellow lines indicate coral collections after peak bleaching (October 2014) and during post-bleaching recovery (January 2015). (**b**) Daily light integral (DLI), (**c**) daily mean, (**d**) daily maximum (*Max*) and minimum (*Min*) temperatures at Reef 44 (*blue*) and HIMB (*red*). *Symbols* (*) indicate significant site effects ($p <$ 0.05).

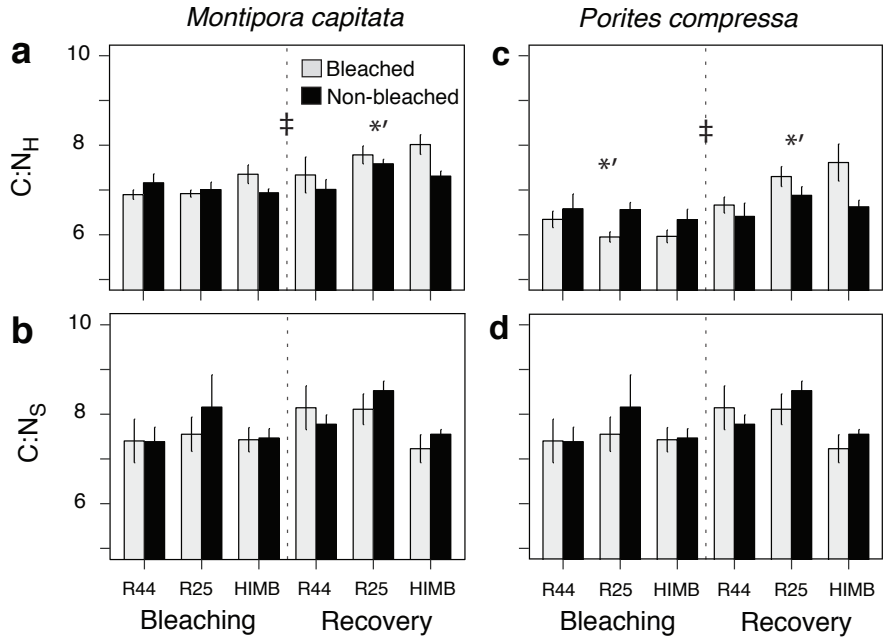

Appendix Figure 3.S2. Biomass carbon:nitrogen (C:N) molar ratios in (**a**,**c**) host ($C:N_H$) and (**b**,**d**) symbionts ($C:N_S$) from bleached (*gray*) and non-bleached (*black*) *Montipora capitata* (*left*) and *Porites compressa* (*right*) at three reefs [Reef 44 (R44), Reef 25 (R25) and HIMB] during (October 2014: Bleaching) and after (January 2015: Recovery) a regional bleaching event. Values are mean ± SE ($n = 4 – 5$). *Symbols* indicate significant differences ($p < 0.05$) between periods (‡) and between bleached and non-bleached corals within a period (*').

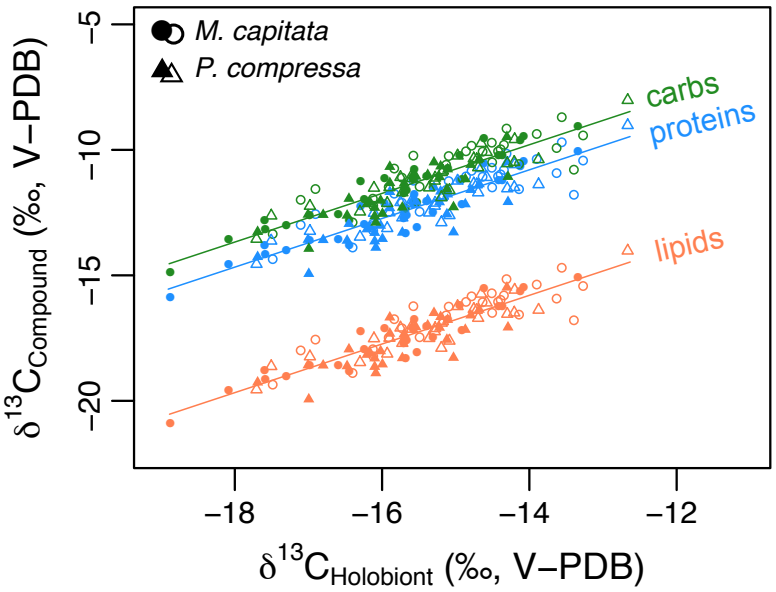

Appendix Figure 3.S3. Modeled relationship between $\delta^{13}C$ of the coral holobiont and constituent tissue compounds (Hayes 2001) for *Montipora capitata* (*circles*) and *Porites compressa* (*triangles*) pooled among sites and time periods for bleached colonies (*open* symbols) and non-bleached colonies (*filled* symbols). Lines represent linear regression of $\delta^{13}C_{Compound}$ and $\delta^{13}C_{Holobiont}$ for data pooled across all levels.

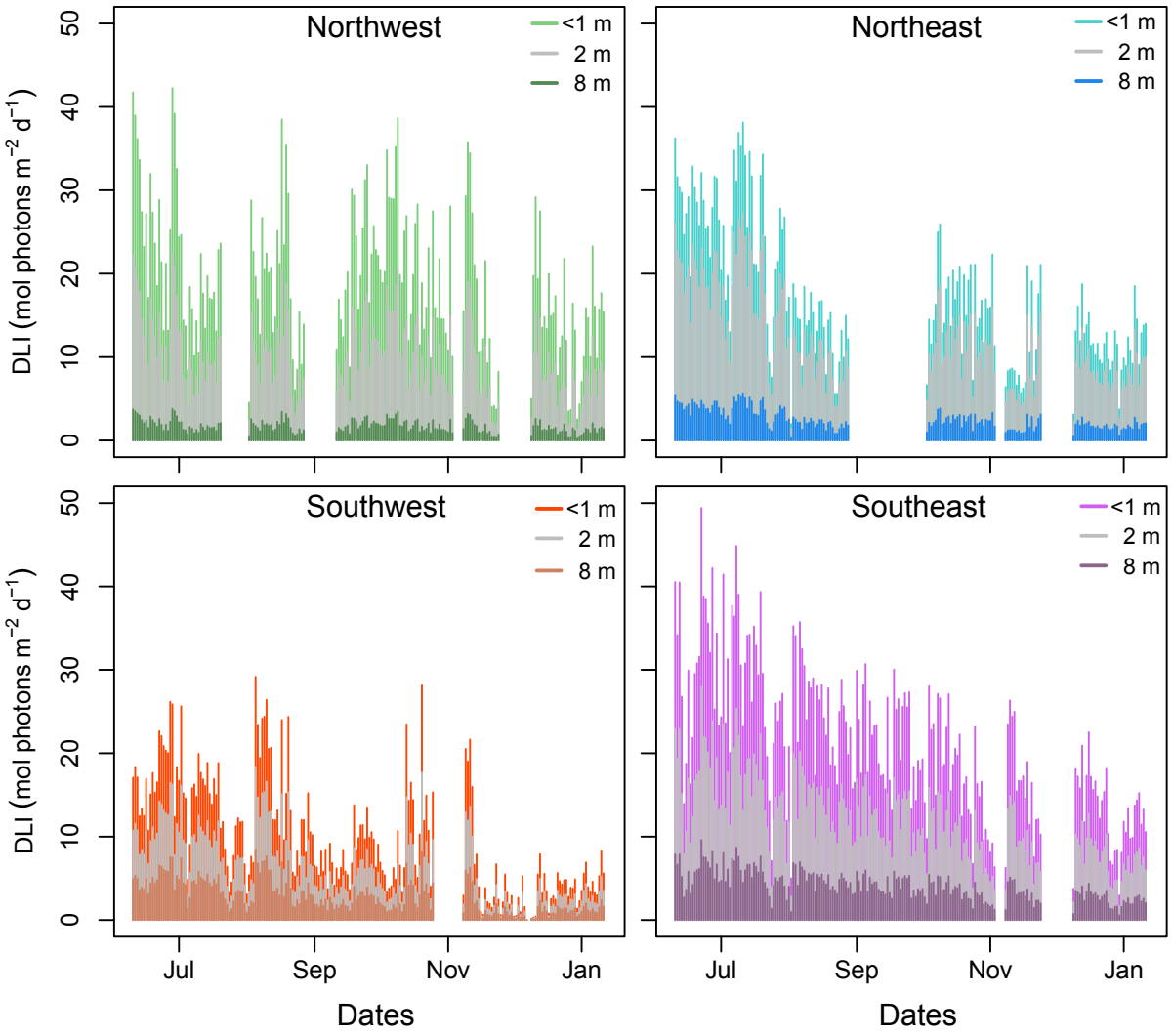

Appendix Figure 4.S1. Light availability (daily light interval [DLI]) at four Kāneʻohe Bay reefs from June – January 2016. DLI values are based on measured values at 2 m depth and calculating light at <1 m and 8 m according to a modified Beer-Lambert equation for light attenuation in water, described in *Materials and Methods*.

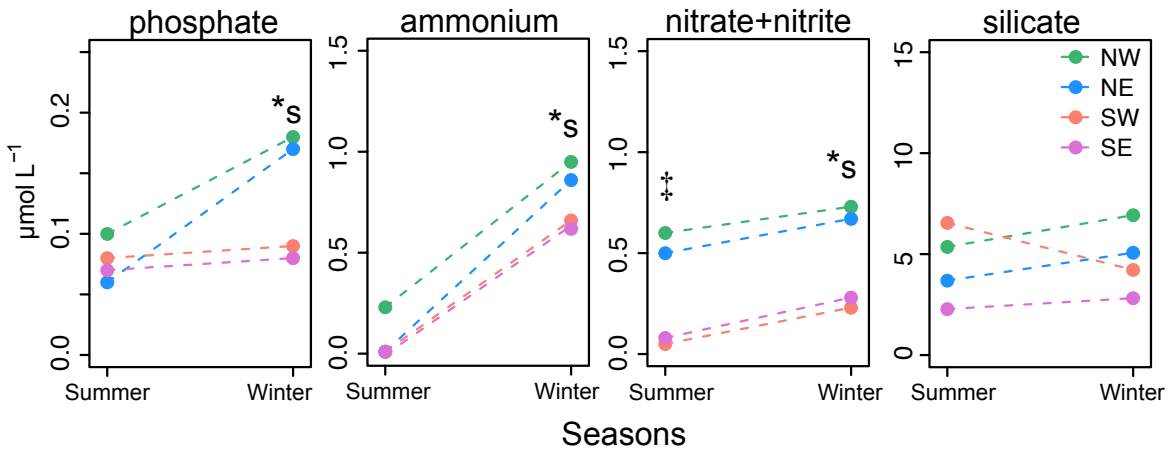

Appendix Figure 4.S2. Molar concentrations of the dissolved inorganic nutrients (µmol L^{-1}) phosphate (PO_4^{3-}), ammonium (NH_4^+), nitrate+nitrite (NO_3^- + NO_2^- or N+N) and silicate ($Si(OH)_4$) in seawater (points, n = 1) collected during two sampling periods in summer and winter 2016 from four reef locations, described in *Figure 1*. *Symbols* indicate significant differences ($p < 0.05$) between seasons (**s*) and among locations (‡).

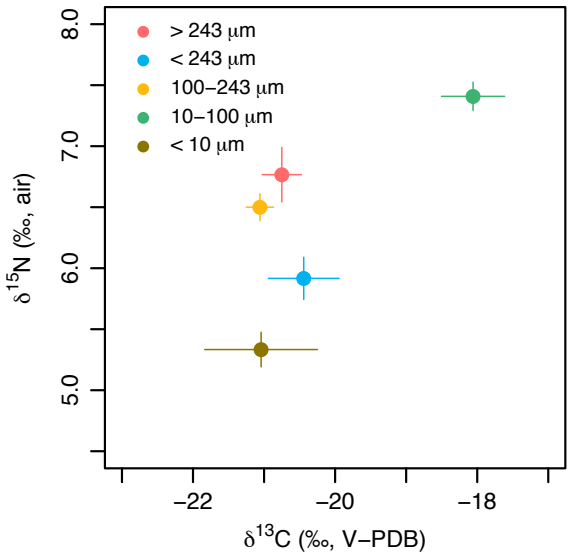

Appendix Figure 4.S3. Size fractioned organic materials and plankton in seawater. Values are mean ± SE (n = 12) in permil (‰) relative to standards for carbon (Vienna-Pee Dee Belemnite: V-PDB) and nitrogen (air).

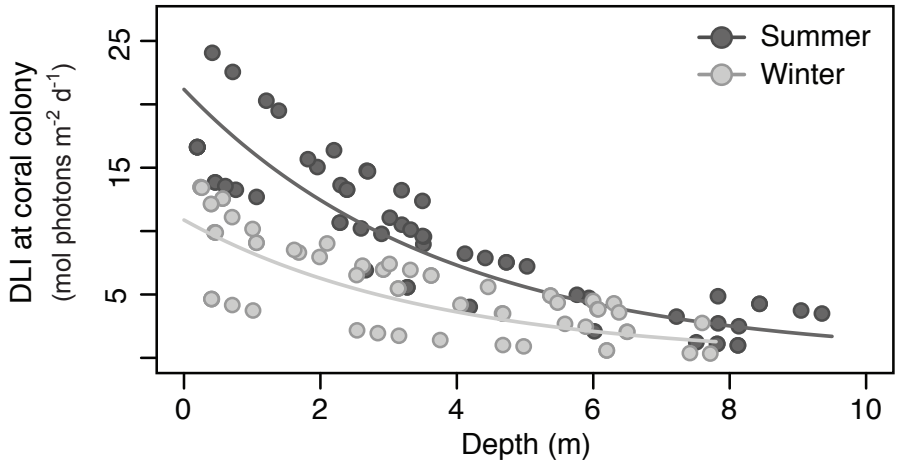

Appendix Figure 4.S4. The daily light integral (DLI) and the depth (m) where *Montipora capitata* coral fragments were collected during two periods (summer and winter) in 2016 in Kāneʻohe Bay, Hawaiʻi. Solid lines represent model fit to log(DLI) and depth relationship.

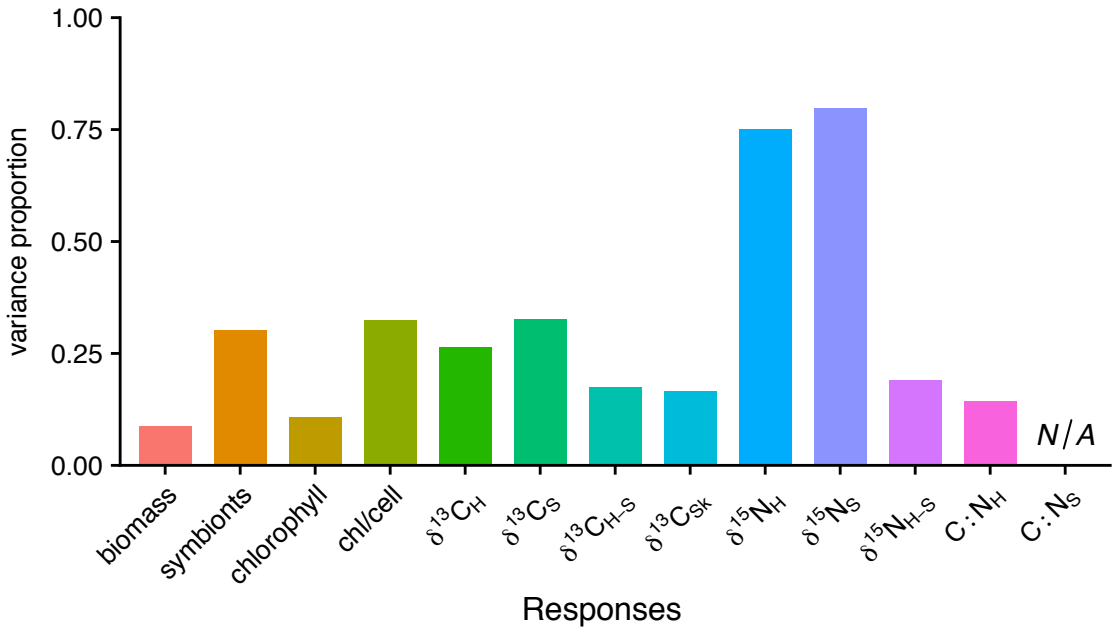

Appendix Figure 4.S5. Proportion of linear mixed effect model variance explained by the random effects of *Location* for each response metric. *N/A* represents models where variance proportion was not different from zero.

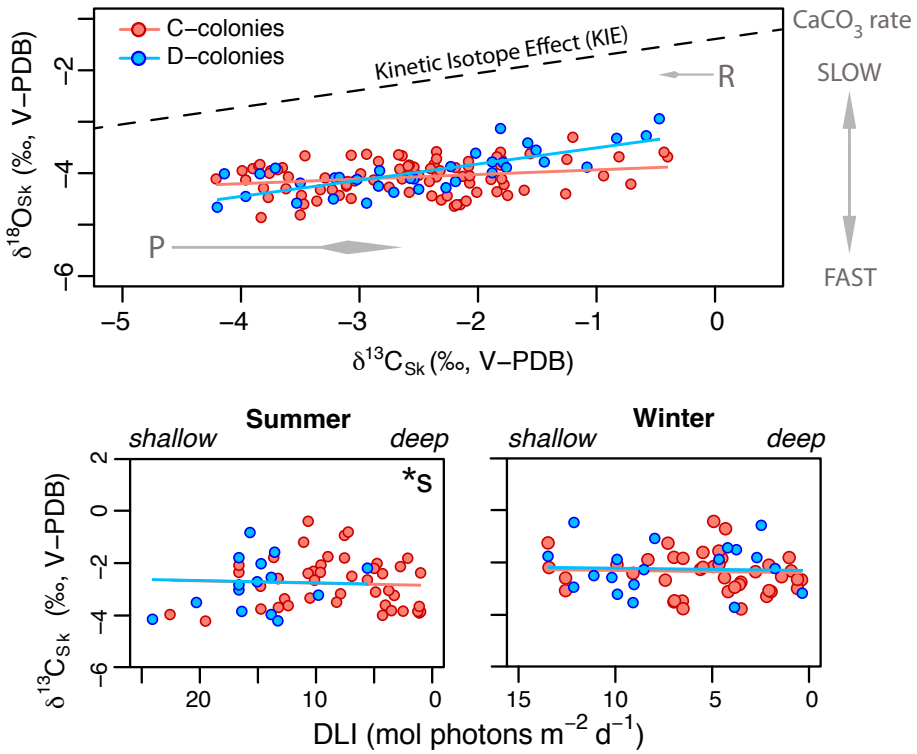

Appendix Figure 4.S6. Stable isotope values skeletal carbonates from *Montipora capitata* colonies dominated by C (*Cladocopium* spp.) or D (*Durusdinium* spp.) symbionts. (*Top*) The relationship between oxygen $\delta^{18}O$ and carbon isotopes $\delta^{13}C_{Sk}$, and (*bottom*) carbon isotopes in skeletal material across seasons in response to light availability. Letters *P* and *R* represent carbon isotope offset from metabolic effects of photosynthesis and respiration, respectively. *Slow* and *fast* refer to skeletal growth effects ($CaCO_3$ rate) effects on $\delta^{18}O$; Kinetic Isotope Effect (KIE) is line where kinetic isotope effects occur, departing from seawater isotopic equilibrium (approx. -1.24 ‰ $\delta^{18}O$ and 2.85 ‰ $\delta^{13}C$). Values are permil (‰) relative to standards for carbon and oxygen (Vienna-Pee Dee Belemnite: V-PDB). Solid lines represent linear mixed effect model fits. *Asterisk-letter* (**s*) indicates significant differences ($p < 0.05$) between seasons.

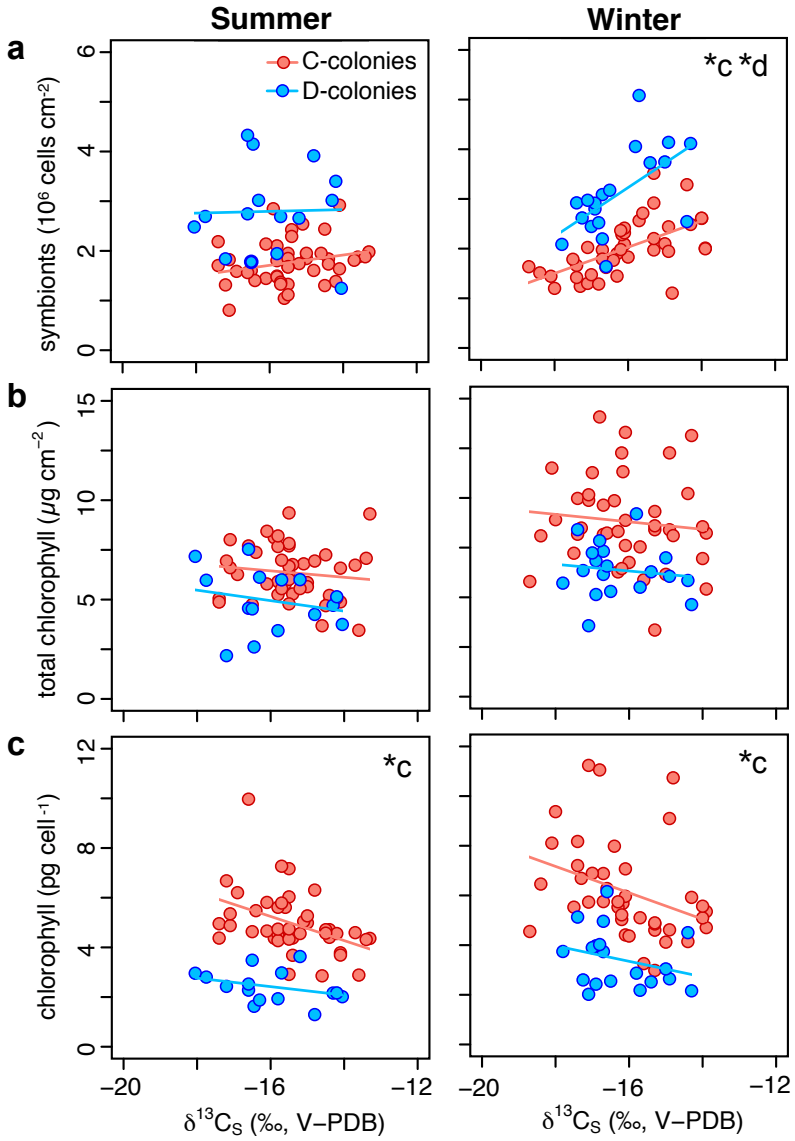

Appendix Figure 4.S7. The relationship between symbiont isotope values ($\delta^{13}C_S$) and (**a**) symbiont densities, (**b**) total chlorophyll, and (**c**) chlorophyll per symbiont cells and for *Montipora capitata* colonies dominated by C (*Cladocopium* spp.) or D (*Durusdinium* spp.) symbionts collected in summer (*left*) and winter (*right*). Solid lines represent linear model fits. *Asterisk-letters* represent significant relationship ($p < 0.05$) for C- or D-colonies (**c* or **d*, respectively).

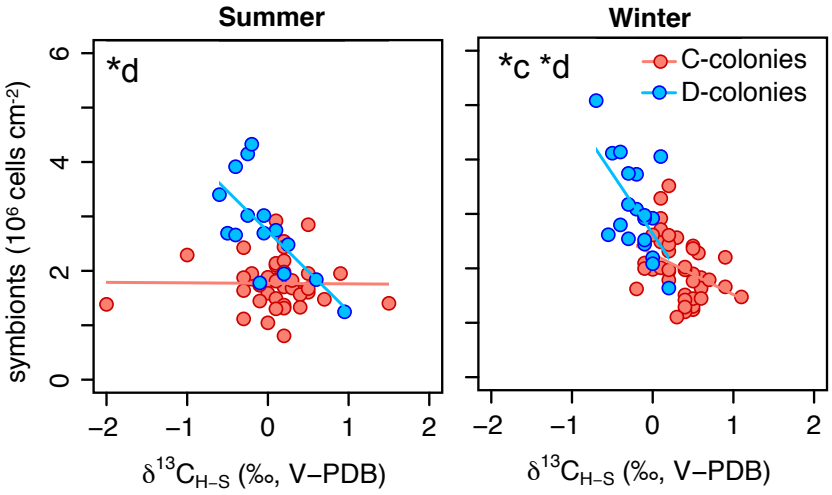

Appendix Figure 4.S7. The relationship between the relative differences in host and symbiont isotope values ($\delta^{13}C_{H-S}$) and symbiont densities for *Montipora capitata* colonies dominated by C (*Cladocopium* spp.) or D (*Durusdinium* spp.) symbionts collected in summer (*left*) and winter (*right*). Solid lines represent linear model fits. *Asterisk-letters* represent significant relationship ($p < 0.05$) for C- or D-colonies (**c* or **d*, respectively).

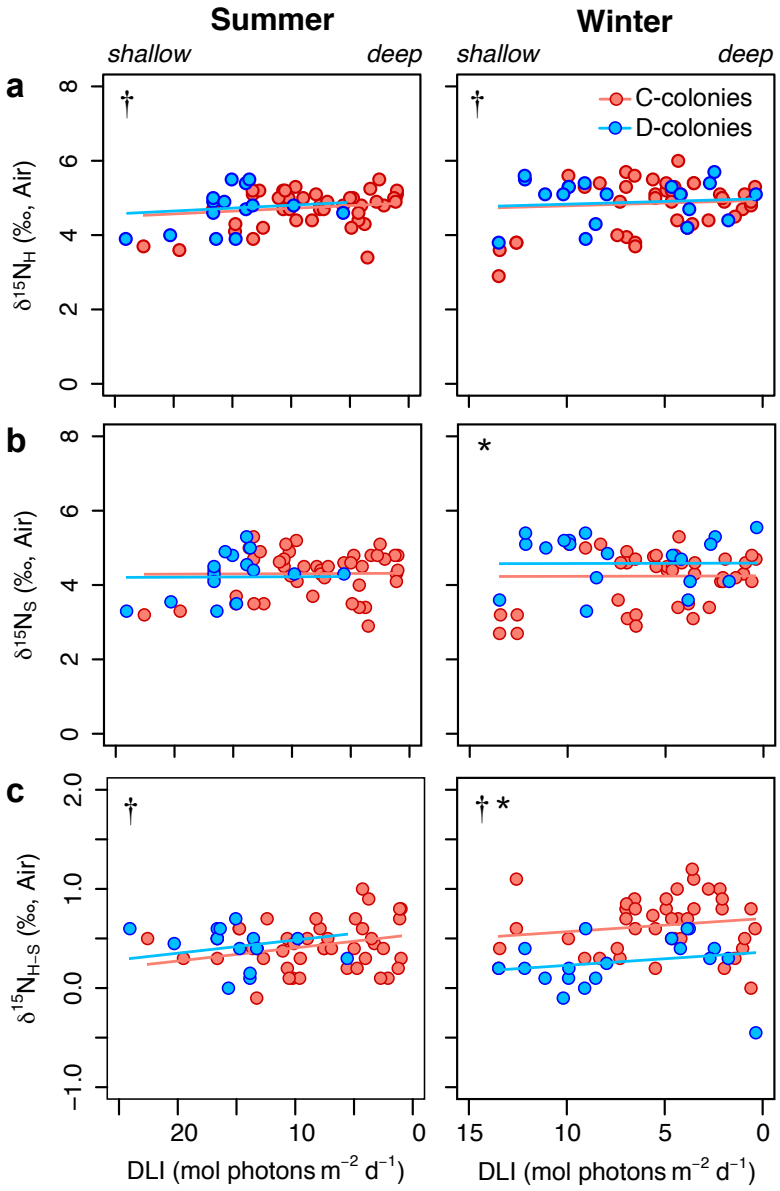

Appendix Figure 4.S9. Nitrogen stable isotope values for *Montipora capitata* dominated by C (*Cladocopium* spp.) or D (*Durusdinium* spp.) symbionts. Colonies were collected from four Kāneʻohe Bay reef locations in summer (*left*) and winter (*right*) spanning a light availability gradient across <1 m – 9 m depth. Values are for (**a**) coral host ($\delta^{15}N_H$) (**b**) symbiont algae ($\delta^{15}N_S$) and (**c**) their relative difference ($\delta^{15}N_{H\text{-}S}$) in permil (‰) relative to nitrogen standards (Air). Lines represent linear mixed effect model fits. *Symbols* indicate significant differences ($p < 0.05$) between symbiont communities (*) or in response to light.

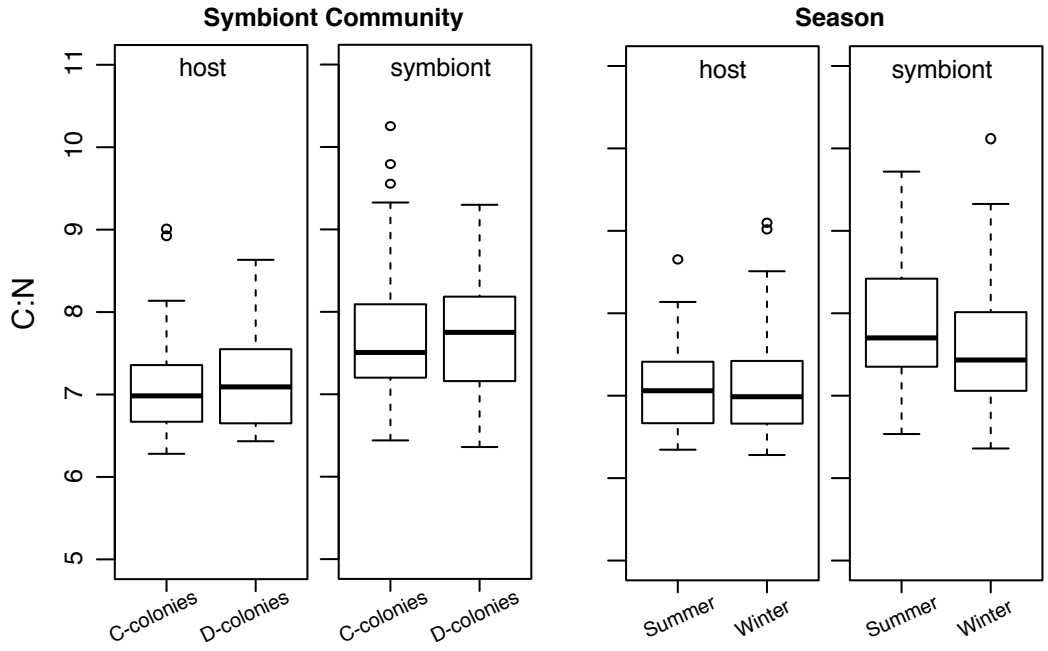

Appendix Figure 4.S10. Biomass molar carbon:nitrogen (C:N) ratios in host and symbiont tissues as a function of symbiont community (C-colonies *vs.* D-colonies) and season (summer *vs*. winter).

REFERENCES

Aeby GS, Williams GJ, Franklin EC, Kenyon J, Cox EF, Coles S, Work TM (2011) Patterns of coral disease across the Hawaiian archipelago: relating disease to environment. PLoS One 6:e20370

Akaike H. (1978) A Bayesian analysis of the minimum AIC procedure. Ann Inst Stat Math 30: 9–14

Alamaru A, Loya Y, Brokovich E, Yam R, Shemesh A (2009) Carbon and nitrogen utilization in two species of Red Sea corals along a depth gradient: Insights from stable isotope analysis of total organic material and lipids. Geochim Cosmochim Acta 73:5333–5342

Albright R, Mason B, Langdon C (2008) Effect of aragonite saturation state on settlement and post-settlement growth of Porites astreoides larvae. Coral Reefs 27:485–490

Allemand D, Tambutté É, Zoccola D, Tambutté S. (2011) Coral calcification, cells to reefs. In Coral Reefs: An Ecosystem in Transition (eds Z. Dubinsky & N. Stambler), pp. 119–150. Dordrecht: Springer Netherlands

Allison N, Cohen I, Finch AA, Erez J, Tudhope AW, Edinburgh Ion Microprobe Facility (2014) Corals concentrate dissolved inorganic carbon to facilitate calcification. Nat Commun 5:5741

Anthony KR, Fabricius KE (2000) Shifting roles of heterotrophy and autotrophy in coral energetics under varying turbidity. J Exp Mar Bio Ecol 252:221–253

Anthony KRN (1999) Coral suspension feeding on fine particulate matter. J Exp Mar Bio Ecol 232:85–106

Anthony KRN (2006) Enhanced energy status of corals on coastal, high-turbidity reefs. Mar Ecol Prog Ser 319:111–116

Anthony KRN, Connolly SR, Hoegh-Guldberg O (2007) Bleaching, energetics, and coral mortality risk: Effects of temperature, light, and sediment regime. Limnol Oceanogr 52:716–726

Anthony KRN, Connolly SR, Willis BL (2002) Comparative analysis of energy allocation to tissue and skeletal growth in corals. Limnol Oceanogr 47:1417–1429

Anthony KRN, Hoegh-Guldberg O (2003a) Kinetics of photoacclimation in corals. Oecologia 134:23–31

Anthony KRN, Hoegh-Guldberg O (2003b) Variation in coral photosynthesis, respiration and growth characteristics in contrasting light microhabitats: An analogue to plants in forest gaps and understoreys? Funct Ecol 17:246–259

Anthony KRN, Hoogenboom MO, Maynard JA, Grottoli AG, Middlebrook R (2009) Energetics approach to predicting mortality risk from environmental stress: A case study of coral bleaching. Funct Ecol 23:539–550

Anthony KRN, Kline DI, Diaz-Pulido G, Dove S, Hoegh-Guldberg O (2008) Ocean acidification causes bleaching and productivity loss in coral reef builders. Proc Natl Acad Sci U S A 105:17442–17446

Anthony KRN, Larcombe P (2002) Coral reefs in turbid waters: sediment-induced stresses in corals and likely mechanisms of adaptation. Proc Int Coral Reef Symp 9:239–244

Bahr KD, Jokiel PL, Rodgers KS (2015) The 2014 coral bleaching and freshwater flood events in Kāneʻohe Bay, Hawaiʻi. PeerJ 3:e1136

Bahr KD, Jokiel PL, Rodgers KS (2016) Relative sensitivity of five Hawaiian coral species to high temperature under high-pCO_2 conditions. Coral Reefs 35:729–738

Bahr KD, Rodgers KS, Jokiel PL (2017) Impact of three bleaching events on the reef resiliency of Kāneʻohe Bay, Hawaiʻi. Front Mar Sci 4:398

Baker AC (2003) Flexibility and specificity in coral-algal symbiosis: Diversity, ecology, and biogeography of *Symbiodinium*. Annu Rev Ecol Evol Syst 34:661–689

Baker AC, McClanahan TR, Starger CJ (2013a) Long-term monitoring of algal symbiont communities in corals reveals stability is taxon dependent and driven by site-specific thermal regime. Mar Ecol Prog Ser 479:85–97

Baker DM, Andras JP, Jordán-Garza AG, Fogel ML (2013b) Nitrate competition in a coral symbiosis varies with temperature among *Symbiodinium* clades. ISME J 7:1248–1251

Baker DM, Freeman CJ, Wong JCY, Fogel ML, Knowlton N (2018) Climate change promotes parasitism in a coral symbiosis. ISME J 12:921–930

Baumann J, Grottoli AG, Hughes AD, Matsui Y (2014) Photoautotrophic and heterotrophic carbon in bleached and non-bleached coral lipid acquisition and storage. J Exp Mar Bio Ecol 461:469–478

Bayliss SLJ, Scott ZR, Coffroth MA, terHorst CP (2019) Genetic variation in *Breviolum antillogorgium*, a coral reef symbiont, in response to temperature and nutrients. Ecol Evol 9:2803–2813

Bednarz VN, Grover R, Maguer J-F, Fine M, Ferrier-Pagès C (2017) The assimilation of diazotroph-derived nitrogen by scleractinian corals depends on their metabolic status. MBio 8:e02058–16

Bessell-Browne P, Negri AP, Fisher R, Clode PL, Jones R (2017) Impacts of light limitation on corals and crustose coralline algae. Sci Rep 7:11553

Biquand E, Okubo N, Aihara Y, Rolland V, Hayward DC, Hatta M, Minagawa J, Maruyama T, Takahashi S (2017) Acceptable symbiont cell size differs among cnidarian species and may limit symbiont diversity. ISME J 11:1702–1712

Bongaerts P, Riginos C, Ridgway T, Sampayo EM, van Oppen MJH, Englebert N, Vermeulen F, Hoegh-Guldberg O (2010) Genetic divergence across habitats in the widespread coral *Seriatopora hystrix* and its associated *Symbiodinium*. PLoS One 5:e10871

Brading P, Warner ME, Davey P, Smith DJ, Achterberg EP, Suggett DJ (2011) Differential effects of ocean acidification on growth and photosynthesis among phylotypes of *Symbiodinium* (Dinophyceae). Limnol Oceanogr 56:927–938

Buddemeier RW, Fautin DG (1993) Coral bleaching as an adaptive mechanism. Bioscience 43:320–326

Cai W-J, Ma Y, Hopkinson BM, Grottoli AG, Warner ME, Ding Q, Hu X, Yuan X, Schoepf V, Xu H, Han C, Melman TF, Hoadley KD, Pettay DT, Matsui Y, Baumann JH, Levas S, Ying Y, Wang Y (2016) Microelectrode characterization of coral daytime interior pH and carbonate chemistry. Nat Commun 7:11144

Cantin NE, van Oppen M, Willis BL, Mieog JC, Negri AP (2009) Juvenile corals can acquire more carbon from high-performance algal symbionts. Coral Reefs 28:405–414

Chalker BE (1981) Simulating light-saturation curves for photosynthesis and calcification by reef-building corals. Mar Biol 63:135–141

Chan NCS, Connolly SR (2013) Sensitivity of coral calcification to ocean acidification: A meta-analysis. Glob Chang Biol 19:282–290

Coles SL, Jokiel PL, Lewis CR (1976) Thermal tolerance in tropical versus subtropical Pacific reef corals. Pac Sci 30:159–166

Comeau S, Carpenter RC, Edmunds PJ (2013a) Coral reef calcifiers buffer their response to ocean acidification using both bicarbonate and carbonate. Proc Biol Sci 280:20122374

Comeau S, Carpenter RC, Edmunds PJ (2013b) Effects of feeding and light intensity on the response of the coral *Porites rus* to ocean acidification. Mar Biol 160:1127–1134

Comeau S, Carpenter RC, Edmunds PJ (2014a) Effects of irradiance on the response of the coral *Acropora pulchra* and the calcifying alga *Hydrolithon reinboldii* to temperature elevation and ocean acidification. J Exp Mar Bio Ecol 453:28–35

Comeau S, Carpenter RC, Edmunds PJ (2017) Effects of pCO_2 on photosynthesis and respiration

of tropical scleractinian corals and calcified algae. ICES J Mar Sci 74:1092–1102

Comeau S, Carpenter RC, Nojiri Y, Putnam HM, Sakai K, Edmunds PJ (2014b) Pacific-wide contrast highlights resistance of reef calcifiers to ocean acidification. Proc Biol Sci 281:20141339–20141339

Comeau S, Edmunds PJ, Lantz CA, Carpenter RC (2014c) Water flow modulates the response of coral reef communities to ocean acidification. Sci Rep 4:6681

Comeau S, Edmunds PJ, Spindel NB (2013c) The responses of eight coral reef calcifiers to increasing partial pressure of CO_2 do not exhibit a tipping point. Limnol Oceanogr 58:388–398

Comeau S, Edmunds PJ, Spindel NB, Carpenter RC (2014d) Fast coral reef calcifiers are more sensitive to ocean acidification in short-term laboratory incubations. Limnol Oceanogr 59:1081–1091

Connolly SR, Lopez-Yglesias MA, Anthony KRN (2012) Food availability promotes rapid recovery from thermal stress in a scleractinian coral. Coral Reefs 31:951–960

Cooper TF, Berkelmans R, Ulstrup KE, Weeks S, Radford B, Jones AM, Doyle J, Canto M, O'Leary RA, van Oppen MJH (2011a) Environmental factors controlling the distribution of *Symbiodinium* harboured by the coral *Acropora millepora* on the Great Barrier Reef. PLoS One 6:e25536

Cooper TF, Lai M, Ulstrup KE, Saunders SM, Flematti GR, Radford B, van Oppen MJH (2011b) *Symbiodinium* genotypic and environmental controls on lipids in reef building corals. PLoS One 6:e20434

Cooper TF, Ulstrup KE, Dandan SS, Heyward AJ, Kühl M, Muirhead A, O'Leary RA, Ziersen BEF, Van Oppen MJH (2011c) Niche specialization of reef-building corals in the mesophotic zone: Metabolic trade-offs between divergent *Symbiodinium* types. Proc Biol Sci 278:1840–1850

Couch CS, Burns JHR, Liu G, Steward K, Gutlay TN, Kenyon J, Eakin CM, Kosaki RK (2017) Mass coral bleaching due to unprecedented marine heatwave in Papahānaumokuākea Marine National Monument (Northwestern Hawaiian Islands). PLoS One 12:e0185121

Crossland CJ, Barnes DJ, Borowitzka MA (1980) Diurnal lipid and mucus production in the staghorn coral Acropora acuminata. Mar Biol 60:81–90

Cunning R, Baker AC (2012) Excess algal symbionts increase the susceptibility of reef corals to bleaching. Nat Clim Chang 3:259

Cunning R, Baker AC (2014) Not just who, but how many: the importance of partner abundance in reef coral symbioses. Front Microbiol 5:400

Cunning R, Gillette P, Capo T, Galvez K, Baker AC (2015) Growth tradeoffs associated with

thermotolerant symbionts in the coral *Pocillopora damicornis* are lost in warmer oceans. Coral Reefs 34:155–160

Cunning R, Ritson-Williams R, Gates RD (2016) Patterns of bleaching and recovery of *Montipora capitata* in Kāneʻohe Bay, Hawaiʻi, USA. Mar Ecol Prog Ser 551:131–139

D'Angelo C, Denzel A, Vogt A, Matz MV, Oswald F, Salih A, Nienhaus GU, Wiedenmann J (2008) Blue light regulation of host pigment in reef-building corals. Mar Ecol Prog Ser 364:97–106

Dailer ML, Knox RS, Smith JE, Napier M, Smith CM (2010) Using delta ^{15}N values in algal tissue to map locations and potential sources of anthropogenic nutrient inputs on the island of Maui, Hawai'i, USA. Mar Pollut Bull 60:655–671

Dale JJ, Wallsgrove NJ, Popp BN, Holland KN (2011) Nursery habitat use and foraging ecology of the brown stingray *Dasyatis lata* determined from stomach contents, bulk and amino acid stable isotopes. Mar Ecol Prog Ser 433:221–236

Davies PS (1984) The role of zooxanthellae in the nutritional energy requirements of *Pocillopora eydouxi*. Coral Reefs 2:181–186

Davy SK, Cook CB (2001) The influence of "host release factor"on carbon release by zooxanthellae isolated from fed and starved *Aiptasia pallida* (Verrill). Comp Biochem Phys A

DeNiro MJ, Epstein S (1977) Mechanism of carbon isotope fractionation associated with lipid synthesis. Science 197:261–263

Dennison WC, Barnes DJ (1988) Effect of water motion on coral photosynthesis and calcification. J Exp Mar Bio Ecol 115:67–77

Dickson AG, Sabine CL, Christian JR (2007) Guide to best practices for ocean CO_2 measurements. PICES Special Publication 3; 2007. http://cdiac.ornl.gov/oceans/Handbook_2007.html

Drenkard EJ, Cohen AL, McCorkle DC, de Putron SJ, Starczak VR, Repeta DJ (2018) Juveniles of the Atlantic coral, *Favia fragum* (Esper, 1797) do not invest energy to maintain calcification under ocean acidification. J Exp Mar Bio Ecol 507:61–69

Drenkard EJ, Cohen AL, McCorkle DC, de Putron SJ, Starczak VR, Zicht AE (2013) Calcification by juvenile corals under heterotrophy and elevated CO_2. Coral Reefs 32:727–735

Dove S, Ortiz JC, Enríquez S, Fine M, Fisher P, Iglesias-Prieto R, Thornhill D, Hoegh-Guldberg O (2006) Response of holosymbiont pigments from the Scleractinian coral *Montipora monasteriata* to short-term heat stress. Limnol Oceanogr 51:1149–1158

Drupp P, De Carlo EH, Mackenzie FT, Bienfang P, Sabine CL (2011) Nutrient inputs,

phytoplankton response, and CO_2 variations in a semi-enclosed subtropical embayment, Kaneohe Bay, Hawaii. Aquat Geochem 17:473–498

Drupp PS, De Carlo EH, Mackenzie FT, Sabine CL, Feely RA, Shamberger KE (2013) Comparison of CO_2 dynamics and air–sea gas exchange in differing tropical reef environments. Aquat Geochem 19:371–397

Dubinsky Z, Jokiel PL (1994) Ratio of energy and nutrient fluxes regulates symbiosis between zooxanthellae and corals. Pac Sci 48:313–324

DuBois M, Gilles KA, Hamilton JK, Rebers PA, Smith F (1956) Colorimetric method for determination of sugars and related substances. Anal Chem 28:350–356

Dufault AM, Ninokawa A, Bramanti L, Cumbo VR, Fan T-Y, Edmunds PJ (2013) The role of light in mediating the effects of ocean acidification on coral calcification. J Exp Biol 216:1570–1577

Dulai H, Kleven A, Ruttenberg K, Briggs R, Thomas F (2016) Evaluation of submarine groundwater discharge as a coastal nutrient source and its role in coastal groundwater quality and quantity. In: Fares A. (eds) Emerging Issues in Groundwater Resources. Springer International Publishing, Cham, pp 187–221

Edmunds P, Gates R (2002) Normalizing physiological data for scleractinian corals. Coral Reefs 21:193–197

Edmunds PJ (2011) Zooplanktivory ameliorates the effects of ocean acidification on the reef coral *Porites* spp. Limnol Oceanogr 56:2402–2410

Edmunds PJ, Brown D, Moriarty V (2012) Interactive effects of ocean acidification and temperature on two scleractinian corals from Moorea, French Polynesia. Glob Chang Biol 18:2173–2183

Edmunds PJ, Cumbo VR, Fan T-Y (2013) Metabolic costs of larval settlement and metamorphosis in the coral *Seriatopora caliendrum* under ambient and elevated pCO_2. J Exp Mar Bio Ecol 443:33–38

Edmunds PJ, Gates RD, Gleason DF (2003) The tissue composition of *Montastraea franksi* during a natural bleaching event in the Florida Keys. Coral Reefs 22:54–62

Edmunds PJ, Wall CB (2014) Evidence that high pCO_2 affects protein metabolism in tropical reef corals. Biol Bull 227:68–77

Einbinder S, Mass T, Brokovich E, Dubinsky Z, Erez J, Tchernov D (2009) Changes in morphology and diet of the coral Stylophora pistillata along a depth gradient. Mar Ecol Prog Ser 381:167–174

Enochs IC, Manzello DP, Carlton R, Schopmeyer S, van Hooidonk R, Lirman D (2014) Effects of light and elevated pCO_2 on the growth and photochemical efficiency of *Acropora cervicornis*. Coral Reefs 33:477–485

Eyre BD, Cyronak T, Drupp P, De Carlo EH, Sachs JP, Andersson AJ (2018) Coral reefs will transition to net dissolving before end of century. Science 359:908–911

Ezzat L, Fine M, Maguer J-F, Grover R, Ferrier-Pagès C (2017) Carbon and nitrogen Acquisition in shallow and deep holobionts of the scleractinian coral *S. pistillata*. Mar Sci 4:102

Ezzat L, Jean-François M, Renaud G, Ferrier-Pagès C (2015) New insights into carbon acquisition and exchanges within the coral–dinoflagellate symbiosis under NH_4^+ and NO_3^- supply. Proc Roy Soc B 282:20150610

Fabricius KE (2005) Effects of terrestrial runoff on the ecology of corals and coral reefs: Review and synthesis. Mar Pollut Bull 50:125–146

Falkowski PG, Dubinsky Z, Muscatine L, McCloskey L (1993) Population control in symbiotic corals. Bioscience 43:606–611f

Falkowski PG, Dubinsky Z, Muscatine L, Porter JW (1984) Light and the bioenergetics of a symbiotic coral. Bioscience 34:705–709

Falkowski PG, Raven JA (2007) Aquatic Photosynthesis. Princeton University Press,

Ferrier-Pages C, Allemand D, Gattuso JP, Jaubert J, Rassoulzadegan F (1998) Microheterotrophy in the zooxanthellate coral *Stylophora pistillata*: Effects of light and ciliate density. Limnol Oceanogr 43:1639–1648

Ferrier-Pagès C, Leal MC (2018) Stable isotopes as tracers of trophic interactions in marine mutualistic symbioses. Ecol Evol 8:661–618

Ferrier-Pagès C, Rottier C, Beraud E, Levy O (2010) Experimental assessment of the feeding effort of three scleractinian coral species during a thermal stress: Effect on the rates of photosynthesis. J Exp Mar Bio Ecol 390:118–124

Ferrier-Pagès C, Witting J, Tambutté E, Sebens KP (2003) Effect of natural zooplankton feeding on the tissue and skeletal growth of the scleractinian coral *Stylophora pistillata*. Coral Reefs 22:229–240

Fitt WK, Spero HJ, Halas J, White MW, Porter JW (1993) Recovery of the coral *Montastrea annularis* in the Florida Keys after the 1987 Caribbean "bleaching event." Coral Reefs 12:57–64

Fitt WK, McFarland FK, Warner ME, Chilcoat GC (2000) Seasonal patterns of tissue biomass and densities of symbiotic dinoflagellates in reef corals and relation to coral bleaching. Limnol Oceanogr 45:677–685

Fox J, Weisberg S. 2011. An {R} Companion to Applied Regression, Second Edition. Thousand Oaks CA: Sage. http://socserv.socsci.mcmaster.ca/jfox/Books/Companion

Fox MD, Williams GJ, Johnson MD, Radice VZ, Zgliczynski BJ, Kelly ELA, Rohwer FL, Sandin SA, Smith JE (2018) Gradients in primary production predict trophic strategies of mixotrophic corals across spatial scales. Curr Biol 28:3355–3363.e4

Frade PR, Bongaerts P, Winkelhagen AJS, Tonk L, Bak RPM (2008a) In situ photobiology of corals over large depth ranges: A multivariate analysis on the roles of environment, host, and algal symbiont. Limnol Oceanogr 53:2711–2723

Frade PR, De Jongh F, Vermeulen F, van Bleijswijk J, Bak RPM (2008b) Variation in symbiont distribution between closely related coral species over large depth ranges. Mol Ecol 17:691–703

Frade PR, Englebert N, Faria J, Visser PM, Bak RPM (2008c) Distribution and photobiology of *Symbiodinium* types in different light environments for three colour morphs of the coral *Madracis pharensis*: Is there more to it than total irradiance? Coral Reefs 27:913–925

Friedlander A, Aeby G, Brown E, Clark A, Coles S, Dollar S, Hunter C, Jokiel P, Smith J, Walsh B, Williams I, Wiltse W (2005) The State of Coral Reef Ecosystems of the Main Hawaiian Islands. In: Waddell J. (eds) The State of Coral Reef Ecosystems of the United States and Pacific Freely Associated States. NOAA Technical Memorandum NOS NCCOS II, NOAA/NCCOS, pp 222–269

Gates RD, Hoegh-Guldberg O (1995) Free amino acids exhibit anthozoan“ host factor” activity: They induce the release of photosynthate from symbiotic dinoflagellates in vitro. 92:7430–7434

Gattuso J-P, Allemand D, Frankignoulle M (1999) Photosynthesis and calcification at cellular, organismal and community levels in coral reefs: A review on interactions and control by carbonate chemistry. Integr Comp Biol 39:160–183

Gattuso JP, Epitalon JM, Lavigne H. 2015 seacarb: seawater carbonate chemistry. R package, version 3.0.11. https://cran.r-project.org/package=seacarb

Gaylord B, Kroeker KJ, Sunday JM, Anderson KM, Barry JP, Brown NE, Connell SD, Dupont S, Fabricius KE, Hall-Spencer JH, Klinger T, Milazzo M, Munday PL, Russell BD, Sanford E, Schreiber SJ, Thiyagarajan V, Vaughan MLH, Widdicombe S, Harley CDG (2015) Ocean acidification through the lens of ecological theory. Ecology 96:3–15

Hoegh-Guldberg O (2010) Genetic divergence across habitats in the widespread coral *Seriatopora hystrix* and its associated *Symbiodinium*. PLoS One 5:e10871

Schoepf V, Grottoli AG, Levas SJ, Aschaffenburg MD, Baumann JH, Matsui Y, Warner ME (2015) Annual coral bleaching and the long-term recovery capacity of coral. Proc Biol Sci 282:20151887

Schoepf V, Grottoli AG, Warner ME, Cai W-J, Melman TF, Hoadley KD, Pettay DT, Hu X, Li Q, Xu H, Wang Y, Matsui Y, Baumann JH (2013) Coral energy reserves and calcification in a high-CO_2 world at two temperatures. PLoS One 8:e75049

Schoepf V, Levas SJ, Rodrigues LJ, McBride MO, Aschaffenburg MD, Matsui Y, Warner ME, Hughes AD, Grottoli AG (2014) Kinetic and metabolic isotope effects in coral skeletal carbon isotopes: A re-evaluation using experimental coral bleaching as a case study. Geochim Cosmochim Acta 146:164–178

Selph KE, Goetze E, Jungbluth MJ, Lenz PH, Kolker G (2018) Microbial food web connections and rates in a subtropical embayment. Mar Ecol Prog Ser 590:19–34

Shick JM, Lesser MP, Jokiel PL (1996) Effects of ultraviolet radiation on corals and other coral reef organisms. Glob Chang Biol 2:527–545

Sigman DM, Casciotti KL (2001) Nitrogen Isotopes in the Ocean. In: Steele J.H. (eds) Encyclopedia of Ocean Sciences. Academic Press, Oxford, pp 1884–1894

Sigman DM, Casciotti KL, Andreani M, Barford C, Galanter M, Böhlke JK (2001) A bacterial method for the nitrogen isotopic analysis of nitrate in seawater and freshwater. Anal Chem 73:4145–4153

Silbiger NJ, Nelson CE, Remple K, Sevilla JK, Quinlan ZA, Putnam HM, Fox MD, Donahue MJ (2018) Nutrient pollution disrupts key ecosystem functions on coral reefs. Proc Biol Sci 285:20172718–20172719

Silverman J, Lazar B, Cao L, Caldeira K, Erez J (2009) Coral reefs may start dissolving when atmospheric CO 2doubles. Geophys Res Lett 36:L05606

Smith JN, De'ath G, Richter C, Cornils A, Hall-Spencer JM, Fabricius KE (2016) Ocean acidification reduces demersal zooplankton that reside in tropical coral reefs. Nat Clim Chang 6:1124

Smith PK, Krohn RI, Hermanson GT, Mallia AK, Gartner FH, Provenzano MD, Fujimoto EK, Goeke NM, Olson BJ, Klenk DC (1985) Measurement of protein using bicinchoninic acid. Anal Biochem 150:76–85

Smith SV, Kimmerer WJ, Laws EA, Brock RE, Walsh TW (1981) Kaneohe Bay sewage diversion experiment: perspectives on ecosystem responses to nutritional perturbation. Science 35:279–395

Sogin EM, Putnam HM, Nelson CE, Anderson P, Gates RD (2017) Correspondence of coral holobiont metabolome with symbiotic bacteria, archaea and *Symbiodinium* communities. Environ Microbiol Rep 9:310–315

Spalding C, Finnegan S (2017) Energetic costs of calcification under ocean acidification. Global Biogeochem Cycles 31:866–877

Spencer Davies P (1989) Short-term growth measurements of corals using an accurate buoyant weighing technique. Mar Biol 101:389–395

Starzak DE, Quinnell RG, Nitschke MR, Davy SK (2014) The influence of symbiont type on photosynthetic carbon flux in a model cnidarian–dinoflagellate symbiosis. Mar Biol 161:711–724

Stat M, Carter D, Hoegh-Guldberg O (2006) The evolutionary history of *Symbiodinium* and scleractinian hosts—Symbiosis, diversity, and the effect of climate change. Perspect Plant Ecol Evol Syst 8:23–43

Stat M, Gates RD (2010) Clade D Symbiodinium in Scleractinian corals: A "nugget" of hope, a selfish opportunist, an ominous sign, or all of the above? J Mar Biol 2011:1–9

Stat M, Morris E, Gates RD (2008) Functional diversity in coral–dinoflagellate symbiosis. Proc Natl Acad Sci U S A 105:9256–9261

Stat M, Pochon X, Cowie ROM, Gates RD (2009) Specificity in communities of *Symbiodinium* in corals from Johnston Atoll. Mar Ecol Prog Ser 386:83–96

Stat M, Pochon X, Franklin EC, Bruno JF, Casey KS, Selig ER, Gates RD (2013) The distribution of the thermally tolerant symbiont lineage (*Symbiodinium* clade D) in corals from Hawaii: Correlations with host and the history of ocean thermal stress. Ecol Evol 3:1317–1329

Stat M, Yost DM, Gates RD (2015) Geographic structure and host specificity shape the community composition of symbiotic dinoflagellates in corals from the Northwestern Hawaiian Islands. Coral Reefs 34:1075–1086

Stimson J, Kinzie RA (1991) The temporal pattern and rate of release of zooxanthellae from the reef coral *Pocillopora damicornis* (Linnaeus) under nitrogen-enrichment and control conditions. J Exp Mar Bio Ecol 153:63–74

Stimson JS (1987) Location, quantity and rate of change in quantity of lipids in t issue of Hawaiian hermatypic corals. Bull Mar Sci 41:889–904

Storlazzi CD, Norris BK, Rosenberger KJ (2015) The influence of grain size, grain color, and suspended-sediment concentration on light attenuation: Why fine-grained terrestrial sediment is bad for coral reef ecosystems. Coral Reefs 34:967–975

Suggett DJ, Dong LF, Lawson T, Lawrenz E, Torres L, Smith DJ (2013) Light availability determines susceptibility of reef building corals to ocean acidification. Coral Reefs 32:327–337

Swart PK, Leder JJ, Szmant AM, Dodge RE (1996) The origin of variations in the isotopic

record of scleractinian corals: II. Carbon. Geochim Cosmochim Acta 60:2871–2885

Swart PK, Saied A, Lamb K (2005a) Temporal and spatial variation in the $\delta^{15}N$ and $\delta^{13}C$ of coral tissue and zooxanthellae in *Montastraea faveolata* collected from the Florida reef tract. Limnol Oceanogr 50:1049–1058

Swart PK, Szmant A, Porter JW, Dodge RE, Tougas JI, Southam JR (2005b) The isotopic composition of respired carbon dioxide in scleractinian corals: Implications for cycling of organic carbon in corals. Geochim Cosmochim Acta 69:1495–1509

Szmant AM, Gassman NJ (1990) The effects of prolonged "bleaching" on the tissue biomass and reproduction of the reef coral *Montastrea annularis*. Coral Reefs 8:217–224

Tambutté E, Venn AA, Holcomb M, Segonds N, Techer N, Zoccola D, Allemand D, Tambutté S (2015) Morphological plasticity of the coral skeleton under CO_2-driven seawater acidification. Nat Commun 6:7368

Tanaka Y, Miyajima T, Koike I, Hayashibara T, Ogawa H (2006) Translocation and conservation of organic nitrogen within the coral-zooxanthella symbiotic system of *Acropora pulchra*, as demonstrated by dual isotope-labeling techniques. J Exp Mar Bio Ecol 336:110–119

Terán E, Méndez ER, Enríquez S, Iglesias-Prieto R (2010) Multiple light scattering and absorption in reef-building corals. Appl Opt 49:5032–5042

Thomas L, Palumbi SR (2017) The genomics of recovery from coral bleaching. Proc Biol Sci 284:20171790–20171799

Tolosa I, Treignier C, Grover R, Ferrier-Pagès C (2011) Impact of feeding and short-term temperature stress on the content and isotopic signature of fatty acids, sterols, and alcohols in the scleractinian coral *Turbinaria reniformis*. Coral Reefs 30:763

Towle EK, Enochs IC, Langdon C (2015) Threatened Caribbean coral is able to mitigate the adverse effects of ocean acidification on calcification by increasing feeding Rate. PLoS One 10:e0139398

Tremblay P, Ferrier-Pagès C, Maguer JF, Rottier C, Legendre L, Grover R (2012a) Controlling effects of irradiance and heterotrophy on carbon translocation in the temperate coral *Cladocora caespitosa*. PLoS One 7:e44672

Tremblay P, Fine M, Maguer JF, Grover R, Ferrier-Pagès C (2013) Photosynthate translocation increases in response to low seawater pH in a coral–dinoflagellate symbiosis. Biogeosciences 10:3997–4007

Tremblay P, Grover R, Maguer JF, Hoogenboom M, Ferrier-Pagès C (2014) Carbon translocation from symbiont to host depends on irradiance and food availability in the tropical coral *Stylophora pistillata*. Coral Reefs 33:1–13

Tremblay P, Naumann MS, Sikorski S, Grover R, Ferrier-Pages C (2012b) Experimental assessment of organic carbon fluxes in the scleractinian coral *Stylophora pistillata* during a thermal and photo stress event. Mar Ecol Prog Ser 453:63–77

Trench RK (1971a) The physiology and biochemistry of zooxanthellae symbiotic with marine coelenterates. I. The assimilation of photosynthetic products of zooxanthellae by two marine coelenterates. Proc R Soc Lond B Biol Sci 177:225–235

Trench RK (1971b) The physiology and biochemistry of zooxanthellae symbiotic with marine coelenterates III. The effect of homogenates of host tissues on the excretion of photosynthetic products in vitro by zooxanthellae from two marine coelenterates.
Proc R Soc Lond B Biol Sci 177:251–264

Trench RK (1971c) The physiology and biochemistry of zooxanthellae symbiotic with marine coelenterates. II. Liberation of fixed 14C by zooxanthellae in vitro. Proc R Soc Lond B Biol Sci 177:237–250

Glynn PW (1993) Coral reef bleaching: ecological perspectives. Coral Reefs 12:1–17

Glynn PW, D'croz L (1990) Experimental evidence for high temperature stress as the cause of El Niño-coincident coral mortality. Coral Reefs 8:181–191

Glynn PW, Maté JL, Baker AC, Calderón MO (2001) Coral bleaching and mortality in Panama and Ecuador During the 1997–1998 El Niño–Southern Oscillation event: Spatial/temporal patterns and comparisons with the 1982–1983 event. Bull Mar Sci 69:79–109

Gnaiger E, Bitterlich G (1984) Proximate biochemical composition and caloric content calculated from elemental CHN analysis: A stoichiometric concept. Oecologia 62:289–298

Granger J, Sigman DM, Needoba JA, Harrison PJ (2004) Coupled nitrogen and oxygen isotope fractionation of nitrate during assimilation by cultures of marine phytoplankton. Limnol Oceanogr 49:1763–1773

Grant AJ, Rémond M, Hinde R (1998) Low molecular-weight factor from *Plesiastrea versipora* (Scleractinia) that modifies release and glycerol metabolism of isolated symbiotic algae. Mar Biol 130:553–557

Grottoli AG, Rodrigues LJ (2011) Bleached *Porites compressa* and *Montipora capitata* corals catabolize δ^{13}C-enriched lipids. Coral Reefs 30:687

Grottoli AG, Rodrigues LJ, Juarez C (2004) Lipids and stable carbon isotopes in two species of Hawaiian corals, *Porites compressa* and *Montipora verrucosa*, following a bleaching event. Mar Biol 145:621–631

Grottoli AG, Rodrigues LJ, Matthews KA, Palardy JE, Gibb OT (2005) Pre-treatment effects on coral skeletal $\delta^{13}C$ and $\delta^{18}O$. Chem Geol 221:225–242

Grottoli AG, Rodrigues LJ, Palardy JE (2006) Heterotrophic plasticity and resilience in bleached corals. Nature 440:1186–1189

Grottoli AG, Tchernov D, Winters G (2017) Physiological and biogeochemical responses of super-corals to thermal stress from the Northern Gulf of Aqaba, Red Sea. Front Mar Sci 4:215

Grottoli AG, Warner ME, Levas SJ, Aschaffenburg MD, Schoepf V, McGinley M, Baumann J, Matsui Y (2014) The cumulative impact of annual coral bleaching can turn some coral species winners into losers. Glob Chang Biol 20:3823–3833

Grottoli AG, Wellington GM (1999) Effect of light and zooplankton on skeletal $\delta^{13}C$ values in the eastern Pacific corals *Pavona clavus* and *Pavona gigantea*. Coral Reefs 18:29–41

Grover R, Maguer J-F, Allemand D, Ferrier-Pagès C (2006) Urea uptake by the scleractinian coral *Stylophora pistillata*. J Exp Mar Bio Ecol 332:216–225

Halpern BS, Walbridge S, Selkoe KA, Kappel CV, Micheli F, D'Agrosa C, Bruno JF, Casey KS, Ebert C, Fox HE, Fujita R, Heinemann D, Lenihan HS, Madin EMP, Perry MT, Selig ER, Spalding M, Steneck R, Watson R (2008) A global map of human impact on marine ecosystems. Science 319:948–952

Harii S, Yamamoto M, Hoegh-Guldberg O (2010) The relative contribution of dinoflagellate photosynthesis and stored lipids to the survivorship of symbiotic larvae of the reef-building corals. Mar Biol 157:1215–1224

Haubert D, Langel R, Scheu S, Ruess L (2005) Effects of food quality, starvation and life stage on stable isotope fractionation in Collembola. Pedobiologia 49:229–237

Hayes JM (2001) Fractionation of carbon and hydrogen isotopes in biosynthetic processes. Rev Mineral Geochem 43:225–277

Heikoop JM, Dunn JJ, Risk MJ, Sandeman IM, Schwartz HP, Waltho N (1998) Relationship between light and the $\delta^{15}N$ of coral tissue: Examples from Jamaica and Zanzibar. Limnol Oceanogr 43:909–920

Heikoop JM, Dunn JJ, Risk MJ, Tomascik T, Schwarcz HP, Sandeman IM, Sammarco PW (2000) $\delta^{15}N$ and $\delta^{13}C$ of coral tissue show significant inter-reef variation. Coral Reefs 19:189–193

Heron SF, Maynard JA, van Hooidonk R, Eakin CM (2016) Warming trends and bleaching stress of the world's coral reefs 1985-2012. Sci Rep 6:38402

Hoadley KD, Pettay DT, Grottoli AG, Cai W-J, Melman TF, Schoepf V, Hu X, Li Q, Xu H,

Wang Y, Matsui Y, Baumann JH, Warner ME (2015) Physiological response to elevated temperature and pCO_2 varies across four Pacific coral species: Understanding the unique host+symbiont response. Sci Rep 5:18371

Hoegh-Guldberg O (1999) Climate change, coral bleaching and the future of the world's coral reefs. Mar Freshwater Res 50:839–866

Holcomb M, McCorkle DC, Cohen AL (2010) Long-term effects of nutrient and CO_2 enrichment on the temperate coral *Astrangia poculata* (Ellis and Solander, 1786). J Exp Mar Bio Ecol 386:27–33

Holcomb M, Venn AA, Tambutté E, Tambutté S, Allemand D, Trotter J, McCulloch M (2014) Coral calcifying fluid pH dictates response to ocean acidification. Sci Rep 4:5207

Hoogenboom MO, Connolly SR, Anthony KRN (2009) Effects of photoacclimation on the light niche of corals: A process-based approach. Mar Biol 156:2493–2503

Hoogenboom MO, Connolly SR, Anthony KRN (2011) Biotic and abiotic correlates of tissue quality for common scleractinian corals. Mar Ecol Prog Ser 438:119–128

Houlbrèque F, Ferrier-Pagès C (2009) Heterotrophy in tropical scleractinian corals. Biol Rev Camb Philos Soc 84:1–17

Houlbrèque F, Tambutté E, Ferrier-Pagès C (2003) Effect of zooplankton availability on the rates of photosynthesis, and tissue and skeletal growth in the scleractinian coral *Stylophora pistillata*. J Exp Mar Bio Ecol 296:145–166

Hughes AD, Grottoli AG (2013) Heterotrophic compensation: A possible mechanism for resilience of coral reefs to global warming or a sign of prolonged stress? PLoS One 8:e81172

Hughes AD, Grottoli AG, Pease TK, Matsui Y (2010) Acquisition and assimilation of carbon in non-bleached and bleached corals. Mar Ecol Prog Ser 420:91–101

Hughes TP, Baird AH, Bellwood DR, Card M, Connolly SR, Folke C, Grosberg R, Hoegh-Guldberg O, Jackson JBC, Kleypas J, Lough JM, Marshall P, Nyström M, Palumbi SR, Pandolfi JM, Rosen B, Roughgarden J (2003) Climate change, human impacts, and the resilience of coral reefs. Science 301:929–933

Hughes TP, Barnes ML, Bellwood DR, Cinner JE, Cumming GS, Jackson JBC, Kleypas J, van de Leemput IA, Lough JM, Morrison TH, Palumbi SR, van Nes EH, Scheffer M (2017a) Coral reefs in the Anthropocene. Nature 546:82–90

Hughes TP, Kerry JT, Álvarez-Noriega M, Álvarez-Romero JG, Anderson KD, Baird AH, Babcock RC, Beger M, Bellwood DR, Berkelmans R, Bridge TC, Butler IR, Byrne M, Cantin NE, Comeau S, Connolly SR, Cumming GS, Dalton SJ, Diaz-Pulido G, Eakin CM, Figueira WF, Gilmour JP, Harrison HB, Heron SF, Hoey AS, Hobbs J-PA, Hoogenboom MO, Kennedy EV,

Kuo C-Y, Lough JM, Lowe RJ, Liu G, McCulloch MT, Malcolm HA, McWilliam MJ, Pandolfi JM, Pears RJ, Pratchett MS, Schoepf V, Simpson T, Skirving WJ, Sommer B, Torda G, Wachenfeld DR, Willis BL, Wilson SK (2017b) Global warming and recurrent mass bleaching of corals. Nature 543:373–377

Innis T, Cunning R, Ritson-Williams R, Wall CB, Gates RD (2018) Coral color and depth drive symbiosis ecology of Montipora capitata in Kāneʻohe Bay, Oʻahu, Hawaiʻi. Coral Reefs 37:423–430

Jeffrey SW, Humphrey GF (1975) New spectrophotometric equations for determining chlorophylls *a*, *b*, c_1 and c_2 in higher plants, algae and natural phytoplankton. Biochem Physiol Pflanz 167:191–194

Jokiel PL (2011) Ocean acidification and control of reef coral calcification by boundary layer limitation of proton flux. Bull Mar Sci 87:639–657

Jokiel PL, Brown EK (2004) Global warming, regional trends and inshore environmental conditions influence coral bleaching in Hawaii. Glob Chang Biol 10:1627–1641

Jones A, Berkelmans R (2010) Potential costs of acclimatization to a warmer climate: Growth of a reef coral with heat tolerant vs. sensitive symbiont types. PLoS One 5:e10437

Jones AM, Berkelmans R (2011) Tradeoffs to Thermal Acclimation: Energetics and reproduction of a reef coral with heat tolerant *Symbiodinium* type-D. J Mar Biol 2011:1–12

Jones AM, Berkelmans R, van Oppen MJH, Mieog JC, Sinclair W (2008) A community change in the algal endosymbionts of a scleractinian coral following a natural bleaching event: field evidence of acclimatization. Proc Biol Sci 275:1359–1365

Jones RJ, Hoegh-Guldberg O (2001) Diurnal changes in the photochemical efficiency of the symbiotic dinoflagellates (Dinophyceae) of corals: photoprotection, photoinactivation and the relationship to coral bleaching. Plant Cell Environ 24:89–99

Kaniewska P, Campbell PR, Kline DI, Rodriguez-Lanetty M, Miller DJ, Dove S, Hoegh-Guldberg O (2012) Major cellular and physiological impacts of ocean acidification on a reef building coral. PLoS One 7:e34659

Kenkel CD, Matz MV (2016) Gene expression plasticity as a mechanism of coral adaptation to a variable environment. Nat Ecol Evol 1:14

Kenkel CD, Meyer E, Matz MV (2013) Gene expression under chronic heat stress in populations of the mustard hill coral (*Porites astreoides*) from different thermal environments. Mol Ecol 22:4322–4334

Kenyon JC, Brainard RE (2006) Second recorded episode of mass coral bleaching in the Northwestern Hawaiian Islands. Atoll Res Bull 543:505–523

Kleypas JA, Buddemeier RW, Archer D, Gattuso JP, Langdon C, Opdyke BN (1999) Geochemical consequences of increased atmospheric carbon dioxide on coral reefs. Science 284:118–120

Kopp C, Pernice M, Domart-Coulon I, Djediat C, Spangenberg JE, Alexander DTL, Hignette M, Meziane T, Meibom A (2013) Highly dynamic cellular-level response of symbiotic coral to a sudden increase in environmental nitrogen. MBio 4:e00052–13

Krief S, Hendy EJ, Fine M, Yam R, Meibom A, Foster GL, Shemesh A (2010) Physiological and isotopic responses of scleractinian corals to ocean acidification. Geochim Cosmochim Acta 74:4988–5001

Kroeker KJ, Kordas RL, Crim RN, Singh GG (2010) Meta-analysis reveals negative yet variable effects of ocean acidification on marine organisms. Ecol Lett 13:1419–1434

Kroeker KJ, Micheli F, Gambi MC (2012) Ocean acidification causes ecosystem shifts via altered competitive interactions. Nat Clim Chang 3:156

Kuznetsova A, Brockhoff PB, Christensen RHB (2017) lmerTest package: Tests in linear mixed effects models. J Stat Softw 82:1–26

LaJeunesse TC, Parkinson JE, Gabrielson PW, Jeong HJ, Reimer JD, Voolstra CR, Santos SR (2018) Systematic revision of Symbiodiniaceae highlights the antiquity and diversity of coral endosymbionts. Curr Biol 28:2570–2580.e6

LaJeunesse TC, Thornhill DJ, Cox EF, Stanton FG, Fitt WK, Schmidt GW (2004) High diversity and host specificity observed among symbiotic dinoflagellates in reef coral communities from Hawaii. Coral Reefs 23:596–603

Land LS, Lang JC, Smith BN (1975) Preliminary observations on the carbon isotopic composition of some reef coral tissues and symbiotic zooxanthellae1. Limnol Oceanogr 20:283–287

Laws EA, Popp BN, Bidigare RR, Kennicutt MC, Macko SA (1995) Dependence of phytoplankton carbon isotopic composition on growth rate and $[CO_2]_{aq}$: Theoretical considerations and experimental results. Geochim Cosmochim Acta 59:1131–1138

Leal MC, Hoadley K, Pettay DT, Grajales A, Calado R, Warner ME (2015) Symbiont type influences trophic plasticity of a model cnidarian-dinoflagellate symbiosis. J Exp Biol 218:858–863

Lenth R (2019) Emmeans: Estimated marginal means, aka least-squares means. R package version 1.3.3. https://CRAN.R-project.org/package=emmeans

Lenth R (2019) Least-squares means: The R package lsmeans. J Stat Softw 69: 1–33

Lenz EA, Edmunds PJ (2017) Branches and plates of the morphologically plastic coral *Porites rus* are insensitive to ocean acidification and warming. J Exp Mar Bio Ecol 486:188–194

Lesser MP (1997) Oxidative stress causes coral bleaching during exposure to elevated temperatures. Coral Reefs 16:187–192

Lesser MP (2013) Using energetic budgets to assess the effects of environmental stress on corals: are we measuring the right things? Coral Reefs 32:25–33

Lesser MP, Slattery M, Stat M, Ojimi M, Gates RD, Grottoli A (2010) Photoacclimatization by the coral *Montastraea cavernosa* in the mesophotic zone: Light, food, and genetics. Ecology 91:990–1003

Lesser MP, Stat M, Gates RD (2013) The endosymbiotic dinoflagellates (*Symbiodinium* sp.) of corals are parasites and mutualists. Coral Reefs 32:603–611

Lesser MP, Stochaj WR, Tapley DW, Shick JM (1990) Bleaching in coral reef anthozoans: Effects of irradiance, ultraviolet radiation, and temperature on the activities of protective enzymes against active oxygen. Coral Reefs 8:225–232

Leuzinger S, Willis BL, Anthony KRN (2012) Energy allocation in a reef coral under varying resource availability. Mar Biol 159:177–186

Levas S, Grottoli AG, Schoepf V, Aschaffenburg M, Baumann J, Bauer JE, Warner ME (2016) Can heterotrophic uptake of dissolved organic carbon and zooplankton mitigate carbon budget deficits in annually bleached corals? Coral Reefs 35:495–506

Levas SJ, Grottoli AG, Hughes A, Osburn CL, Matsui Y (2013) Physiological and biogeochemical traits of bleaching and recovery in the mounding species of coral *Porites lobata*: Implications for resilience in mounding corals. PLoS One 8:e63267

Levitan DR, Boudreau W, Jara J, Knowlton N (2014) Long-term reduced spawning in *Orbicella* coral species due to temperature stress. Mar Ecol Prog Ser 515:1–10

Lewis C, Neely K, Rodriguez-Lanetty M (2019) Recurring episodes of thermal stress shift the balance from a dominant host-specialist to a background host-generalist zooxanthella in the threatened pillar coral, *Dendrogyra cylindrus*.

Logan JM, Jardine TD, Miller TJ, Bunn SE, Cunjak RA, Lutcavage ME (2008) Lipid corrections in carbon and nitrogen stable isotope analyses: Comparison of chemical extraction and modelling methods. J Anim Ecol 77:838–846

Long MH, Rheuban JE, Berg P, Zieman JC (2012) A comparison and correction of light intensity loggers to photosynthetically active radiation sensors: Comparison of light loggers and PAR sensors. Limnol Oceanogr Methods 10:416–424

Loram JE, Trapido-Rosenthal HG, Douglas AE (2007) Functional significance of genetically different symbiotic algae Symbiodinium in a coral reef symbiosis. Mol Ecol 16:4849–4857

Lowe RJ, Falter JL, Monismith SG, Atkinson MJ (2009) A numerical study of circulation in a coastal reef-lagoon system. J Geophys Res 114:997

Loya Y, Sakai K, Yamazato K, Nakano Y, Sambali H, van Woesik R (2001) Coral bleaching: the winners and the losers. Ecol Lett 4:122–131

Maier C, Pätzold J, Bak RPM (2003) The skeletal isotopic composition as an indicator of ecological and physiological plasticity in the coral genus *Madracis*. Coral Reefs 22:370–380

Maier C, Weinbauer MG, Pätzold J (2010) Stable isotopes reveal limitations in C and N assimilation in the Caribbean reef corals *Madracis auretenra*, *M. carmabi* and *M. formosa*. Mar Ecol Prog Ser 412:103–112

Manzello DP, Brandt M, Smith TB, Lirman D, Hendee JC, Nemeth RS (2007) Hurricanes benefit bleached corals. Proc Natl Acad Sci U S A 104:12035–12039

Marubini F, Barnett H, Langdon C (2001) Dependence of calcification on light and carbonate ion concentration for the hermatypic coral *Porites compressa*. Mar Ecol Prog Ser 220:153–162

Marubini F, Davies PS (1996) Nitrate increases zooxanthellae population density and reduces skeletogenesis in corals. Mar Biol 127:319–328

Mass T, Drake JL, Haramaty L, Kim JD, Zelzion E, Bhattacharya D, Falkowski PG (2013) Cloning and characterization of four novel coral acid-rich proteins that precipitate carbonates in vitro. Curr Biol 23:1126–1131

Mass T, Einbinder S, Brokovich E, Shashar N, Vago R, Erez J, Dubinsky Z (2007) Photoacclimation of *Stylophora pistillata* to light extremes: Metabolism and calcification. Mar Ecol Prog Ser 334:93–102

Mass T, Kline DI, Roopin M, Veal CJ, Cohen S, Iluz D, Levy O (2010) The spectral quality of light is a key driver of photosynthesis and photoadaptation in *Stylophora pistillata* colonies from different depths in the Red Sea. J Exp Biol 213:4084–4091

Matthews JL, Crowder CM, Oakley CA, Lutz A, Roessner U, Meyer E, Grossman AR, Weis VM, Davy SK (2017) Optimal nutrient exchange and immune responses operate in partner specificity in the cnidarian-dinoflagellate symbiosis. Proc Natl Acad Sci U S A 114:13194–13199

Matthews Jennifer L., Oakley Clinton A., Lutz Adrian, Hillyer Katie E., Roessner Ute, Grossman Arthur R., Weis Virginia M., Davy Simon K. (2018) Partner switching and metabolic flux in a model cnidarian–dinoflagellate symbiosis. Proc R Soc B 285:20182336

McCloskey LR, Muscatine L (1984) Production and respiration in the Red Sea coral *Stylophora pistillata* as a function of depth. Proc R Soc Lond B Biol Sci 222:215–230

McCulloch M, Falter J, Trotter J, Montagna P (2012) Coral resilience to ocean acidification and global warming through pH up-regulation. Nat Clim Chang 2:623

McConnaughey TA (2003) Sub-equilibrium oxygen-18 and carbon-13 levels in biological carbonates: carbonate and kinetic models. Coral Reefs 22:316–327

McIlvin MR, Casciotti KL (2011) Technical updates to the bacterial method for nitrate isotopic analyses. Anal Chem 83:1850–1856

Mills MM, Lipschultz F, Sebens KP (2004) Particulate matter ingestion and associated nitrogen uptake by four species of scleractinian corals. Coral Reefs 23:311–323

Mills MM, Sebens KP (2004) Ingestion and assimilation of nitrogen from benthic sediments by three species of coral. Mar Biol 145:1097–1106

Minagawa M, Wada E (1984) Stepwise enrichment of ^{15}N along food chains: Further evidence and the relation between $\delta^{15}N$ and animal age. Geochim Cosmochim Acta 48:1135–1140

Moss RH, Edmonds JA, Hibbard KA, Manning MR, Rose SK, van Vuuren DP, Carter TR, Emori S, Kainuma M, Kram T, Meehl GA, Mitchell JFB, Nakicenovic N, Riahi K, Smith SJ, Stouffer RJ, Thomson AM, Weyant JP, Wilbanks TJ (2010) The next generation of scenarios for climate change research and assessment. Nature 463:747–756

Muscatine L, Cernichiari E (1969) Assimilation of photosynthetic products of zooxanthellae by a reef coral. Biol Bull 137:506–523

Muscatine L, Falkowski PG, Porter JW, Dubinsky Z (1984) Fate of Photosynthetic Fixed Carbon in Light- and Shade-Adapted Colonies of the Symbiotic Coral *Stylophora pistillata*. Proc R Soc Lond B Biol Sci 222:181–202

Muscatine L, Goiran C, Land L, Jaubert J, Cuif J-P, Allemand D (2005) Stable isotopes ($\delta^{13}C$ and $\delta^{15}N$) of organic matrix from coral skeleton. Proc Natl Acad Sci U S A 102:1525–1530

Muscatine L, Kaplan IR (1994) Resource partitioning by reef corals as determined from stable isotope composition II. $\delta^{15}N$ of zooxanthellae and animal tissue versus depth. Pac Sci 48:304–312

Muscatine L, Porter JW (1977) Reef corals: Mutualistic symbioses adapted to nutrient-poor environments. Bioscience 27:454–460

Muscatine L, Porter JW, Kaplan IR (1989) Resource partitioning by reef corals as determined from stable isotope composition: I. $\delta^{13}C$ of zooxanthellae and animal tissue vs depth. Mar Biol

100:185–193

Muscatine L, R. McCloskey L, E. Marian R (1981) Estimating the daily contribution of carbon from zooxanthellae to coral animal respiration. Limnol Oceanogr 26:601–611

Nahon S, Richoux NB, Kolasinski J, Desmalades M, Ferrier Pages C, Lecellier G, Planes S, Berteaux Lecellier V (2013) Spatial and temporal variations in stable carbon ($\delta^{13}C$) and nitrogen ($\delta^{15}N$) isotopic composition of symbiotic scleractinian corals. PLoS One 8:e81247

Nakamura T, van Woesik R (2001) Water-flow rates and passive diffusion partially explain differential survival of corals during the 1998 bleaching event. Mar Ecol Prog Ser 212:301–304

NOAA Coral Reef Watch (2018) Main Hawaiian Islands 5-km Bleaching Heat Stress Gauges (Version 3). Jan 2014 – Jan 2015. College Park, Maryland, USA: NOAA Coral Reef Watch. [accessed: May 21 2018] https://coralreefwatch.noaa.gov/vs/gauges/hawaii.php

NOAA (2017) Tides and Currents. Mokuoloe, Hawaii, Station ID: 1612480. National Oceanic and Atmospheric Administration, USA. [accessed: March 01 2017] https://tidesandcurrents.noaa.gov/stationhome.html?id=16124 80.

NOAA (2018) Central Pacific Hurricane Center, National Atmospheric and Oceanic Administration. [accessed: May 21 2018] http://www.prh.noaa.gov/cphc/tcpages/archive.php?stormid=CP022014.

Noonan SHC, Fabricius KE (2016) Ocean acidification affects productivity but not the severity of thermal bleaching in some tropical corals. ICES J Mar Sci 73:715–726

Oku H, Yamashiro H, Onaga K, Iwasaki H, Takara K (2002) Lipid distribution in branching coral *Montipora digitata*. Fish Sci 68:517–522

van Oppen MJ, Palstra FP, Piquet AM, Miller DJ (2001) Patterns of coral-dinoflagellate associations in *Acropora*: Significance of local availability and physiology of *Symbiodinium* strains and host-symbiont selectivity. Proc Biol Sci 268:1759–1767

Oswald F, Schmitt F, Leutenegger A, Ivanchenko S, D'Angelo C, Salih A, Maslakova S, Bulina M, Schirmbeck R, Nienhaus GU, Matz MV, Wiedenmann J (2007) Contributions of host and symbiont pigments to the coloration of reef corals. FEBS J 274:1102–1109

Pacherres CO, Schmidt GM, Richter C (2013) Autotrophic and heterotrophic responses of the coral *Porites lutea* to large amplitude internal waves. J Exp Biol 216:4365–4374

PacIOOS (2018) Pacific Island Ocean Observing System. http://www.pacioos.hawaii.edu/weather/obs-mokuoloe/

Palardy JE, Grottoli AG, Matthews KA (2005) Effects of upwelling, depth, morphology and polyp size on feeding in three species of Panamanian corals. Mar Ecol Prog Ser 300:79–89

Palardy JE, Grottoli AG, Matthews KA (2006) Effect of naturally changing zooplankton concentrations on feeding rates of two coral species in the Eastern Pacific. J Exp Mar Bio Ecol 331:99–107

Palardy JE, Rodrigues LJ, Grottoli AG (2008) The importance of zooplankton to the daily metabolic carbon requirements of healthy and bleached corals at two depths. J Exp Mar Bio Ecol 367:180–188

Palmer AR (1992) Calcification in marine molluscs: how costly is it? Proc Natl Acad Sci U S A 89:1379–1382

Palumbi SR, Barshis DJ, Traylor-Knowles N, Bay RA (2014) Mechanisms of reef coral resistance to future climate change. Science 344:895–898

Pan T-CF, Applebaum SL, Manahan DT (2015) Experimental ocean acidification alters the allocation of metabolic energy. Proc Natl Acad Sci U S A 112:4696–4701

Pandolfi JM, Jackson JBC, Baron N, Bradbury RH, Guzman HM, Hughes TP, Kappel CV, Micheli F, Ogden JC, Possingham HP, Sala E (2005) Ecology. Are U.S. coral reefs on the slippery slope to slime? Science 307:1725–1726

Papina M, Meziane T, van Woesik R (2003) Symbiotic zooxanthellae provide the host-coral *Montipora digitata* with polyunsaturated fatty acids. Comp Biochem Physiol B Biochem Mol Biol 135:533–537

Patton JS, Abraham S, Benson AA (1977) Lipogenesis in the intact coral *Pocillopora capitata* and its isolated zooxanthellae: Evidence for a light-driven carbon cycle between symbiont and host. Mar Biol 44:235–247

Pernice M, Dunn SR, Tonk L, Dove S, Domart-Coulon I, Hoppe P, Schintlmeister A, Wagner M, Meibom A (2015) A nanoscale secondary ion mass spectrometry study of dinoflagellate functional diversity in reef-building corals. Environ Microbiol 17:3570–3580

Pinzón JH, Kamel B, Burge CA, Harvell CD, Medina M, Weil E, Mydlarz LD (2015) Whole transcriptome analysis reveals changes in expression of immune-related genes during and after bleaching in a reef-building coral. R Soc Open Sci 2:140214

Pochon X, Putnam HM, Gates RD (2014) Multi-gene analysis of *Symbiodinium* dinoflagellates: a perspective on rarity, symbiosis, and evolution. PeerJ 2:e394

Porter JW (1976) Autotrophy, heterotrophy, and resource partitioning in Caribbean reef-building corals. Am Nat 110:731–742

Porter JW, Fitt WK, Spero HJ, Rogers CS, White MW (1989) Bleaching in reef corals: Physiological and stable isotopic responses. Proc Natl Acad Sci U S A 86:9342–9346

R Core Team (2016) R: A language and environment for statistical computing. R foundation for statistical computing, Vienna, Austria. https://www.R-project.org/

R Core Team (2018) R: A language and environment for statistical computing. R foundation for statistical computing, Vienna, Austria. https://www.R-project.org/

R Core Team (2019) R: A language and environment for statistical computing. R foundation for statistical computing, Vienna, Austria. https://www.R-project.org/

Radice VZ, Hoegh-Guldberg O, Fry B, Fox MD, Dove SG (2019) Upwelling as the major source of nitrogen for shallow and deep reef-building corals across an oceanic atoll system. Funct Ecol 73:5333

Rahav O, Dubinsky Z, Achituv Y, Falkowski PG (1989) Ammonium metabolism in the zooxanthellate coral, *Stylophora pistillata*. Proc R Soc Lond B Biol Sci 236:325–337

Raven JA (2005) *Ocean acidification due to increasing atmospheric carbon dioxide*. The Royal Society. https://royalsociety.org/topics-policy/publications/2005/ocean-acidification/ The Clyvedon Press Ltd, Cardiff, UK

Reynaud S, Ferrier-Pages C, Sambrotto R (2002) Effect of feeding on the carbon and oxygen isotopic composition in the tissues and skeleton of the zooxanthellate coral *Stylophora pistillata*. Mar Ecol 238:81–89

Reynaud S, Leclercq N, Romaine-Lioud S, Ferrier-Pages C, Jaubert J, Gattuso J-P (2003) Interacting effects of CO_2 partial pressure and temperature on photosynthesis and calcification in a scleractinian coral. Glob Chang Biol 9:1660–1668

Reynaud S, Martinez P, Houlbrèque F, Billy I, Allemand D, Ferrier-Pagès C (2009) Effect of light and feeding on the nitrogen isotopic composition of a zooxanthellate coral: role of nitrogen recycling. Mar Ecol Prog Ser 392:103–110

Ries JB (2011) A physicochemical framework for interpreting the biological calcification response to CO_2-induced ocean acidification. Geochim Cosmochim Acta 75:4053–4064

Ritson-Williams, R., and R. D. Gates. 2016a. Kaneohe Bay light data 2014 and 2015 [Data set]. Zenodo. doi:10.5281/zenodo.160214

Ritson-Williams, R., and R. D. Gates. 2016b. Kaneohe Bay seawater temperature data 2014 and 2015 [Data set]. Zenodo. superseded.doi:10.5281/zenodo.46366

Ritson-Williams, R., and R.D. Gates. 2016c. Kaneohe Bay sediment data 2015 [Data set]. Zenodo. doi:10.5281/zenodo.61137

Ritson-Williams, R., C. Wall, R. Cunning, and R. Gates. 2019. Kaneohe Bay nutrient data 2014-2016 [Data set]. Zenodo. http://doi.org/10.5281/zenodo.2538121

Rodolfo-Metalpa R, Houlbrèque F, Tambutté É, Boisson F, Baggini C, Patti FP, Jeffree R, Fine M, Foggo A, Gattuso J-P, Hall-Spencer JM (2011) Coral and mollusc resistance to ocean acidification adversely affected by warming. Nat Clim Chang 1:308

Rodrigues LJ, Grottoli AG (2006) Calcification rate and the stable carbon, oxygen, and nitrogen isotopes in the skeleton, host tissue, and zooxanthellae of bleached and recovering Hawaiian corals. Geochim Cosmochim Acta 70:2781–2789

Rodrigues LJ, Grottoli AG (2007) Energy reserves and metabolism as indicators of coral recovery from bleaching. Limnol Oceanogr 52:1874–1882

Rodrigues LJ, Grottoli AG, Pease TK (2008) Lipid class composition of bleached and recovering *Porites compressa* Dana, 1846 and *Montipora capitata* Dana, 1846 corals from Hawaii. J Exp Mar Bio Ecol 358:136–143

Rosset S, Wiedenmann J, Reed AJ, D'Angelo C (2017) Phosphate deficiency promotes coral bleaching and is reflected by the ultrastructure of symbiotic dinoflagellates. Mar Pollut Bull 118:180–187

Rost B, Zondervan I, Riebesell U (2002) Light-dependent carbon isotope fractionation in the coccolithophorid *Emiliania huxleyi*. Limnol Oceanogr 47:120–128

Rowan R, Knowlton N, Baker A, Jara J (1997) Landscape ecology of algal symbionts creates variation in episodes of coral bleaching. Nature 388:265–269

Sampayo EM, Dove S, Lajeunesse TC (2009) Cohesive molecular genetic data delineate species diversity in the dinoflagellate genus *Symbiodinium*. Mol Ecol 18:500–519

Sampayo EM, Franceschinis L, Hoegh-Guldberg O, Dove S (2007) Niche partitioning of closely related symbiotic dinoflagellates. Mol Ecol 16:3721–3733

Sampayo EM, Ridgway T, Bongaerts P, Hoegh-Guldberg O (2008) Bleaching susceptibility and mortality of corals are determined by fine-scale differences in symbiont type. Proc Natl Acad Sci U S A 105:10444–10449

Sawall Y, Al-Sofyani A, Banguera-Hinestroza E, Voolstra CR (2014) Spatio-temporal analyses of Symbiodinium physiology of the coral *Pocillopora verrucosa* along large-scale nutrient and temperature gradients in the Red Sea. PLoS One 9:e103179

Scheufen T, Krämer WE, Iglesias-Prieto R, Enríquez S (2017) Seasonal variation modulates coral sensibility to heat-stress and explains annual changes in coral productivity. Sci Rep 7:4937

Schlacher TA, Connolly RM (2014) Effects of acid treatment on carbon and nitrogen stable isotope ratios in ecological samples: a review and synthesis. Methods Ecol Evol 5:541–550

Schmidt-Roach S, Miller KJ, Lundgren P, Andreakis N (2014) With eyes wide open: a revision of species within and closely related to the *Pocillopora damicornis* species complex (Scleractinia; Pocilloporidae) using morphology and genetics: *Pocillopora* Species. Zool J Linn Soc 170:1–33

Strahl J, Stolz I, Uthicke S, Vogel N, Noonan SHC, Fabricius KE (2015) Physiological and ecological performance differs in four coral taxa at a volcanic carbon dioxide seep. Comparative Biochemistry and Physiology, Part A 184:179–186.

Teece MA, Estes B, Gelsleichter E, Lirman D (2011) Heterotrophic and autotrophic assimilation of fatty acids by two scleractinian corals, *Montastraea faveolata* and *Porites astreoides*. Limnol Oceanogr 56:1285–1296

Vega Thurber RL, Burkepile DE, Fuchs C, Shantz AA, McMinds R, Zaneveld JR (2014) Chronic nutrient enrichment increases prevalence and severity of coral disease and bleaching. Glob Chang Biol 20:544–554

Venn A, Tambutté E, Holcomb M, Allemand D, Tambutté S (2011) Live tissue imaging shows reef corals elevate pH under their calcifying tissue relative to seawater. PLoS One 6:e20013

Venn AA, Tambutté E, Holcomb M, Laurent J, Allemand D, Tambutté S (2013) Impact of seawater acidification on pH at the tissue-skeleton interface and calcification in reef corals. Proc Natl Acad Sci U S A 110:1634–1639

Vidal-Dupiol J, Zoccola D, Tambutté E, Grunau C, Cosseau C, Smith KM, Freitag M, Dheilly NM, Allemand D, Tambutté S (2013) Genes related to ion-transport and energy production are upregulated in response to CO_2-driven pH decrease in corals: new insights from transcriptome analysis. PLoS One 8:e58652

Vogel N, Meyer FW, Wild C, Uthicke S (2015) Decreased light availability can amplify negative impacts of ocean acidification on calcifying coral reef organisms. Mar Ecol Prog Ser 521:49–61

Von Euw S, Zhang Q, Manichev V, Murali N, Gross J, Feldman LC, Gustafsson T, Flach C, Mendelsohn R, Falkowski PG (2017) Biological control of aragonite formation in stony corals. Science 356:933–938

van Vuuren DP, Edmonds J, Kainuma M, Riahi K, Thomson A, Hibbard K, Hurtt GC, Kram T, Krey V, Lamarque J-F, Masui T, Meinshausen M, Nakicenovic N, Smith SJ, Rose SK (2011) The representative concentration pathways: An overview. Clim Change 109:5

Wagner DE, Kramer P, Van Woesik R (2010) Species composition, habitat, and water quality influence coral bleaching in southern Florida. Mar Ecol Prog Ser 408:65–78

Wall C (2019) cbwall/Energetics-and-isotopes-in-bleached-and-recovering-corals: Physiology and isotopes values of bleached and recovering corals (Version v1.0-pub). Zenodo. http://doi.org/10.5281/zenodo.2587467

Wall CB, Fan T-Y, Edmunds PJ (2014) Ocean acidification has no effect on thermal bleaching in the coral *Seriatopora caliendrum*. Coral Reefs 33:119–130

Wall CB, Mason RAB, Ellis WR, Cunning R, Gates RD (2017a) Data from: Elevated pCO_2 affects tissue biomass composition, but not calcification, in a reef coral under two light regimes. Dryad Digital Repository. https://doi.org/10.5061/dryad.5vg70.3

Wall CB, Mason RAB, Ellis WR, Cunning R, Gates RD (2017b) Elevated pCO_2 affects tissue biomass composition, but not calcification, in a reef coral under two light regimes. R Soc Open Sci 4:170683

Wall CB, Ritson-Williams R, Popp BN, and Gates RD (2019) Spatial variation in the biochemical and isotopic composition of corals during bleaching and recovery. Limnol Oceanogr https://doi.org/10.1002/lno.11166

Wang J, Douglas AE (1998) Nitrogen recycling or nitrogen conservation in an alga-invertebrate symbiosis? J Exp Biol 201:2445–2453

Ward S (1995) Two patterns of energy allocation for growth, reproduction and lipid storage in the scleractinian coral *Pocillopora damicornis*. Coral Reefs 14:87–90

Weis VM (2008) Cellular mechanisms of Cnidarian bleaching: Stress causes the collapse of symbiosis. J Exp Biol 211:3059–3066

Wham DC, Ning G, LaJeunesse TC (2017) *Symbiodinium glynnii* sp. nov., a species of stress-tolerant symbiotic dinoflagellates from pocilloporid and montiporid corals in the Pacific Ocean. Phycologia 56:396–409

Whiteman J, Elliott Smith E, Besser A, Newsome S (2019) A guide to using compound-specific stable isotope analysis to study the fates of molecules in organisms and ecosystems. Diversity 11:8–18

Wiedenmann J, D'Angelo C, Smith EG, Hunt AN, Legiret F-E, Postle AD, Achterberg EP (2012) Nutrient enrichment can increase the susceptibility of reef corals to bleaching. Nat Clim Chang 3:160

Wild C, Hoegh-Guldberg O, Naumann MS, Florencia Colombo-Pallotta M, Ateweberhan M, Fitt WK, Iglesias-Prieto R, Palmer C, Bythell JC, Ortiz J-C, Loya Y, van Woesik R (2011) Climate change impedes scleractinian corals as primary reef ecosystem engineers. Mar Freshwater Res 62:205–215

Wilkinson C, Lindén O, Cesar H, Hodgson G, Rubens J, Strong AE (1999) Ecological and

socioeconomic impacts of 1998 coral mortality in the Indian Ocean: An ENSO impact and a warning of future change? Ambio 28:188–196

Wooldridge SA (2009) Water quality and coral bleaching thresholds: Formalising the linkage for the inshore reefs of the Great Barrier Reef, Australia. Mar Pollut Bull 58:745–751

Wright RM, Strader ME, Genuise HM, Matz M (2019) Effects of thermal stress on amount, composition, and antibacterial properties of coral mucus. PeerJ 7:e6849